

OROBOROS INSTRUMENTS  
high-resolution respirometry

**Mitochondrial Physiology Network**



# **Mitochondrial Pathways and Respiratory Control**

## **An Introduction to OXPHOS Analysis**

**Erich Gnaiger**

**Mitochondr Physiol Network 19.12**

**OROBOROS MiPNet Publications 2014**



# **Mitochondrial Pathways and Respiratory Control**

## **An Introduction to OXPHOS Analysis**

**Erich Gnaiger**

Mitochondr Physiol Network 19.12

OROBOROS MiPNet Publications 2014

**©2014 OROBOROS INSTRUMENTS Corp, Innsbruck, Austria**  
Printed by Steiger Druck GmbH, Axams, Austria [steigerdruck@tirol.com](mailto:steigerdruck@tirol.com)

**4<sup>th</sup> edition 2014:** 4000 prints

**ISBN 978-3-9502399-8-0**

2012 3<sup>rd</sup> edition: 2400 prints; ISBN 978-3-9502399-6-6

2007 1<sup>st</sup> edition: 1000 prints; electronic 1<sup>st</sup> edition, ISBN 978-3-9502399-0-4

Open Access: [www.bioblast.at/index.php/Gnaiger\\_2014\\_MitoPathways](http://www.bioblast.at/index.php/Gnaiger_2014_MitoPathways)

OROBOROS INSTRUMENTS Corp.  
high-resolution respirometry  
Schöpfstr. 18  
A-6020 Innsbruck, Austria  
[erich.gnaiger@oroboros.at](mailto:erich.gnaiger@oroboros.at)  
[www.oroboros.at](http://www.oroboros.at)

D. Swarovski Research Lab.  
Dept. Visceral, Transplant and  
Thoracic Surgery  
Medical University of Innsbruck  
A-6020 Innsbruck, Austria  
[www.bioblast.at](http://www.bioblast.at)

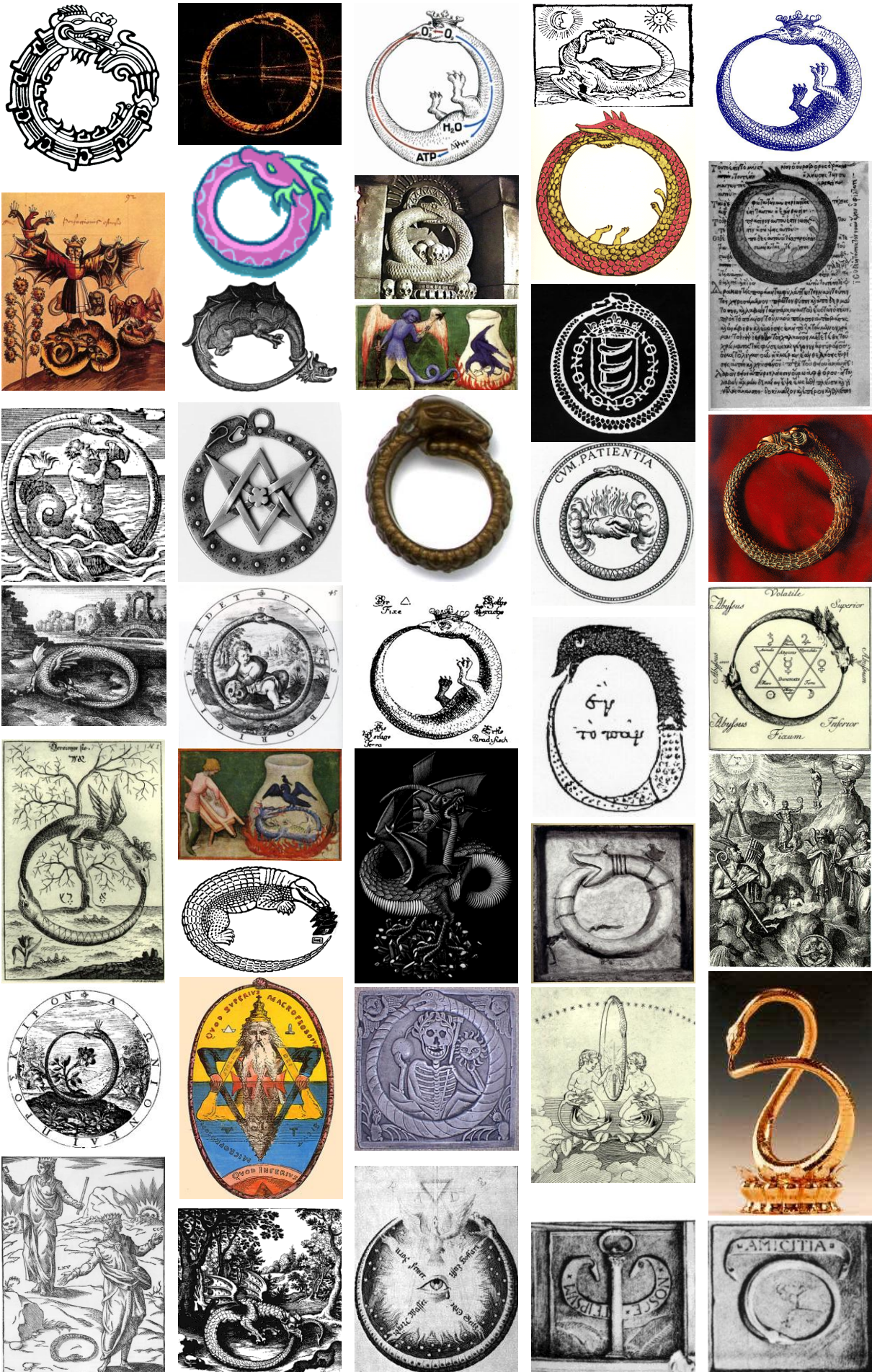


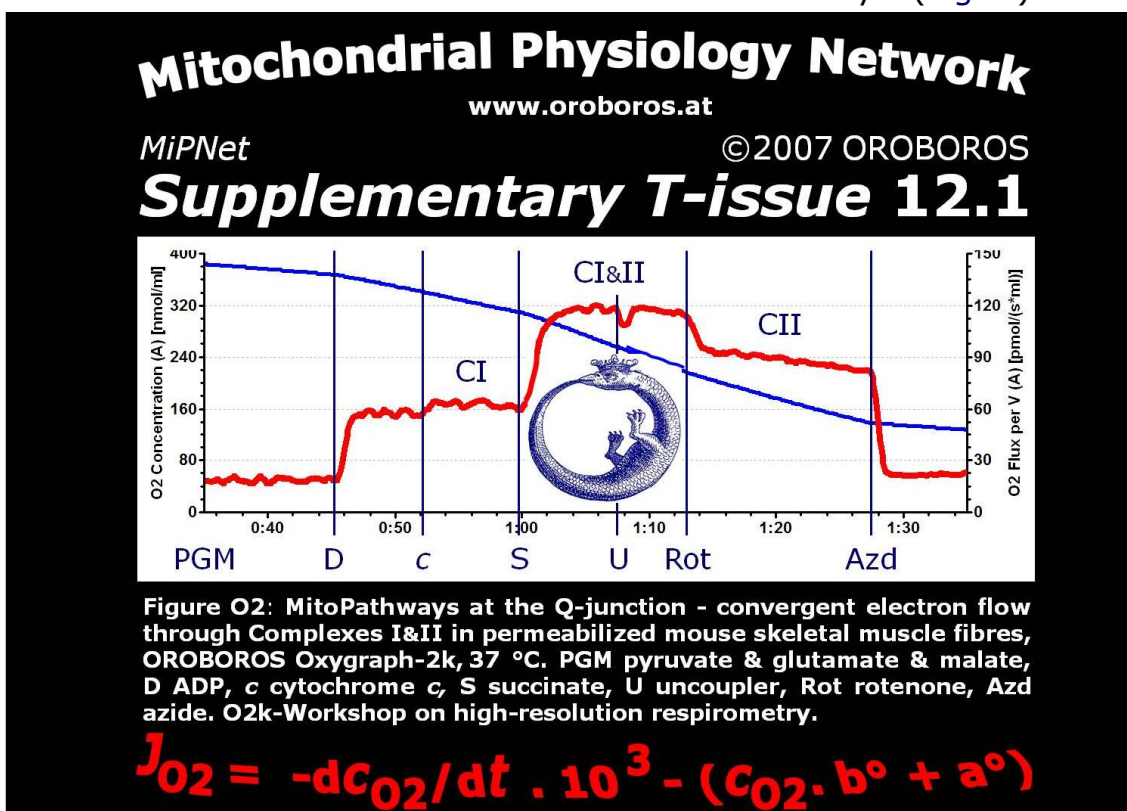


Fig. 1. The Blue Book: Mitochondrial Pathways and Respiratory Control 1<sup>st</sup> edition (2007). 1<sup>st</sup> Mitochondrial Physiology Summer School, MiPsummer July 2007, Schröcken, Austria.

# Mitochondrial Pathways and Respiratory Control

## Preface

The 'Blue Book' is an introduction to the analysis of oxidative phosphorylation (OXPHOS). It combines concepts of bioenergetics and biochemical pathways related to mitochondrial (mt) core energy metabolism and provides the basis for the design of substrate-uncoupler-inhibitor titration (SUIT) protocols in O<sub>2</sub>k-assays established since publication of the first edition of 'Mitochondrial Pathways' (Fig. 1).



**Fig. 2.** High-resolution respirometry (HRR) and OXPHOS analysis presented as supplementary *T-issue* (OROBOROS *T-shirt*). Oxygraph-2k experiment 2007-04-14 P1-03 (chamber A) performed at an O<sub>2</sub>k-Workshop on HRR (IOC39, April 2007, Schröcken, Vorarlberg, Austria).



We live with mitochondrial physiology. Your OXPHOS capacity is essential for your quality of life, for brain and muscle function, resistance against preventable and age-related degenerative diseases. Genetic background and life style determine mitochondrial competence, which is OXPHOS capacity and multiple mt-functions. Comprehensive OXPHOS analysis is vital for your cells, vital for our health care system, and vitally deserves reliability of experimental and diagnostic approaches.

Application of SUIT protocols for real-time OXPHOS analysis is a component of metabolic phenotyping (Fig. 2). OXPHOS analysis extends conventional bioenergetics to the level of mitochondrial physiology for functional diagnosis in health and disease. The OROBOROS Oxygraph-2k (O2k) represents the unique instrument for HRR. No other platform is suited for application of SUIT protocols. The O2k overcomes restrictions of the number of titrations available in multiwell systems, or the insufficient signal stability and limited oxygen capacity in small chambers.

A *Mitochondrial Physiology Network* has evolved as (i) a network of scientists linked by applications of the O2k (WorldWide MiPNet: [http://wiki.orooboros.at/index.php/MiPNet\\_Reference\\_Laboratories](http://wiki.orooboros.at/index.php/MiPNet_Reference_Laboratories)), and (ii) a format of publications available on the OROBOROS website, which summarizes protocols, introductory guidelines and discussions of concepts (MiPNet Protocols: <http://wiki.orooboros.at/index.php/O2k-Protocols>). (iii) Beyond the restricted space for references selected in the printed edition, O2k-Publications are listed as supplementary information that is updated continuously ([http://wiki.orooboros.at/index.php/O2k-Publications: Topics](http://wiki.orooboros.at/index.php/O2k-Publications:_Topics)). The number of O2k-Publications increases rapidly (presently >1.300) with extending basic, biomedical and clinical applications of the OROBOROS Oxygraph-2k. (iv) Bioblast Glossaries are presented with emphasis on developing a consistent terminology in mitochondrial physiology ([http://wiki.orooboros.at/index.php/Bioblast\\_Glossaries](http://wiki.orooboros.at/index.php/Bioblast_Glossaries)).

'MitoPathways' is an element of high-resolution respirometry and mitochondrial physiology. A mosaic evolves by combining the elements into a picture of modern mitochondrial respiratory physiology.

I thank all contributors to the *Mitochondrial Physiology Network* for their cooperation and feedback. In particular, I acknowledge experimental contributions from the K-regio project *Mitocom Tyrol* and the authors and co-authors of various publications emerging from international cooperations. Without the team of OROBOROS INSTRUMENTS, including the partners in electromechanical engineering (Oxygraph-2k; Philipp Gradl, WGT-Elektronik, Kolsass, Austria) and software development (DatLab; Lukas Gradl, software security networks, Innsbruck, Austria) the experimental advances on 'MitoPathways' would not have been possible.

For references and notes see Bioblast online information:



[www.bioblast.at/index.php/Gnaiger\\_2014\\_MitoPathways](http://www.bioblast.at/index.php/Gnaiger_2014_MitoPathways)



Erich Gnaiger  
Innsbruck, Jul 2007 - Sep 2014



## Contents

<b>1. Real-time OXPHOS analysis</b> .....	7
<b>2. Respiratory states:</b> Coupling control .....	19
<b>3. MitoPathways to Complex I.</b> Respiratory substrate control with pyruvate, malate, glutamate .....	32
<b>4. MitoPathways to Complexes II,</b> glycerophosphate dehydrogenase and ETF .....	39
<b>5. MitoPathways to Complexes I&amp;II.</b> Convergent electron transfer at the Q-junction .....	43
<b>6. Normalization of flux - past the RCR:</b> On efficiency, coupling and substrate control factors .....	58
<b>7. Conversions of metabolic fluxes</b> .....	64
<b>A. Abbreviations</b> .....	67
<b>References</b> .....	72
<a href="http://www.bioblast.at/index.php/Gnaiger_2014_MitoPathways">www.bioblast.at/index.php/Gnaiger_2014_MitoPathways</a>	
<b>Bioblast Wiki</b> – Gentle Science .....	74
<i>MiP Art – Mitchell's dream – Mitchell's equation</i> .....	75
<b>The OROBOROS</b> - feeding on negative entropy .....	79



Mitochondrial Orobos by Odra Noel

Cover: Suspended human umbilical vein endothelial cells by Gunde Rieger



## OROBOROS INSTRUMENTS high-resolution respirometry

The OROBOROS Oxygraph-2k (O2k) provides the basis for high-resolution respirometry (HRR) and represents world-wide the technologically leading instrument for diagnostic evaluation of mitochondrial respiratory function, represented in 42 countries (2014). The new development of the high-resolution O2k-Fluorometer builds upon the OROBOROS Oxygraph-2k developed and extended since 2001 by OROBOROS INSTRUMENTS and WGT-Elektronik (Austria).

Integration of fluorometry and spectrophotometry into the O2k opens up the potential for the analysis of various diagnostically significant cellular functions, simultaneously with the measurement of mitochondrial respiration. In particular, HRR is now combined with new modules for the fluorometric detection of reactive oxygen species (ROS; oxidative stress) and mitochondrial membrane potential using established fluorescent dyes. This innovation further extends the technological leadership and sole-source status of the O2k as a high-end diagnostic instrument.

The new edition of 'Mitochondrial Pathways' presents the conceptual basis of established and continuously emerging SUIT protocols for the study of respiratory control, and for the design and optimization of new experimental protocols to support innovative applications of HRR at an advanced level of real-time OXPHOS analysis.

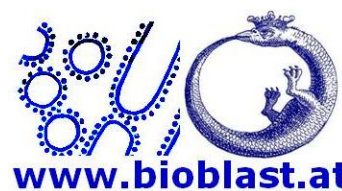
### Citation

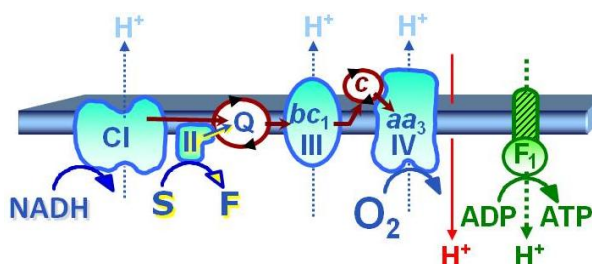
Gnaiger E (2014) Mitochondrial Pathways and Respiratory Control. An Introduction to OXPHOS Analysis. 4<sup>th</sup> ed. Mitochondr Physiol Network 19.12. OROBOROS MiPNet Publications, Innsbruck: 80 pp.

References: [www.bioblast.at/index.php/Gnaiger\\_2014\\_MitoPathways](http://www.bioblast.at/index.php/Gnaiger_2014_MitoPathways)



OROBOROS Oxygraph-2k, TIP2k and O2k-Fluorescence LED2-Module.

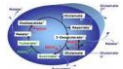




## Chapter 1. Real-time OXPHOS analysis

*The protoplasm is a colony of bioblasts. Microorganisms and granula are at an equivalent level and represent elementary organisms, which are found wherever living forces are acting, thus we want to describe them by the common term bioblasts.*

Richard Altmann (1894)

Section		Page
	1. Chemiosmotic coupling .....	7
	2. From oxygen concentration to oxygen flux .....	8
	3. Oxygen flow and flux: open the black box .....	11
	4. Metabolic forces: electric and chemical .....	12
	5. Fluxes and forces: coupling and efficiency .....	14
	6. Electron gating .....	15
	7. Electron transfer: Q-junction .....	16
	8. Biochemical thresholds and the Q-junction.....	16
	9. Boundary conditions .....	17

Oxidative phosphorylation (OXPHOS) is a key element of bioenergetics, extensively studied to resolve the mechanisms of energy transduction in the mitochondrial electron transfer system and to analyze various modes of mitochondrial respiratory control in health and disease. Respiratory flux control is exerted by (i) the density of mitochondria as the functional units of cell respiration; (ii) biochemical composition and structure of the mitochondrial-cytosolic network; (iii) respiratory coupling and substrate states in substrate-uncoupler-inhibitor titrations (SUIT) with saturating concentrations; (iv) allosteric kinetic and concentration-dependent substrate-uncoupler-inhibitor kinetic (SUIK) control.

### 1. Chemiosmotic coupling

Peter Mitchell's chemiosmotic coupling theory explains the fundamental mechanism of mitochondrial and microbial energy transformation, marking Richard Altmann's 'bioblasts' as the systematic unit of bioenergetics and of the human symbiotic 'supraorganism' with microbial-mammalian co-metabolic pathways. The transmembrane protonmotive, chemiosmotic force or electrochemical mt-proton potential,  $\Delta p_{mt}$ , provides the link between electron transfer and phosphorylation of ADP to ATP (Fig. 1.1).  $\Delta p_{mt}$  has an electric component (mt-membrane potential difference,  $\Delta \Psi_{mt}$ ) and a chemical component (pH difference,  $\Delta pH$ ; p. 76),

$$\Delta p_{mt} = \Delta \Psi_{mt} - 2.3 \cdot RT/F \cdot \Delta pH \quad (1.1)$$

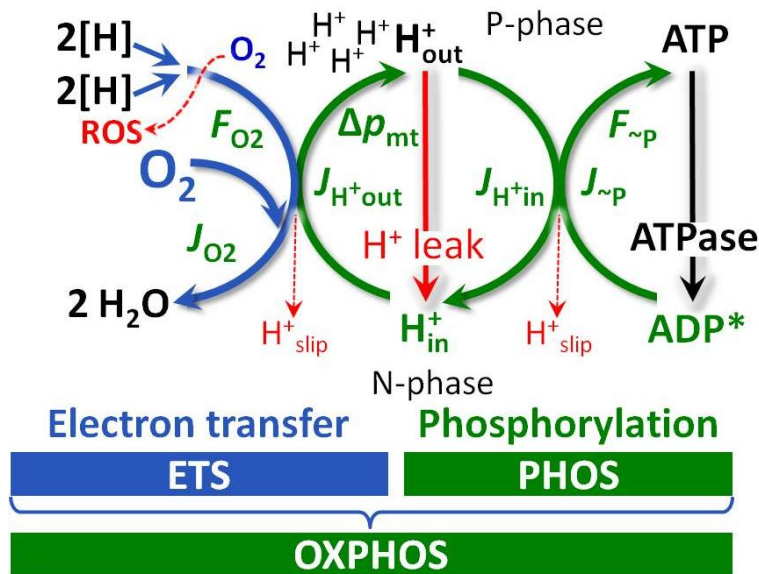


**Fig. 1.1. Energy transformation** in coupled fluxes,  $J$ , and forces,  $F$  and  $\Delta p_{mt}$ , of oxidative phosphorylation.  $2[H]$  indicates the reduced hydrogen equivalents of fuel substrates (CHO) and electron transfer to oxygen.  $J_{H^+out}$  is coupled output flux. Proton leaks dissipate energy of translocated protons from low pH in the positive P-phase to the negative N-phase.

Mitochondrial respiration is the exergonic input tightly but not fully coupled to the endergonic output of phosphorylation. OXPHOS capacity ( $P$ ) is measured at saturating ADP concentration ( $ADP^*$ , Fig. 1.1), which cannot be tested in living cells. ETS capacity ( $E$ ) is quantified by uncoupler (protonophore) titrations to obtain maximum flux in mitochondrial preparations or living cells (Fig. 1.2).  $E$  and  $P$  are numerically identical only if the phosphorylation system (adenylate nucleotide translocase, phosphate carrier, ATP synthase; Fig. 2.6) does not exert control over coupled respiration. A shift towards control of OXPHOS by the phosphorylation system is observed when ETS capacity is increased by the additive effect of convergent electron input into the Q-junction.

LEAK respiration is the LEAK oxygen flux,  $L$ , compensating for proton leak, slip and cation cycling, with ROS production usually playing a minor role (Fig. 1.1). LEAK respiration is measured as mitochondrial respiration in the LEAK state, in the presence of fuel substrate(s), but absence of ADP or after inhibition of the phosphorylation system (oligomycin or carboxyatractyloside; Fig. 1.2). In this non-phosphorylating resting state, the protonmotive force is maintained at a maximum, exerting feedback control by depressing oxygen flux to a level determined by the proton leak and the  $H^+/O_2$  ratio ( $H^+/O$  ratio). In this state of maximum protonmotive force, LEAK respiration represents an estimate of the upper limit of the LEAK component in ADP-stimulated respiration (OXPHOS capacity).

## 2. From oxygen concentration to oxygen flux

Real-time OXPHOS analysis uses respirometry as a fundamental approach to study oxygen consumption as an element of mitochondrial function in aerobic core metabolism. Oxygen flux times the driving force of the oxidation reaction provide the input power into the OXPHOS system. In a closed Oxygraph chamber, the oxygen concentration declines over time as a result of respiratory processes. The time derivative, therefore, is a negative number. Why is then the 'rate of oxygen consumption' not



expressed as a negative value? Why do we use the term 'oxygen flux' in this context of chemical reactions? The rationale is based on fundamental concepts of physical chemistry and the thermodynamics of irreversible processes in open and closed systems (Gnaiger 1993).

Concentration,  $c_B$  [ $\text{mol}\cdot\text{dm}^{-3}$ ], is the amount of substance,  $n_B$  [ $\text{mol}$ ], per unit of volume,  $V$ . The amount of elemental oxygen dissolved per volume of aqueous medium in the Oxygraph chamber is the oxygen concentration,  $c_{O_2}$  or  $[O_2]$ , measured by the polarographic oxygen sensor as an electric current,  $I$  [ $A$ ], and converted into a voltage [ $V$ ]. This raw signal is calibrated to record the oxygen concentration  $c_{O_2,t}$  over time  $t$  [ $s$ ] (Fig. 1.2). For units of oxygen concentration, see Chapter 7.2.

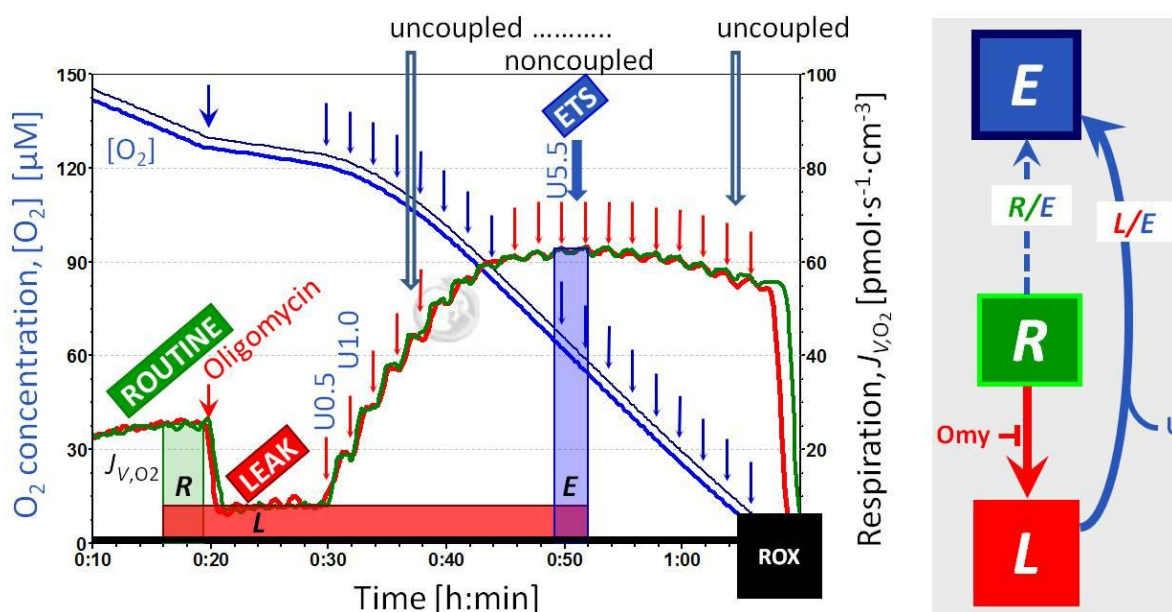


**Fig. 1.2. Oxygen concentration and oxygen flux in intact cells with phosphorylation control protocol, PCP.** High-resolution respirometry (OROBOROS Oxygraph-2k with TIP2k) with parental hematopoietic 32D cells at  $1.1\cdot 10^6$  cells/ $\text{cm}^3$  suspended in culture medium RPMI at 37 °C. Replicate measurements in the two O2k-chambers (2  $\text{cm}^3$ ). Superimposed plots of oxygen concentration  $[O_2]$  and volume-specific oxygen flux,  $J_{v,O_2}$ , calculated as the negative time derivative of oxygen concentration. **ROUTINE** respiration (R) is followed by inhibition of ATP synthase (manual titration of oligomycin,  $2\ \mu\text{g}\cdot\text{ml}^{-1}$ ) to induce the non-phosphorylating **LEAK** state (L). Automatic titration of uncoupler (10 mM FCCP in the TIP2k) in steps of  $0.1\ \mu\text{l}$  corresponding to a step increase in the final concentration of  $0.5\ \mu\text{M}$  FCCP at intervals of 120 s. Maximum noncoupled flux (capacity of the electron transfer system, ETS; state E) is reached at  $5.5\ \mu\text{M}$  FCCP. The L/E ratio is 0.10. Respiration is inhibited at higher  $[FCCP]$ , unrelated to sample dilution ( $<1\%$ ). O2k-experiment 2005-04-09 P3-03, carried out by participants of O2k-Workshop IOC30. Modified after Gnaiger (2008).

The oxygen concentration in pure water at equilibrium with air at standard barometric pressure of 100 kPa is 254.8 to 207.3  $\mu\text{mol/litre}$  in the range of 25 °C to 37 °C. In the 'open' Oxgraph chamber, in which the



aqueous medium is in equilibrium with a gas phase (such as air), the partial oxygen pressure,  $p_{O_2}$  [kPa] is identical in the gas phase and aqueous phase. The oxygen concentration, however, is very different in air and water. At equilibrium, the gas concentration in the gas phase is much higher than in aqueous solution. The dissolved oxygen concentration is proportional to the partial oxygen pressure at constant temperature and composition of the aqueous medium. This proportionality is expressed as the oxygen solubility,  $S_{O_2}$  [ $\mu\text{M}/\text{kPa}$ ]. In pure water at 25 °C (37 °C), the oxygen solubility is 12.56 (10.56)  $\mu\text{M}/\text{kPa}$ , but reduced by a factor of 0.89 to 0.92 in various culture and respiration media (0.92 for MiR06).

Cell respiration is an exergonic process by which fuel substrates (CHO) are oxidised internally and molecular oxygen (or another electron acceptor) is consumed in exchange with the environment. In the 'closed' Oxygraph chamber, which is sealed against any exchange of oxygen across the chamber walls and sealings, all oxygen consuming reactions cause the oxygen concentration to decline with time. If oxygen consumption is stimulated, then  $c_{O_2}$  falls off more steeply (Fig. 1.2). When all processes reacting with oxygen are fully inhibited, oxygen concentration remains constant over time and the slope is zero.

A linear negative slope, i.e. a constant drop of oxygen concentration with time in the closed Oxygraph chamber, is the result of a constant rate of the chemical reaction. Defining the reaction as



then the oxygen consumption rate per unit volume (= oxygen flux, volume-specific) is proportional to the negative slope of oxygen concentration with time. Take the difference of oxygen concentration (left Y-axis) between two time points (X-axis in Fig. 1.2),

$$\text{Concentration axis: } \Delta c_{O_2} = c_{O_2,2} - c_{O_2,1} \quad (1.3a)$$

$$\text{Time axis: } \Delta t = t_2 - t_1 \quad (1.3b)$$

The slope between these points is the rate of concentration change,

$$r_{O_2} = \Delta c_{O_2} / \Delta t \quad (1.4)$$

Metabolic flux (reaction 1.2), however, is the *negative* slope (see Eq. 1.6),

$$J_{V,O_2} = -(\Delta c_{O_2} / \Delta t) \quad (1.5)$$

In differential form ( $dt$  = infinitesimally small  $\Delta t$ ), the expression becomes

$$\text{Closed system: } J_{V,O_2} = -(dc_{O_2} / dt) \quad (1.6a)$$

$$\text{General: } J_{V,O_2} = d_r n_{O_2} / dt \cdot v_{O_2}^{-1} \cdot V^1 = d_r \xi_{O_2} / dt \cdot V^1 \quad (1.6b)$$

With the differential form (Eq. 1.6), gradual changes of oxygen flux can be evaluated (Fig. 1.2), in contrast to the assumption of linearity in the difference form of Eq. 1.5. Generalization from closed to open systems is achieved by the concept of *advancement* of reaction,  $d_r \xi_{O_2} = d_r n_{O_2} \cdot v_{O_2}^{-1}$ . The



subscript  $O_2$  in  $d_{r\xi_{O_2}}$  indicates that the stoichiometric number of oxygen in reaction 1.2 is taken as unity ( $v_{O_2} = -1$ ). Hence respiratory flux,  $J_{V,O_2}$ , refers to a stoichiometric form of oxygen-consuming reactions, where 1 mol of  $O_2$  is transformed. The negative sign in  $v_{O_2}$  yields  $J_{V,O_2}$  with a positive value.

### 3. Oxygen flow and flux: open the black box

Volume-specific oxygen flux,  $J_{V,O_2}$  (Eq. 1.6; Fig. 1.2 [ $\text{pmol}\cdot\text{s}^{-1}\cdot\text{ml}^{-1}$ ]) is a quantitative measure of the internal reaction per volume of the *experimental* chamber. What does it mean? The 'black box' is opened at three levels by expressing cell respiration per biological system (oxygen flow per cell), per cell size (cell-size specific oxygen flux) and per functional element (mt-specific oxygen flux; Fig. 1.3).

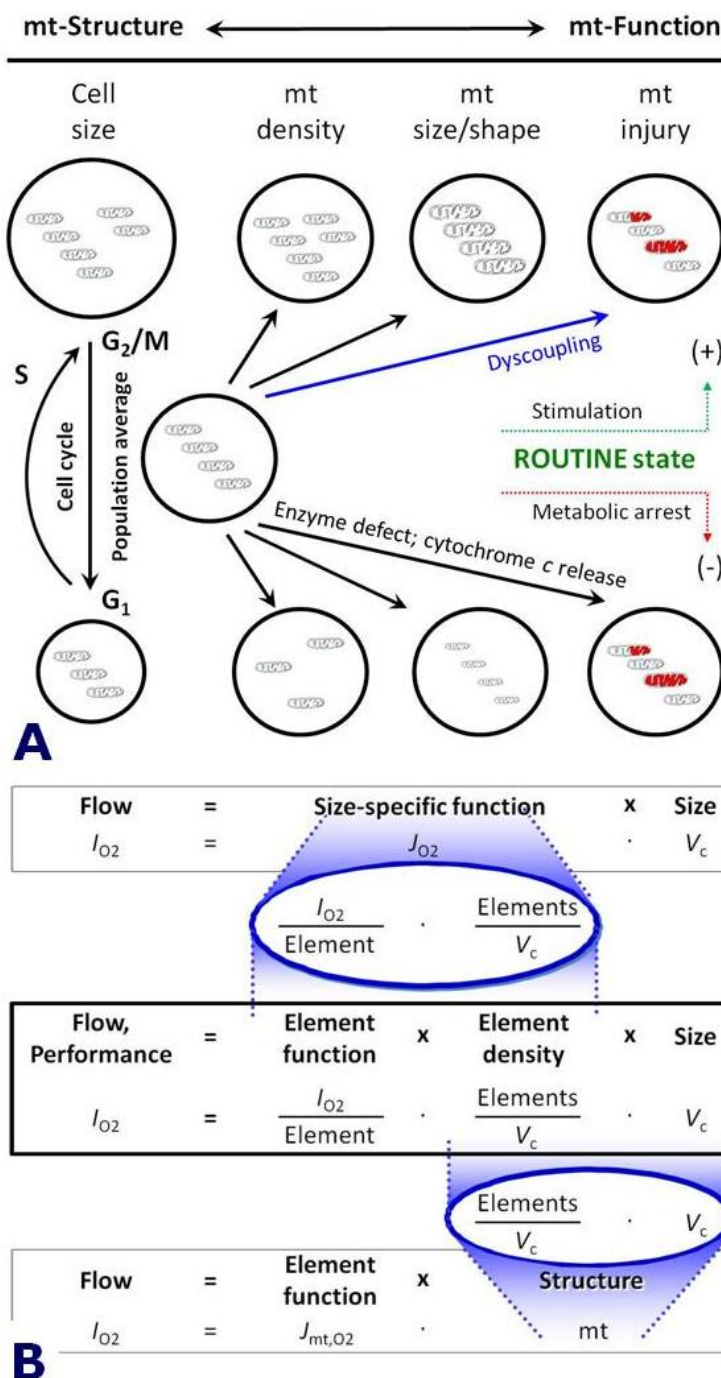


**Fig. 1.3. From oxygen flow ( $I_{O_2}$ , per cell) to cell-size specific oxygen flux ( $J_{O_2}$ , per cell size) and mt-specific oxygen flux (per mitochondrial marker). A. Oxygen flow depends on cell size, mt-density and mt-quality. ROUTINE activity is a function of metabolic state. Modified after Renner et al (2003).**

**B.** Structure-function analysis: Performance ( $I_{O_2}$ ) is the product of performance per functional element ( $J_{mt,O_2} = I_{O_2}$  per mt), element density (mt per cell size) and cell size (cell volume,  $V_c$ ). Cell-size specific oxygen flux,  $J_{O_2}$ , is the product of mt-quality (element function) and mt-density (elements/ $V_c$ ):

$$J_{O_2} = J_{mt,O_2} \cdot \text{mt}/V_c$$

(i) Dividing  $J_{V,O_2}$  [ $\text{pmol}\cdot\text{s}^{-1}\cdot\text{ml}^{-1}$  chamber] in cell respiration by cell density (number of cells per chamber volume [ $10^6\cdot\text{ml}^{-1}$ ]) converts



oxygen *flux per chamber volume* to oxygen *flow*,  $I_{O_2}$  [ $\text{pmol}\cdot\text{s}^{-1}\cdot 10^{-6}$  cells]. Flow per cell (or  $10^6$  cells) is a measure of system performance. Flow (per system) is an *extensive* quantity that changes with the size of the system (Fig. 1.3). No information is provided on internal structure.

(ii) Unstructured analysis: A *specific* quantity is obtained when the extensive quantity  $I_{O_2}$  is divided by *system size* (e.g. cell mass). Then *cell-mass specific* oxygen flux,  $J_{O_2}$  [ $\text{pmol}\cdot\text{s}^{-1}\cdot\text{mg}^{-1}$ ], is flow per cell ( $I_{O_2}$  [ $\text{pmol}\cdot\text{s}^{-1}\cdot 10^{-6}$  cells]), divided by mass per cell ( $m_c$  [ $\text{mg}\cdot 10^{-6}$  cells]); or  $J_{O_2}$  is calculated by dividing volume-specific flux ( $J_{V,O_2}$  [ $\text{pmol}\cdot\text{s}^{-1}\cdot\text{ml}^{-1}$  chamber volume]) by mass concentration (mass per chamber volume [ $\text{mg}\cdot\text{ml}^{-1}$ ]).

(iii) Structured analysis: Mitochondrial markers are used to determine mt-content in cells or tissues and to express oxygen flux in terms of a mt-marker (Fig. 1.3). Mitochondria are the structural and functional elemental units of cell respiration. Flux control ratios are based on a functional mt-marker. Other commonly used mt-markers are activities of citrate synthase (mt-matrix marker) and cytochrome c oxidase (inner mt-membrane marker), or mt-protein mass for isolated mitochondria.

#### 4. Metabolic forces: electric and chemical potentials

Power is energy per time, integrating flows and forces, the basis for efficiency or irreversible entropy production. Flow times force yields power. For the chemical reaction,  $r$  (Eq. 1.6b),

$$\text{Flow times force: } P_r = I_{O_2}\cdot F_{O_2,r} \quad I_{O_2} = d_r\xi_{O_2}/dt = d_r n_{O_2}/dt \cdot v_{O_2}^{-1} \quad (1.7a)$$

$$\text{Flux times force: } P_{V,r} = J_{V,O_2}\cdot F_{O_2,r} \quad J_{V,O_2} = d_r\xi_{O_2}/dt \cdot V^{-1} \quad (1.7b)$$

Electric power is flow or current ( $I_{el}$ ; units ampere [ $\text{A}=\text{C}\cdot\text{s}^{-1}$ ]) times force or electric potential difference ( $F_{el}$ ; units volt [ $\text{V}=\text{J}\cdot\text{C}^{-1}$ ]) where electric charge is expressed in coulombs [C].

$$\text{Electric, el: } P_{el} = I_{el}\cdot F_{el} \quad F_{el} = \partial G / \partial_{el}\xi \quad [\text{J}\cdot\text{C}^{-1}] \quad (1.8a)$$

$$\text{Displacement, d: } P_d = I_{B,d}\cdot F_{B,d} \quad F_{B,d} = \partial G / \partial_d\xi_B \quad [\text{J}\cdot\text{mol}^{-1}] \quad (1.8b)$$

$$\text{Reaction, r: } P_r = I_{B,r}\cdot F_{B,r} \quad F_{B,r} = \partial G / \partial_r\xi_B \quad [\text{J}\cdot\text{mol}^{-1}] \quad (1.8c)$$

The power of a transformation,  $P_{tr}$ , is the Gibbs energy change per time,  $P_{tr}=d_{tr}G/dt$  [ $\text{W}=\text{J}\cdot\text{s}^{-1}$ ]. The total Gibbs energy change,  $dG$ , is the sum of all partial energy transformations ( $dG = \sum d_{tr}G = d_{el}G + d_dG + d_rG + ..$ ), which is a concept of eminent importance in the chemiosmotic theory. Gibbs energy change,  $dG$ , measured over a defined period of time,  $\Delta t$ , becomes an energy change of  $\Delta G$  (compare Eq. 1.6 and 1.5).

A glorious didactic pitfall in most famous textbooks of biochemistry and bioenergetics is the confusing presentation of  $\Delta G$ , propagating a mix-up of energy change [J] and driving force of chemical reactions [ $\text{J}\cdot\text{mol}^{-1}$ ]. The generalized scalar forces in thermodynamics are partial changes (derivatives) of Gibbs energy per advancement,  $F_{tr} = \partial G / \partial_{tr}\xi$  (Eq. 1.8). These ergodynamic forces are potential differences between 'substrate' or



source states and 'product' or destination states (Gnaiger 1993). The chemiosmotic potential difference or protonmotive force,  $\Delta p_{mt}$ , is the sum of the partial electric and chemical (osmotic) forces of proton translocation across the mt-membrane (Eq. 1.1). A redox potential difference expresses force on the basis of displaced (motive) electric charge [ $J \cdot C^{-1} = V$ ]. The chemical potential difference,  $\Delta \mu_B$ , expresses chemical force on the basis of displaced or reacting *amount of substance* [ $J \cdot mol^{-1} = Jol$ ]. Unfortunately, the unit 'Jol' – a unit for chemical force – does not exist officially; it should be coined in analogy to the unit volt, facilitating the conceptual distinction between Gibbs energy change [J] and Gibbs force [ $Jol = J \cdot mol^{-1}$ ]. Logically, a *force* cannot be an *energy* difference,  $\Delta G$  [J]. A voltage [V] is not an electric energy difference [J]. Gibbs force is a chemical potential difference,  $\sum \mu_i \nu_i$ , which can be converted to an electric potential difference by multiplication with the number of charges and the Farady constant,  $F = 96\,485.3\ C \cdot mol^{-1}$  or  $F = 0.0964853\ kJol \cdot mV^{-1}$ .

Flows are advancement per time,  $I_{tr} = d_{tr} \xi / dt = d_{tr} X_i / dt \cdot \nu_i^{-1}$  (Eq. 1.6b).  $X_i$  is the generalized property (*transformant*) involved in a transformation, tr.  $X_i(el)$  is charge expressed in coulombs [C].  $X_i(d)$  and  $X_i(r)$  denote the amount of displaced or reacting substance, respectively, expressed as amount of substance [mol] (Eq. 1.8).

Electric force,  $F_{el}$  [V], is an *electric potential difference*, giving rise to the term mitochondrial *membrane potential (difference)*,  $\Delta \psi_{mt}$ . The partial chemical force of proton transduction or dislocation, d, is the *chemical potential difference*,  $\Delta \mu_{H^+}$  [ $kJ \cdot mol^{-1}$ ], which is a function of the proton activity,  $a_{H^+}$  [ $mol \cdot dm^{-3}$ ], or pH at phases  $i$ ,

$$\text{Potential:} \quad \mu_{H^+,i} = -RT \cdot \ln a_{H^+,i} = -RT \cdot \ln(10) \cdot pH_i \quad (1.9a)$$

$$\text{Potential difference:} \quad \Delta \mu_{H^+} = -RT \cdot \ln(10) \cdot \Delta pH = -2.3 \cdot RT \cdot (pH_2 - pH_1) \quad (1.9b)$$

Choosing  $i=1$  as the negative N-phase ( $\nu_{H^+,1} = -1$ ) and  $i=2$  as the positive P-phase ( $\nu_{H^+,2} = 1$ ) defines the direction of translocation against the electrochemical gradient. At 25 °C or 37 °C, a difference of -1 pH yields  $\Delta \mu_{H^+} = 5.7$  or  $5.9\ kJ \cdot mol^{-1}$ , equivalent to 59.2 or 61.5 mV (Chapter 7.3).

Force, energy and power are positive when conserving work by pumping protons uphill from the negative to the positive phase (low to high  $a_{H^+}$ ; Fig. 1.1). Output power requires coupling to input power (Fig. 1.1). Input force, energy and power have a negative sign, indicating the spontaneous downward or dissipative direction of energy transformation, consistent with (positive) entropy production of irreversible processes. Thus, irreversible thermodynamics provides the conceptual framework to describe all partial, simultaneous fluxes and forces in a consistent format of the dissipation function (Prigogine 1967). This unifies the description of chemical and electrochemical energy transformations, achieving a simplification compared to the divergent symbols and sign conventions in classical descriptions (Gnaiger 1993).

Real-time OXPHOS analysis has the potential to combine measurement of flows by HRR (electron transfer quantified by oxygen flow as input, ATP flow as output) and forces, such as the mitochondrial



membrane potential difference,  $\Delta\psi_{mt}$ , in an O2k-MultiSensor System using either potentiometric or fluorometric signals to study the equilibrium distribution of ions across the inner mt-membrane. The chemical  $\Delta pH$  component of the protonmotive force must be determined separately, or is diminished by incubation conditions including a high inorganic phosphate concentration. A shortcircuit ( $H^+$  leak) dissipates the energy of the translocated protons, which otherwise is used to phosphorylate ADP to ATP, with an output force,  $F_{\sim P}$ , of 52 to 66 kJ/mol  $\sim P$  under intracellular conditions. The efficiency of coupling is diminished further by potential proton slips of the proton-energy conserving pumps (Complexes CI, CIII and CIV). While the proton leak depends on  $\Delta p_{mt}$  and is a property of the inner membrane including the boundaries between membrane-spanning proteins and the lipid phase, proton slip is a property of the proton pumps when the proton slips back to the matrix side within the proton pumping process and is thus mainly dependent on flux. Electron leak with production of reactive oxygen species (ROS) is another component reducing the coupling between oxygen flux and ATP turnover.

## 5. Fluxes and forces: coupling and efficiency

The flux ratio between ATP production,  $J_{\sim P}$ , and oxygen consumption,  $J_{O_2}$ , is the  $\sim P/O_2$  ratio (or  $\sim P/O$  ratio with atomic oxygen as a reference). This is frequently referred to as the 'coupling efficiency', with focus on metabolic fluxes in real-time OXPHOS analysis. Coupling efficiency is quantified by the simultaneous determination of input and output fluxes, e.g. by measurement of oxygen flux and ATP flux in the O2k-MultiSensor System, using the O2k-Fluorescence LED2-Module with Mg-green.

An indirect estimate of coupling efficiency is obtained by sequential measurement of LEAK respiration ( $L$ ) and ETS capacity ( $E$ ), which can be obtained in intact cells (Fig. 1.2). ETS coupling efficiency is then expressed as the 'free' ETS capacity ( $E-L$ ) divided by total ETS capacity,  $(E-L)/E = 1-L/E$ , which is 0.0 at zero coupling ( $L=E$ ; LEAK=ETS capacity) and 1.0 at the limit of a fully coupled system ( $L=0$ ).

Efficiency is well defined in thermodynamics based on the entropy law, as an output/input power ratio with a maximum of 1.0. Specific metabolic power [ $J \cdot s^{-1} \cdot g^{-1} = W \cdot g^{-1}$ ] is not identical to metabolic flux [ $mol \cdot s^{-1} \cdot g^{-1}$ ]. Classical thermodynamics considers efficiency as a ratio of work output and heat or enthalpy input (caloric input, the heat engine).

Efficiency in the thermodynamics of irreversible processes takes into account fluxes and forces (specific power = flux times force). Efficiency (ergodynamic efficiency) is the product of coupling efficiency (flux ratio) and a conjugated force ratio. Ergodynamic efficiencies require the combined information on coupling efficiency and force ratios, including evaluation of redox potentials, chemiosmotic potentials and phosphorylation potentials (Gibbs forces). From Fig. 1.1, calculation of ergodynamic OXPHOS efficiency requires simultaneous measurement of



input oxygen flux and force ( $J_{O_2} \cdot F_{O_2}$ ) and output ATP flux and force ( $J_{\sim P} \cdot F_{\sim P}$ ). The Gibbs force of oxygen consumption,  $F_{O_2}$ , is typically  $-470$  kJ/mol  $O_2$ . Efficiency is then calculated as  $-(J_{\sim P} \cdot F_{\sim P}) / (J_{O_2} \cdot F_{O_2})$ . Maximum efficiency can be obtained only by compromising speed and slowing down when approaching equilibrium, whereas maximum power is achieved at the cost of energy required for fast but less efficient processes (Fig. 1.4).

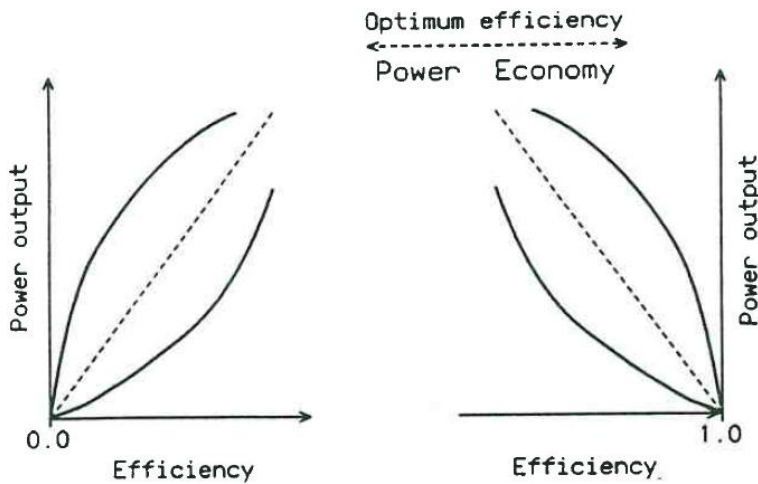


**Fig. 1.4. Optimum efficiency** depends on the strategy of either maximizing output power or efficiency. From Gnaiger E (1993) Efficiency and power strategies under hypoxia. Is low efficiency at high glycolytic ATP production a paradox? In: Surviving Hypoxia: Mechanisms of Control and Adaptation. Hochachka et al eds. CRC Press, Boca Raton, Ann Arbor, London, Tokyo: 77-109.

## 6. Electron gating

Electrons flow to oxygen along linear thermodynamic cascades (electron transfer chains) from either Complex I with three coupling sites, from Complex II with two coupling sites, or from other respiratory complexes which do not have a roman number. The CI- and CII-pathways of electron transfer are conventionally separated by using either NADH-linked substrates, such as pyruvate&malate, or the classical succinate and rotenone combination, to analyze site-specific  $H^+/O$  and  $\sim P/O$  ratios or defects of specific respiratory complexes in functional diagnosis. Electron gating is the experimental separation of various electron transfer pathways converging at the Q-junction (Fig. 1.5). Even without having been properly recognized and defined by a term, electron gating is common to the extent of establishing a bioenergetic paradigm in studies of OXPHOS with isolated mitochondria or permeabilized cells.

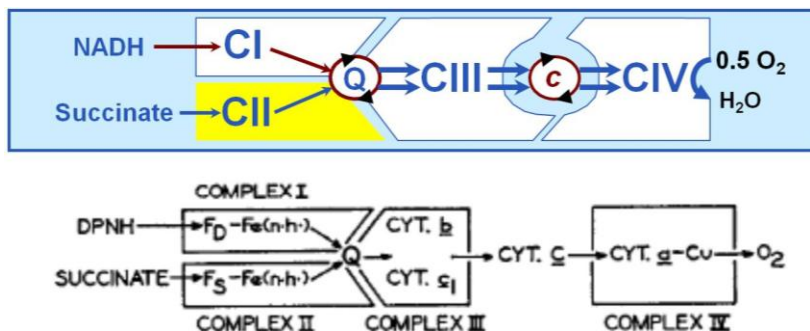


**FIG. 5.** Schematic representation of the four functional primary complexes and their sequential arrangement in the electron transfer system.  $F_D$ , DPNH dehydrogenase flavoprotein;  $F_S$ , succinic dehydrogenase flavoprotein.

**Fig. 1.5. Convergent CI&II-linked electron flow** at the Q-junction, exerting an additive effect on flux, versus electron gating for separation of single input pathways (Hatefi et al 1962; Gnaiger 2009).



## 7. Electron transfer: convergence at the Q-junction

Proper understanding and evaluation of the functional design of the OXPHOS system requires a transition from viewing the electron transfer as a *chain* (ETC) to the recognition of the convergent structure of electron flow to the Q-junction in the electron transfer *system* (ETS; Fig. 1.5). Electron transfer capacity of cells *in vivo* is generally underestimated on the basis of the 'State 3 paradigm' and conventional respiratory protocols applied with isolated mitochondria, permeabilized cells or tissues. Real-time OXPHOS analysis extends this bioenergetic paradigm by a perspective of mitochondrial physiology emerging from a series of studies based on high-resolution respirometry (OROBOROS Oxygraph-2k).

OXPHOS analysis uses an extension of basic bioenergetic respiratory protocols, beyond the important but limited analytical potential offered by oxygen consumption measurements on intact cells. Reconstitution of citric acid cycle function in isolated mitochondria, homogenates or permeabilized cells requires the simultaneous application of CI- and CII-linked substrates. Convergent electron flow through CI *and* CII (CI&II e-input) exerts an additive effect on respiratory flux (Fig. 1.5). OXPHOS capacities are increased up to 2-fold relative to respiratory capacity with CI- *or* CII-linked substrates alone. Operation of OXPHOS in top gear resolves discrepancies between intact cells and isolated mitochondria, with profound implications on evaluation of biochemical thresholds, apparent excess capacities and flux control coefficients of various mitochondrial enzyme systems. The additive effect of convergent electron input into CI and CII indicates a high down-stream excess capacity of respiratory complexes, including cytochrome *c* oxidase, CIV, over the separate convergent upstream pathways through Complex CI or CII (Fig. 1.5).

## 8. Biochemical thresholds and the Q-junction

The additive effect of convergent electron transfer at the Q-junction is highest when electron channelling through supercomplexes is tight (Fig. 1.5). The apparent excess capacity of a downstream step, such as the terminal cytochrome *c* oxidase (CIV), must then be high when related to a single input pathway (Fig. 1.6). This does not represent a functional excess capacity, however, which can only be evaluated relative to the reconstituted pathway flux (CI&II; Fig. 1.6).

Convergent CI&II e-input elicits the most pronounced stimulatory effect on coupled respiration when the phosphorylation system exerts low flux control. Convergent CI&II e-input corresponds to the operation of the citric acid cycle and mitochondrial fuel substrate supply *in vivo*. Importantly, by establishing the reference state of maximum coupled respiration, convergent CI&II e-input provides the proper basis for (i) quantifying excess capacities of Complexes CIII and CIV, (ii) interpreting flux control by various components such as the phosphorylation system or CIV, and (iii) for evaluation of specific enzymatic defects in the context of mitochondrial respiratory physiology and pathology.

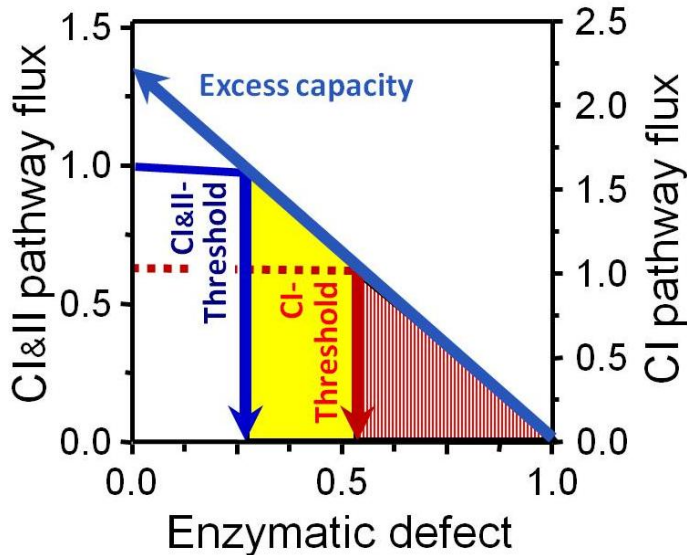


**Fig. 1.6. Biochemical threshold plot** for convergent CI&II-linked (full line, left) and CI-linked pathway flux based on electron gating (dotted line, right). An enzymatic defect of a single step (CIV) exerts no or little effect on pathway flux (horizontal lines) up to a threshold. Beyond the threshold a linear slope is obtained, which is extrapolated to the apparent excess capacity of the single step.

## 9. Boundary conditions

### 8.1. Fuel substrate concentrations

Substrates feeding into the TCA cycle are generally added at saturating concentrations for measurement of mitochondrial respiratory capacity, providing a buffer against fuel substrate depletion in the course of the experiment (Tab. A2.1). During exercise, there is an increase in the concentrations of TCA cycle intermediates, which are not limiting in contracting skeletal muscle. Important anaplerotic reactions, replenishing the pools of metabolic intermediates in the TCA cycle, are catalyzed by malic enzyme and pyruvate carboxylase in the mitochondrial matrix, which synthesize pyruvate from malate and oxaloacetate from pyruvate, respectively. Balanced anaplerosis and cataplerosis (entry and exit of TCA cycle intermediates) is responsible, particularly in metabolism of amino acids and gluconeogenesis (export of malate) and lipogenesis (export of citrate), for maintaining TCA cycle intermediates at steady states which shift under changing metabolic conditions of activity and starvation.

### 8.2. Respiration medium

The respiration medium MiR06 contains 10 mM inorganic phosphate ( $P_i$ ), 3 mM  $Mg^{2+}$ . Saturating ADP concentrations are added to evaluate OXPHOS capacity.  $P_i$  concentrations  $<10$  mM and  $[ADP] <0.4$  mM limit OXPHOS respiration in isolated heart mitochondria. In permeabilized muscle fibre bundles of high respiratory capacity, the apparent  $K_m$  for ADP increases up to 0.5 mM. This implies that  $>90\%$  saturation is reached only  $>5$  mM ADP. Hence, the many studies using lower ADP concentrations in permeabilized tissues and cells may underestimate OXPHOS capacity. Saturating ADP concentrations are essential for evaluation of flux control exerted by the capacity of the phosphorylation system (ATP synthase, adenine nucleotide translocase and phosphate carrier), which is indicated by noncoupled respiration in excess of OXPHOS capacity.



### 8.3. Oxygen concentration

Oxygen is not limiting for respiration of isolated mitochondria and small cells even at 20  $\mu\text{M}$  (20- to 50-fold above the apparent  $K_m$  for dissolved oxygen). In permeabilized muscle fibre bundles, however, diffusion restriction increases the sensitivity to oxygen supply 100-fold (human vastus lateralis, rat soleus and rat heart). It appears, therefore, that most studies carried out below air saturation (about 200  $\mu\text{M}$   $\text{O}_2$ ) imply oxygen limitation of OXPHOS flux in permeabilized fibres. It is recommended to apply increased oxygen levels in the range of 500 to  $>200$   $\mu\text{M}$  to studies of respiratory capacity in muscle fibres.

### 8.4. Cytochrome c retention

Release of cytochrome *c*, either under pathophysiological conditions of the cell or as a result of sample preparation, may limit active respiration. This specific effect can be separated from other OXPHOS defects by addition of cytochrome *c* (10  $\mu\text{M}$ ), which thus provides an essential aspect of quality control of isolated mitochondria or permeabilized tissues and cells.

### 8.5. $\text{Ca}^{2+}$

$\text{Ca}^{2+}$  at optimum concentration is an activator of dehydrogenases and oxidative phosphorylation. Free calcium in MiR05 or MiR06 is kept low by 0.5 mM EGTA. A modest increase of free calcium concentration may stimulate respiration.

### 8.6. Temperature

Experimental temperature is best chosen at or near physiological conditions, else care must be taken when extrapolating results obtained at a different temperature (Chapter 7).

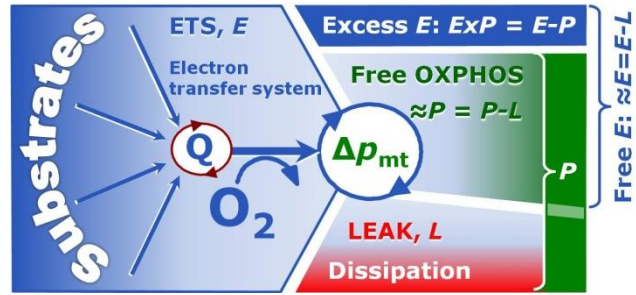
### 8.7. Sample storage

Short-term preservation of mt-preparations including isolated mitochondria on ice in a specific preservation medium increases respiratory capacity in the ADP-activated state when compared to storage in typical isolation medium, and addition of antioxidants even in the isolation medium has a significant beneficial effect.





# Chapter 2. Respiratory states: coupling control



'The growth of any discipline depends on the ability to communicate and develop ideas, and this in turn relies on a language which is sufficiently detailed and flexible.'  
Simon Singh (1997) Fermat's last theorem. Fourth Estate, London.

Section	1. Coupling in oxidative phosphorylation .....	19	Page
	2. Respiratory steady-states .....	19	
	2.1. OXPHOS capacity, <i>P</i> .....	24	
	2.2. Electron transfer system capacity, <i>E</i> .....	26	
	2.3. ROUTINE respiration of the intact cell, <i>R</i> .....	27	
	2.4. LEAK respiration, <i>L</i> .....	28	
	2.5. Uncoupled – noncoupled – dyscoupled? .....	30	
	3. Residual oxygen consumption, ROX .....	31	

## 1. Coupling in oxidative phosphorylation

In oxidative phosphorylation, exergonic electron transfer to oxygen is coupled to endergonic phosphorylation of ADP to ATP. The proton pumps generate and utilize the protonmotive force in a proton circuit across the inner mitochondrial membrane. This proton circuit is partially uncoupled by proton leaks and decoupled by proton slip (Fig. 1.1). Coupling or uncoupling is a key component of mitochondrial respiratory control.

## 2. Respiratory steady-states

Respiratory steady-states have been defined by Chance and Williams (1955 I, III) according to a classical Oxygraph protocol with isolated mitochondria (Fig. 2.1; Tab 2.1).

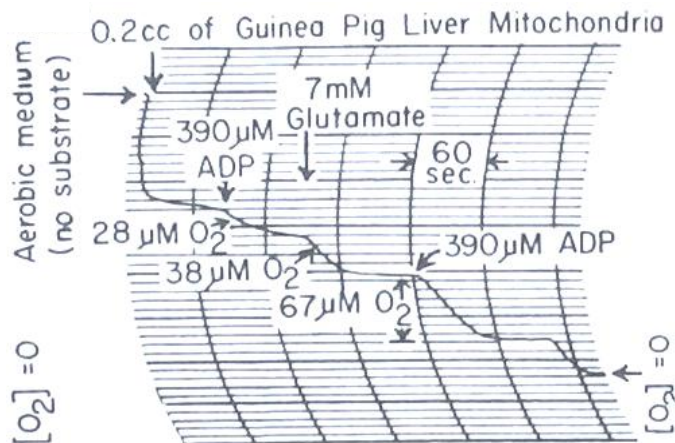


**Fig. 2.1. Respiratory states.** Coupling control in isolated mitochondria: endogenous fuel substrates and added ADP (States 1 and 2), glutamate and respiratory control ratio (RCR=State 3/ State 4); zero oxygen calibration at State 5 (Chance and Williams 1955 I; Fig. 4B).



The titration protocol (Fig. 2.1 and 2.2A) starts with addition of mitochondria to air-saturated isotonic medium with inorganic phosphate in State 1 ( $e_N$ , endogenous substrates; no adenylates, subscript N). ADP (+D) induces a transient activation to effectively exhaust endogenous fuel substrates, after which State 2 is a CHO substrate-depleted state of residual oxygen consumption (ROX). Addition of substrate (Fig. 2.1: glutamate, +G) stimulates respiration while ADP is high ( $G_D$ ; State 3, close to OXPHOS capacity). When ADP is depleted by phosphorylation to ATP ( $\rightarrow T$ ), respiration drops in the transition to State 4, which is an ADP-limited resting state ( $G_{LT}$ , LEAK state,  $L_T$ , in the presence of ATP). A second ADP titration (+D) is followed by another State 3 $\rightarrow$ 4 transition ( $\rightarrow T$ ) while sufficient oxygen is available, which allows calculation of the  $\sim P/O$  ratio (Fig. 5.5). Finally, respiration becomes  $O_2$  limited in the aerobic-anoxic transition ( $\rightarrow$ anox, State 5; Tab. 2.1).

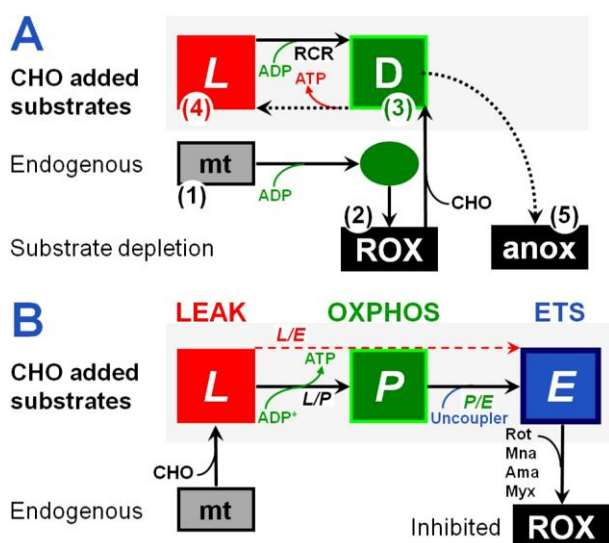


**Fig. 2.2. Coupling control protocols.**

**A:** Classical sequence from States 1 to 5 (numbers in parantheses): Addition of ADP is followed by State 2 (residual oxygen consumption, ROX). CHO fuel substrates stimulate State 3 respiration (D). After ADP $\rightarrow$ ATP phosphorylation ( $\sim P$ ) is complete, State 4 is a LEAK state ( $L_T$ ). State 5 is anoxia. **B:** Initial addition of CHO substrates to induce a LEAK state in the absence of adenylates ( $L_N$ ). Saturating ADP ( $D^*$ ) supports

OXPHOS capacity,  $P$ . Uncoupler titration to maximum oxygen flux induces the noncoupled state of electron transfer system capacity (ETS, state  $E$ ) followed by inhibition of respiratory complexes to determine residual oxygen consumption (ROX) for correction of fluxes in the mt-coupling states. Various ETS competent substrate states  $X$  can be applied.

<b>A</b>	Titration:	mt	+D	+X	$\rightarrow T$	+D	$\rightarrow T$	+D $\rightarrow$ anox
	States:	$e_N$	ROX	$X_D$	$X_{LT}$	$X_D$	$X_{LT}$	anox
		1	2	3	4	3	4	5
<b>B</b>	Titration:	mt	+X	+D		+D*	+U	+Inhibitors
	States:	$e_N$	$X_{LN}$	$X_D$		$X_P$	$X_E$	ROX

**Table 2.1. Metabolic states of mitochondria (Chance and Williams, 1956; TABLE V).**

State	$[O_2]$	ADP level	Substrate level	Respiration rate	Rate-limiting substance	Coupling state with CHO fuel substrate X
1	>0	Low	Low	Slow	ADP	$e_N$ , endogenous, no ADP
2	>0	High	$\sim 0$	Slow	Substrate	$e_D$ , ROX with ADP
3	>0	High	High	Fast	respiratory chain	$X_D$ , OXPHOS capacity?
4	>0	Low	High	Slow	ADP	$X_{LT}$ , LEAK, no ATPase
5	<0	High	High	0	Oxygen	anoxic ( $O_2$ backdiffusion?)

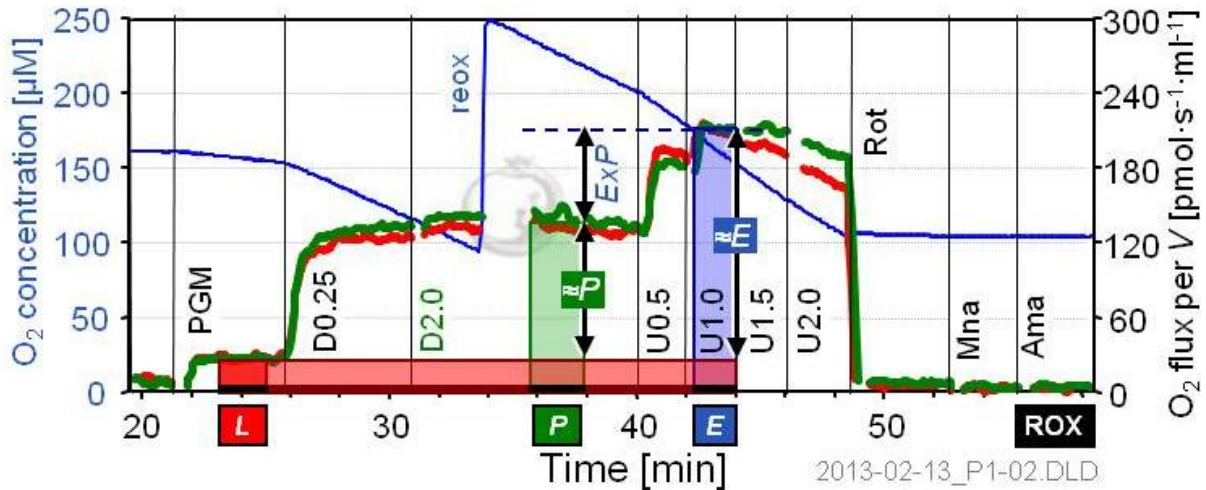


**Fig. 2.3. High-resolution respirometry and coupling control protocol, CCP** (mouse brain homogenate in MiR05). O<sub>2</sub> concentration (blue line; left axis [ $\mu\text{M}$ ]) is shown for one chamber; oxygen flux (red and green lines [ $\text{pmol}\cdot\text{s}^{-1}\cdot\text{ml}^{-1}$ ]) are superimposed for the two chambers of the Oxygraph-2k. Complex I-linked substrates pyruvate, glutamate and malate (PGM; 5, 10 and 2 mM; LEAK state,  $L_N$ , without adenylates), 0.25 mM ADP (D0.25, nonsaturating; State 3), 2 mM ADP\* (OXPHOS capacity,  $P$ ). Uncoupler titration (U, 0.5 to 2.0  $\mu\text{M}$  FCCP) yields maximum flux at 1.0  $\mu\text{M}$  FCCP (ETS capacity,  $E$ ). Residual oxygen consumption (ROX; for correction of total oxygen flux) measured after inhibition of Complexes CI (rotenone, 0.3  $\mu\text{M}$ ), CII (malonate, 5 mM), and CIII (antimycin A; Ama, 2.5  $\mu\text{M}$ ). Reoxygenation with 3  $\mu\text{l}$  H<sub>2</sub>O<sub>2</sub> (200 mM stock). Safranin (2  $\mu\text{M}$ ) added initially for simultaneous fluorometric measurement of  $\Delta\psi_{\text{mt}}$  (not shown) specifically inhibits the phosphorylation system to a larger degree than CI-linked ETS capacity. This explains the large apparent excess ETS-OXPHOS capacity,  $Exp = E - P$  (from Krumschnabel et al 2014; modified).

In an alternative protocol (Fig. 2.2.B) fuel substrates are added first, inducing a LEAK state,  $L_N$  (no ADP; Fig. 5.5: succinate,  $S(\text{Rot})_{L_N}$ ; Fig. 2.3: pyruvate&glutamate&malate,  $\text{PGM}_{L_N}$ ). A four-compartmental model of OXPHOS provides the guideline for experimental design (Fig. 2.4). The critically important steps include testing for saturating [ADP] (+D\*) to quantify OXPHOS capacity, uncoupler titrations (+U) to determine ETS capacity, and inhibition of ETS to correct total oxygen uptake ( $L'$ ,  $P'$ ,  $E'$ ) for residual oxygen consumption, e.g.  $L = L' - \text{ROX}$  and  $E = E' - \text{ROX}$  (Fig. 2.3).

Respiratory coupling states are integrated in the metabolic design of core mitochondrial pathways (Fig. 2.4). Dissipative LEAK respiration,  $L$ , restricts the ETS capacity,  $E$ , to drive coupled transmembrane processes. The remaining free ETS capacity,  $\approx E = E - L$ , is partitioned into the free OXPHOS module,  $\approx P = P - L$ , and the excess capacity module,  $Exp = E - P$ . The excess capacity,  $Exp$ , provides a tool for the diagnosis of a specific impairment of the phosphorylation system in toxicological or pathological states (Fig. 2.3). Diminished OXPHOS at constant ETS or less affected ETS capacity causes  $Exp$  to increase, which leads to the unequivocal distinction between defects of the electron transfer versus phosphorylation system. Both can potentially limit  $\approx P$ , the vital free OXPHOS capacity (Fig. 2.4).

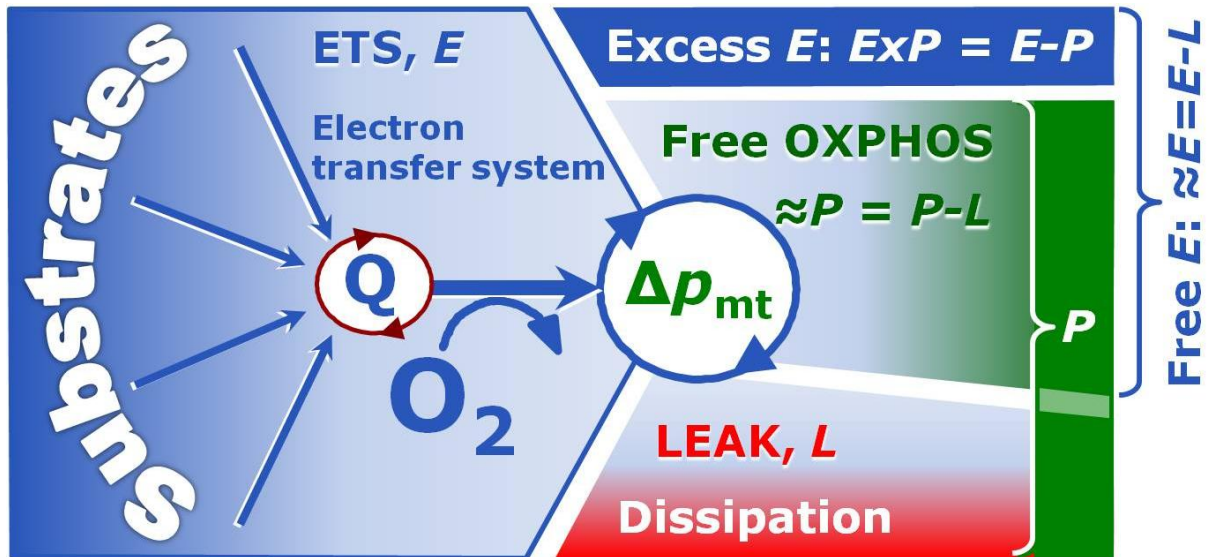


**Figure 2.4. Capacities of ETS, OXPHOS and LEAK respiration ( $E$ ,  $P$ ,  $L$ ) and four-compartmental OXPHOS model.** (i) Capacity of the ETS module is measured in the noncoupled state (Fig. 2.3). OXPHOS capacity,  $P$ , is partitioned into (ii) the dissipative LEAK component,  $L$ , and (iii) the free OXPHOS capacity,  $\approx P = P - L$ . If free OXPHOS capacity is limited by the capacity of the phosphorylation system, then (iv) the apparent ETS excess capacity,  $ExP = E - P$ , is available to drive coupled processes other than phosphorylation without competing with ATP production. Free divided by total ETS capacity,  $\approx E/E$ , is the ETS coupling efficiency. Free divided by total OXPHOS capacity,  $\approx P/P$ , is the OXPHOS coupling efficiency.

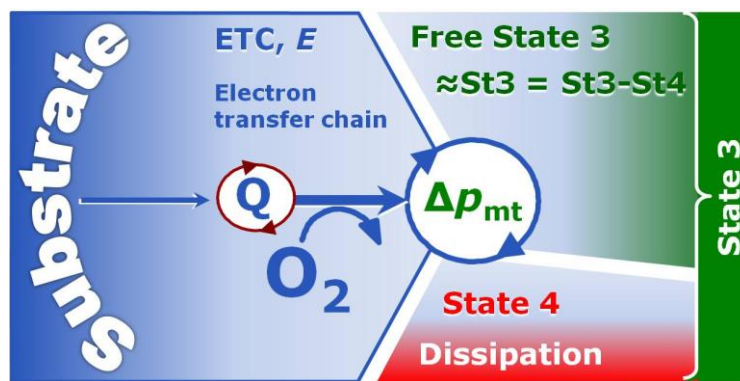
Pronounced differences in the magnitude of the excess  $E - P$  capacity in healthy mitochondria from different species, tissues and life cycle stages challenge comparative mitochondrial physiology to the extent of a paradigm change. Mammalian myocardial mitochondria, particularly of mice and humans, but also skeletal muscle mitochondria, show unexpected diversity of respiratory control, with  $ExP/E$  flux control factors ranging from 0.0 to 0.5. The excess  $E - P$  capacity module,  $ExP$ , needs functional interpretation:  $ExP$  increases the free ETS capacity which then is available to drive  $\Delta\psi_{mt}$  or  $\Delta\mu_{H^+}$  coupled transmembrane processes without competing with phosphorylation:  $\Delta p_{mt}$ -coupled ion transport, including fuel substrates and  $Ca^{2+}$ . The nature of these coupled processes needs to be identified to clarify the functional role of different apparent  $ExP$  excess capacities in various species and tissues. Alternatively, the excess  $E - P$  capacity constitutes a reserve, and the substantial differences in this apparent reserve between species and tissues may then be related to differential challenges and evolutionary risk management.

Generations of students of bioenergetics have adopted a three-compartmental model of mitochondrial respiration as a paradigm for functional separation of three OXPHOS modules (Fig. 2.5): (i) Fuel substrate oxidation (electron transfer chain), (ii) the phosphorylation system (Fig. 2.6) with energy (exergy) conservation as the efficient branch of OXPHOS, and (iii) proton leak and other purely dissipative processes of heat production (dissipation) comprising the inefficient uncoupled respiration (Fig. 2.5).



### Fig. 2.5. Three-compartmental OXPHOS model of respiration.

Electron transfer coupled to phosphorylation in ADP-stimulated State 3, partially uncoupled as observed in the dissipative State 4. State 3 respiration corrected for LEAK is potentially available ('free', symbol  $\approx$ ) for coupled production of ATP ( $\sim P$ ).



Compartmental OXPHOS analysis has been the basis of many important advancements in bioenergetics. However, the three-compartmental OXPHOS model fails to consider the quantitative importance of the excess ETS-OXPHOS capacity,  $Exp = E - P$ . This is reflected by the State 3/State 3u terminology which obscures the fundamental difference between ETS and OXPHOS capacities.

Limitations of the three-compartmental OXPHOS model are tightly linked to traditional protocols restricted to respiratory States 3 and 4 (Fig. 2.5). Experimentally, OXPHOS capacity ( $P$ ) is underestimated at State 3, if the 'high' ADP concentration (Tab. 2.1) is kinetically not saturating. Then an excess ETS-State 3 capacity is due to kinetic limitation of respiration in contrast to differences in catalytic capacities.

Restricted substrate supply in the study of the electron transfer *chain* fails to reveal physiological ETS capacity, since electron gating restricts electron transfer *system* capacity (Fig. 1.5). Downstream excess capacity (CIII, CIV; Fig. 1.6) is overestimated, but excess ETS-OXPHOS capacity is underestimated without reconstitution of TCA cycle function by appropriate substrate supply to mt-preparations. Upstream substrate limitation does not push the capacity of the phosphorylation system to its upper limit and thus masks the functional gap between physiological ETS capacity (noncoupled state) and OXPHOS capacity (coupled state).

Taken together, determination of respiratory capacities in specific coupling states (LEAK, OXPHOS, ETS) require electron transfer system (ETS) competent substrate states, including sufficient oxygen supply. Coupling states and fuel substrate states are complementary: both exert a mutual influence on respiratory control. ETS competence of fuel substrates depends on (i) transport of substrates across the mt-membranes or oxidation by dehydrogenases localized at the outer face of the inner mt-membrane (e.g. glycerophosphate dehydrogenase complex), (ii) oxidation in the mt-matrix (TCA cycle dehydrogenases) or on the inner face of the inner mt-membrane (CII, CETF), and (iii) oxidation of substrates without accumulation of inhibitory endproducts (e.g. oxaloacetate inhibiting CII; NADH and oxaloacetate inhibiting malate dehydrogenase). Products must be either easily transported from the matrix across the inner mt-membrane (e.g. malate formed from succinate via fumarate), or metabolized internally (e.g. malate-derived oxaloacetate forming citrate in the presence of pyruvate), i.e. the topic of MitoPathways Chapters 3 to 5.

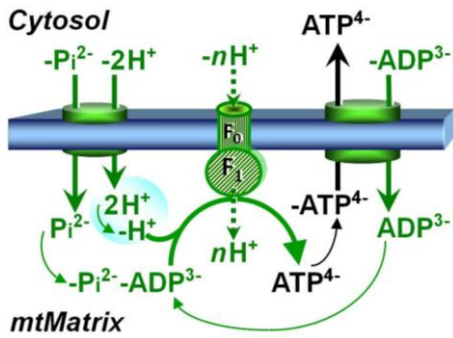


**Fig. 2.6. The phosphorylation system:** ATP synthase, adenine nucleotide translocator and phosphate carrier. OXPHOS is electron transfer (OX) coupled through the proton circuit across the inner mt-membrane to the phosphorylation of ADP to ATP (PHOS; Fig. 1.1). ATP, ADP and  $P_i$  are shown in a reference state of dissociation.

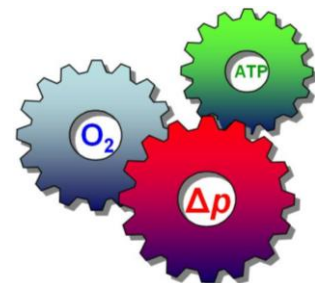
Tab. 2.2 summarizes the free and excess respiratory capacities which constitute the readouts of the coupling control protocol applied to mt-preparations (Fig. 2.3) versus the phosphorylation control protocol applied with intact cells (Fig. 1.2).

**Table 2.2. Free and excess capacities of respiration**, defined by respiratory states in mitochondrial preparations controlled by coupling and ADP, and in intact cells, at saturating oxygen levels and ETS competent substrate states.

Net flux	Symbol	Definition of net respiration	mt-Preparations	Intact cells
		Free (above $L$ ) or excess (above $P$ or $R$ ) capacity	ETS competent substrate states	Intracellular substrates, exogenous or endogenous
$P-L$	$\approx P$	Free OXPHOS capacity, coupled, $\Delta p_{mt}$ supports phosphorylation	Saturating ADP and $P_i$ ; or $J_{max}$ from ADP kinetics, baseline $L$	Difficulties to induce accurately defined state $P$ in intact cells
$R-L$	$\approx R$	Free ROUTINE activity, physiological control in the range from minimum $L$ (baseline) to maximum $P-L$ , variable $\Delta p_{mt}$	Limiting steady-state ADP levels simulating states of routine activity	Physiological control of cellular substrate uptake, intermediary metabolism and energy turnover
$E-L$	$\approx E$	Free ETS capacity, noncoupled, low but not zero $\Delta p_{mt}$	Optimal uncoupler concentration for maximum respiration	Optimal uncoupler concentration for maximum respiration
$E-P$	$ExP$	Excess $E-P$ capacity	See $\approx P$	See $\approx P$
$E-R$	$ExR$	Excess $E-R$ capacity	See $\approx R$	See $\approx R$

## 2.1. OXPHOS capacity

**P** OXPHOS capacity,  $P$ , is the respiratory capacity of mitochondria in the ADP-stimulated state of oxidative phosphorylation (OXPHOS), at saturating concentrations of ADP, inorganic phosphate, oxygen, and defined CHO substrates. OXPHOS involves chemiosmotic contrary to mechanistic coupling between electron transfer and the phosphorylation system. Mechanistic coupling is illustrated by a fully engaged clockwork gear wheel system. When loosening the fit of one gear wheel to the other, intrinsic uncoupling and dyscoupling lower the efficiency and contribute to the control of flux in the OXPHOS state (Fig. 2.7).





## OXPHOS capacity: saturating [ADP]

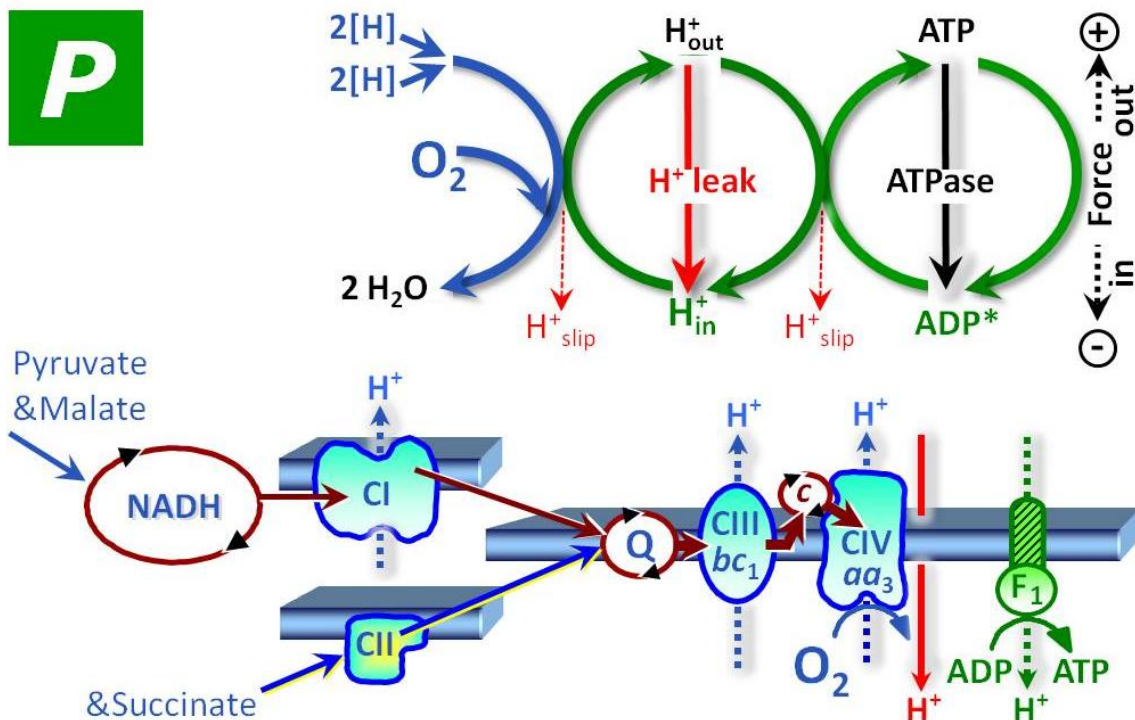


**Fig. 2.7. OXPHOS capacity:** Coupled energy cycles of oxidative phosphorylation stimulated by saturating concentrations of ADP and inorganic phosphate.  $2[H]$  indicates the reduced hydrogen equivalents of CHO fuel substrates and electron transfer to oxygen.  $H^+_{out}$  are protons pumped out of the matrix phase to the positive P-phase. Proton flow to the negative matrix phase ( $H^+_{in}$ ) drives the phosphorylation of ADP to ATP. The capacity of the phosphorylation system may contribute to the limitation of flux. Proton leaks dissipate energy of translocated protons from the P-phase to the negative N-phase. Measurement of OXPHOS capacity is possible in mt-preparations at saturating ADP, supported by an ETS-competent substrate state, exemplified as CI&II-linked substrate supply. For further explanations, see Fig. 1.1.

Mitochondria respiring at OXPHOS capacity generate a chemiosmotic force,  $\Delta p_{mt}$ , by proton pumping through CI, CIII and CIV.  $\Delta p_{mt}$  in turn fuels the ATP synthase to drive phosphorylation (coupled respiration), facilitates transport of charged molecules, and is partially dissipated (uncoupled respiration). In the OXPHOS state, therefore, mitochondria are in a **partially coupled** (loosely coupled) state (Fig. 2.7).

It is difficult to stimulate intact cells to maximum OXPHOS activity, since ADP and inorganic phosphate do not equilibrate across plasma membranes, and thus saturating concentrations of these metabolites can hardly be achieved in living cells. Selective permeabilization of cell membranes with maintenance of intact mitochondria provides a model for biochemical *cell ergometry* (Fig. 2.7; Fig. 5.3).



## Electron transfer system capacity

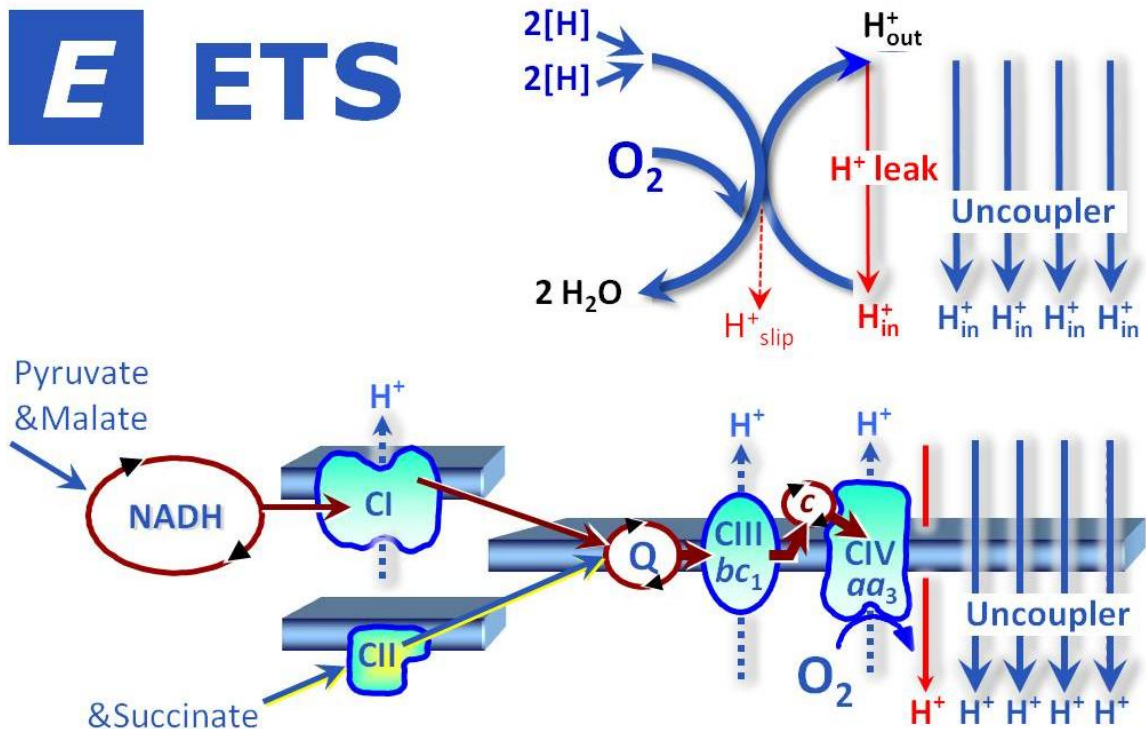


**Fig. 2.8. ETS capacity:** Noncoupled respiration with a shortcircuit of the proton cycle across the inner mt-membrane at optimum uncoupler (protonophore) concentration stimulating maximum oxygen flux. ETS capacity depends not only on the inner membrane-bound ETS (mETS; with respiratory Complexes CI to CIV, electron-transferring flavoprotein complex, CETF, and glycerophosphate dehydrogenase complex, CGpDH), but also integrates transporters across the inner mt-membrane, the TCA cycle and other mt-matrix dehydrogenases.

### 2.2. Electron transfer system capacity

**E** The capacity of the electron transfer system (ETS) is evaluated in an open-circuit operation of the transmembrane proton gradient. State *E* is established experimentally by uncoupler titrations using protonophores (uncouplers, CCCP, FCCP, DNP) at optimum concentrations for stimulation of maximum flux (*noncoupled* state) in intact cells (Fig. 1.2) or mt-preparations supported by an ETS-competent substrate state (Fig. 2.3). Protonophores do not uncouple electron transfer from proton translocation, but dissipate energy of translocated protons as a bypass of ATP synthesis (Fig. 2.6). In state *E* the mt-membrane potential is largely but not fully collapsed. Respiration is inhibited above optimum uncoupler concentrations. ETS potentially exceeds the OXPHOS capacity (Tab. 2.2) since it is not limited by the capacity of the phosphorylation system (uncontrolled state).



## ROUTINE respiration: intact cells

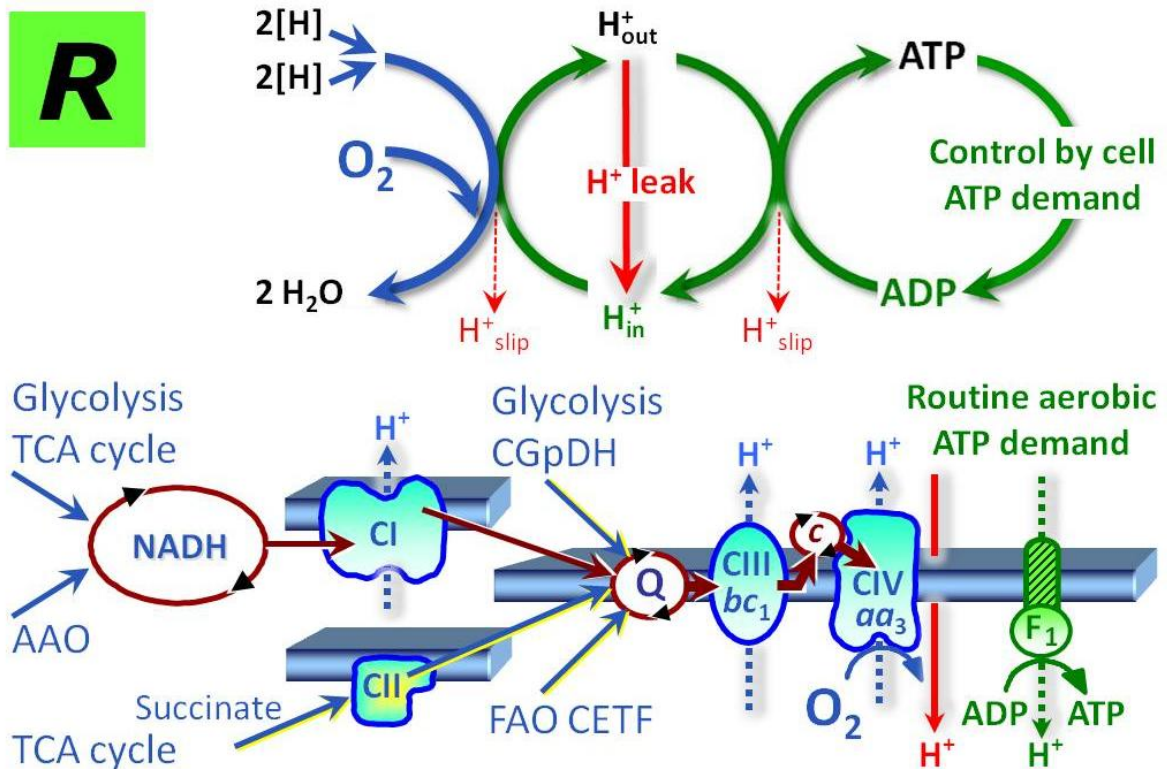


**Fig. 2.9. ROUTINE respiration:** Coupled energy cycles and proton circuit of mitochondrial respiration in intact cells controlled by aerobic ATP demand in the ROUTINE state of activity.  $2[H]$  indicates the reduced hydrogen equivalents of a variety of CHO energy substrates, from carbohydrates through glycolysis to the tricarboxylic acid cycle (TCA) and glycerophosphate dehydrogenase complex (CGpDH), amino acid oxidation (AAO) and fatty acid oxidation (FAO through the electron transferring flavoprotein complex, CETF). Compare Fig. 2.7.

### 2.3. ROUTINE respiration of the intact cell

**R** Cell respiration *in vivo* is regulated according to physiological activity, at intracellular non-saturating ADP levels in ROUTINE states of activity (Fig. 2.9).  $R$  increases under various conditions of activation. When incubated in culture medium, cells maintain a ROUTINE level of activity,  $C_R$  ( $C$ , intact cells;  $R$ , ROUTINE mitochondrial respiration; corrected for residual oxygen consumption due to oxidative side reactions; Fig. 1.2). ROUTINE activity may include aerobic energy requirements for cell growth and is thus fundamentally different from the definition of basal metabolic rate (BMR). When incubated for short experimental periods in a medium devoid of fuel substrates, the cells respire solely on endogenous substrates at the corresponding state of ROUTINE activity,  $C_eR$  ( $e$ , endogenous substrate supply).



## 2.4. LEAK respiration

**L** LEAK respiration compensates for proton leak, proton slip and cation cycling and is, to a small extent, influenced by electron leak linked to ROS production (Fig. 2.10). LEAK or *L* is an acronym beyond the proton leak and is measured as mitochondrial respiration in the presence of fuel substrate(s), absence of ADP, or after enzymatic inhibition of the phosphorylation system. The LEAK state is the *non-phosphorylating* resting state of intrinsic uncoupled or dyscoupled respiration when oxygen flux is minimized by the backpressure of a high chemiosmotic potential generated when ATP synthase is not active. At a given proton leak, *L* depends inversely on the  $H^+/O_2$  ratio and is thus lower for CI-linked compared to CII-linked electron flow. In state *L* at maximum protonmotive force, LEAK respiration is higher than the LEAK component contributing to ROUTINE respiration or OXPHOS capacity. Therefore, *R-L* or *P-L* represent the lower limit of free, phosphorylation-linked net oxygen consumption.

### LEAK respiration: dissipative

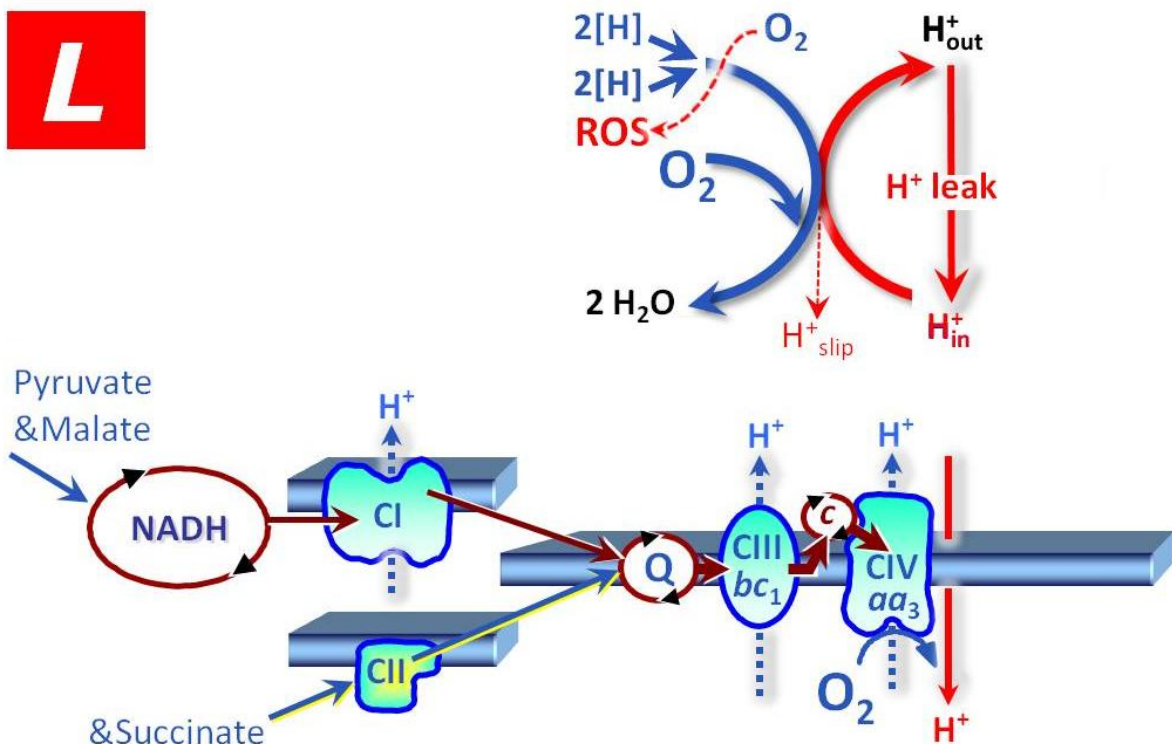


**Fig. 2.10. LEAK respiration:** Resting, non-phosphorylating electron transfer with a shortcircuit of the proton cycle across the inner mt-membrane due to intrinsic uncoupling or dyscoupling, but absence of utilization of the proton motive force for driving ATP synthesis. Proton leak (a property of the inner mt-membrane) dissipates energy of translocated protons, whereas proton slip prevents full translocation of protons across the inner mt-membrane (a property of the proton pumps).



Three experimental LEAK states can be distinguished, which may yield identical estimates of LEAK respiration or may show deviations that help to critically assess the proper protocol to be applied in specific cases. Two LEAK states are based on elimination of the substrate ADP for phosphorylation,  $L_N$  and  $L_T$ , with no adenylates and with ATP but no ADP, respectively. These ADP-limited LEAK states can be induced in mt-preparations but not in intact cells. Effective elimination of inorganic phosphate is more difficult to achieve, exerts additional effects on the control of  $\Delta p_{mt}$  and on substrate antiport, and is therefore not recommended in practice. In intact cells and all mt-preparations, inhibitors of specific components of the phosphorylation system can be applied which are permeable through cell and mt-membranes. Oligomycin, an inhibitor of ATPsynthase, is currently the most frequently applied inhibitor, inducing  $L_{Omy}$ .

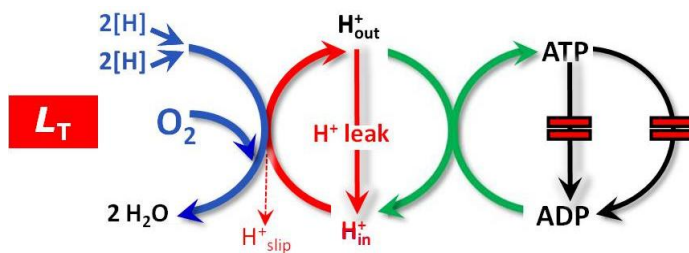


**Fig. 2.11.** The **LEAK state with ATP,  $L_T$** , is the classical State 4 in isolated mitochondria after phosphorylation of ADP to ATP is completed (Tab. 2.1).

*Application:* Highly purified Imt. Not in intact cells. Usually not suitable for permeabilized cells or tissues.

*Caution:*  $L_T$  represents intrinsic LEAK respiration only in the absence of ATPase activity, which would recycle ATP to ADP and thus stimulate coupled respiration. This is easily verified by unchanged respiration upon addition of high ATP in the absence of adenylates ( $L_N$  to  $L_T$  transition) or after inhibition of the phosphorylation system ( $L_T$  to  $L_{Omy}$  transition). ADP has to be phosphorylated to ATP without exhausting the oxygen content in the closed respirometer to zero. Hence 'high ADP' needs to be limited to concentrations  $<1$  mM, which in many cases is not saturating for measurement of OXPHOS even in isolated mitochondria. Assume the oxygen concentration to be  $\approx 200$   $\mu$ M  $O_2$  at air saturation, then oxygen would be completely exhausted until 1 mM ADP is phosphorylated to ATP at a P/ $O_2$  ratio of  $\approx 5$ .

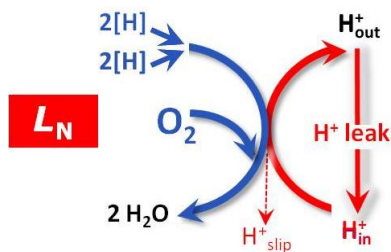


**Fig. 2.12.** The **LEAK state with no adenylates,  $L_N$**  (protocol Fig. 2.2B), is the state of substrate (ADP) limitation of the phosphorylation system, comparable to application of a specific inhibitor,  $L_{Omy}$ .

*Application:* All mt-preparations. Not in intact cells.

*Caution:* Residual and endogenous adenylates may stimulate respiration above the actual LEAK state, which may be checked by addition of oligomycin.

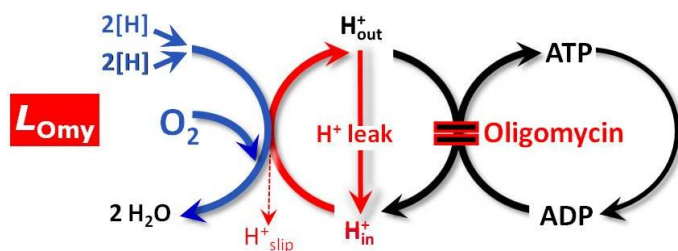


**Fig. 2.13.** In the **LEAK state with oligomycin**,  $L_{Omy}$ , the inhibitor of ATP synthase is used to inhibit the phosphorylation system.

*Application:*  $L_{Omy}$  is frequently used in intact cells,

permeabilized cells and permeabilized tissue preparations or homogenate. It is also applicable for Imt.

*Caution:* Permeabilized muscle fibres and intact yeast cells respond to  $Omy$  very slowly, in contrast to isolated mitochondria and various intact or permeabilized cells. Any subsequent measurements have to be evaluated very critically, since cell metabolism may be dysregulated with the effect of deterioration of respiratory capacity. Experimental artifacts are readily apparent when uncoupler titrations after  $L_{Omy}$  cannot even restore previous OXPHOS or ROUTINE levels of respiration.

## 2.5. Uncoupled - noncoupled - dyscoupled?

Is LEAK respiration *uncoupled*? (i) **Yes:** with respect to the **process**, LEAK respiration is not coupled (non-phosphorylating respiration). (ii) **No:** with respect to the **experimental state**,  $L$  and  $P$  are states of *coupled* mitochondria without addition of an uncoupler, in contrast to protonophore-stimulated ETS capacity measured in the *uncoupled* (noncoupled) state  $E$ . (iii) **Yes:** with respect to a **pathophysiological state**, in which coupling is lost,  $L$  and  $P$  can be observed in a state of *uncoupled* (dyscoupled) mitochondria. To address this confusing state, three different meanings of uncoupling (or coupling) are distinguished by defining intrinsically **uncoupled**, pathologically **dyscoupled**, and experimentally **noncoupled** states of respiration:

1. In the partially uncoupled (or partially coupled) state of respiration, *intrinsic uncoupling* under physiological conditions is a property of the inner mt-membrane (proton leak), proton pumps (proton slip; decoupling), and molecular uncouplers (uncoupling protein, UCP1).

2. *Dyscoupled* respiration under pathological and toxicological conditions is related to states of mitochondrial dysfunction. An explicit distinction is made between physiologically regulated uncoupling and pathologically defective dyscoupling (analogous to distinguishing eustress versus distress, function versus dysfunction). Physiological uncoupling and pathological dyscoupling are evaluated under experimental conditions as respiration in the LEAK state in relation to ETS capacity, i.e. the  $L/E$  coupling control ratio, or as ETS coupling efficiency,  $1-L/E$ .

3. *Noncoupled* respiration in the experimentally controlled uncoupled ( $\equiv$ noncoupled) state is induced by application of established uncouplers (protonophores), with the aim of obtaining a reference state with reduced mt-membrane potential, for evaluation of the respiratory capacity through the electron transfer system (ETS capacity; Fig. 2.8).



### 3. Residual oxygen consumption

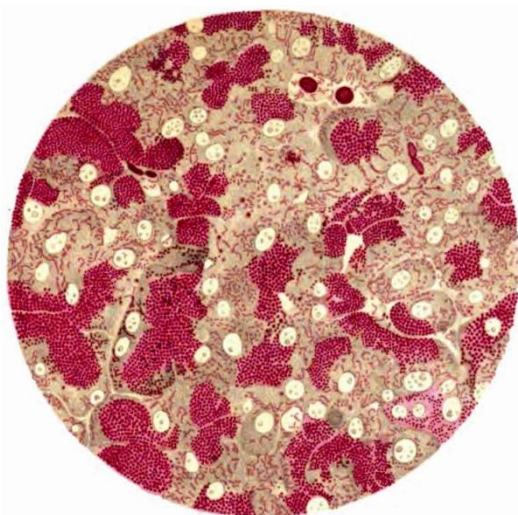
'KCN, H<sub>2</sub>S and CO combine with some of the components of oxidase forming an inactive compound, with the result that cytochrome, or at least its components a' and c', as well as paraphenylenediamine added to the cells, are not oxidised. The respiratory process can be still carried out through the medium of some autoxidisable carriers such as haemochromogens, haematins, the component b' of cytochrome, or some as yet unknown autoxidisable substances. This residual respiration, according to the nature of the cell, may represent a larger or smaller fraction of the total respiration of the cell.'

Keilin D (1929) Cytochrome and respiratory enzymes. Proc R Soc London Ser B 104: 206-52.

#### ROX

Residual oxygen consumption is the respiration due to oxidative side reactions remaining after application of ETS inhibitors acting downstreams of any fuel substrates supplied to mitochondrial preparations or cells, or in mt-preparations incubated without substrates. Mitochondrial respiration is frequently corrected for ROX, then distinguishing ROX-corrected ROUTINE, LEAK, OXPHOS or ETS (*P*, *E*, *R*, *L*) from the corresponding apparent fluxes that have not been corrected for ROX (*P'*, *E'*, *R'*, *L'*). When expressing ROX as a fraction of total respiration (flux control ratio), apparent flux not corrected for ROX should be taken as the reference. ROX may be related to, but is of course different from ROS production.

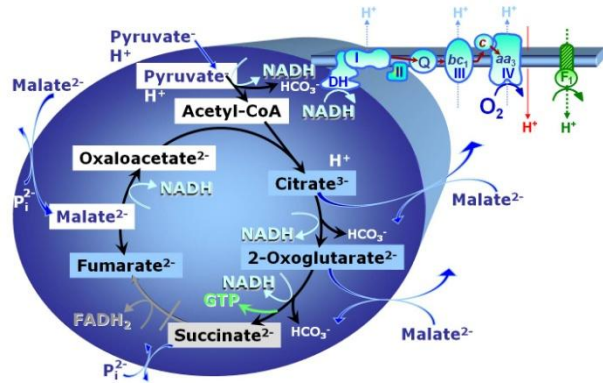
The original definition of State 2 (Tab. 2.1) is opposite to the state obtained in the absence of ADP but presence of fuel substrate (Fig. 2.10). State 2 is ROX. *'We have sought independent controls on whether State 2 corresponds to complete oxidation of the system. It is logical that this be so, for respiration is zero in State 2 because substrate, not phosphate acceptor, is limiting'* (Chance and Williams 1955). ROX in the absence of fuel substrate may be lower than ROX measured in the presence of inhibitors of the ETS (rotenone, malonic acid, antimycin A, myxothiazol) when various fuel substrates with or without uncoupler are added.



**Bioblaster.** *Left:* Richard Altmann (1894). *Right:* Odra Noel (2010) Homage to pioneers – Altmann's bioblast (Bioblast 2012).



## Chapter 3. Mitochondrial pathways to Complex I: respiratory substrate control with pyruvate, malate and glutamate



Section		Page
1. Malate, M.....	33	
2. Pyruvate & Malate, PM .....	34	
3. Glutamate, G .....	35	
4. Glutamate & Malate, GM .....	36	

Mitochondrial respiration depends on a continuous flow of fuel substrates and products across the mt-membranes between the matrix and cytosolic space. Glutamate and malate are anions which cannot permeate through the lipid bilayer of membranes and hence require carriers, which is also true for pyruvate. Anion carriers in the inner mt-membrane catalyze the transport of mitochondrial metabolites. Metabolite distribution across the mt-membrane varies mainly with  $\Delta\text{pH}$  and not  $\Delta\psi_{\text{mt}}$ , since most carriers (but not the glutamate-aspartate carrier) operate non-electrogenic by anion exchange or co-transport of protons.

Depending on the concentration gradients, these carriers also allow for the transport of mitochondrial metabolites from the mitochondria into the cytosol, or for the loss of intermediary metabolites into the incubation medium. Export of intermediates of the tricarboxylic acid (TCA) cycle plays an important metabolic role in the intact cell. This must be considered when interpreting the effect on respiration of specific substrates used in studies of mitochondrial preparations.

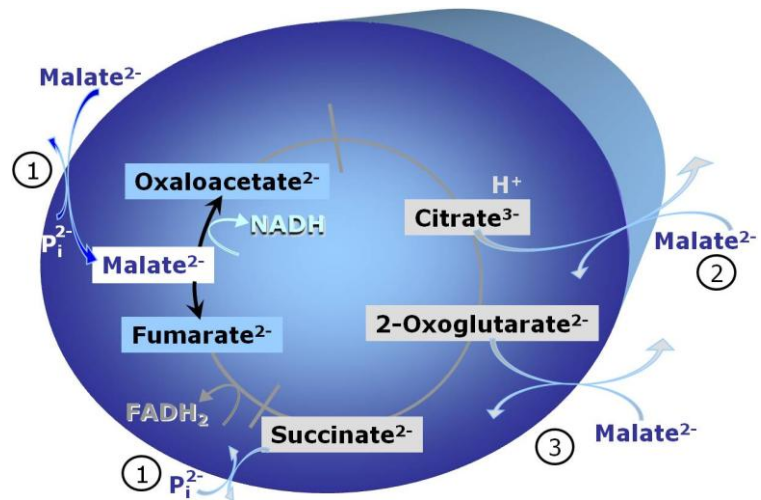
Substrate combinations of pyruvate&malate (PM) and glutamate&malate (GM) stimulate dehydrogenases with reduction of nicotinamide adenine dinucleotide (NADH), then feeding electrons into Complex I (NADH-UQ oxidoreductase) and down the thermodynamic cascade through the Q-cycle and Complex III of the electron transfer system to Complex IV and  $\text{O}_2$ .



## 1. Malate, M

OXPPOS capacity with malate alone is only 1.3% of that with pyruvate & malate in isolated rat skeletal muscle mitochondria.

**Fig. 3.1. Malate** alone does not support respiration of mt-preparations if oxaloacetate cannot be metabolized further in the absence of a source of acetyl-CoA. Transport of oxaloacetate across the inner mt-membrane is restricted particularly in liver. Mitochondrial citrate and 2-oxoglutarate ( $\alpha$ -ketoglutarate) are depleted by antiport with malate. Succinate is lost from the mitochondria through the dicarboxylate carrier.



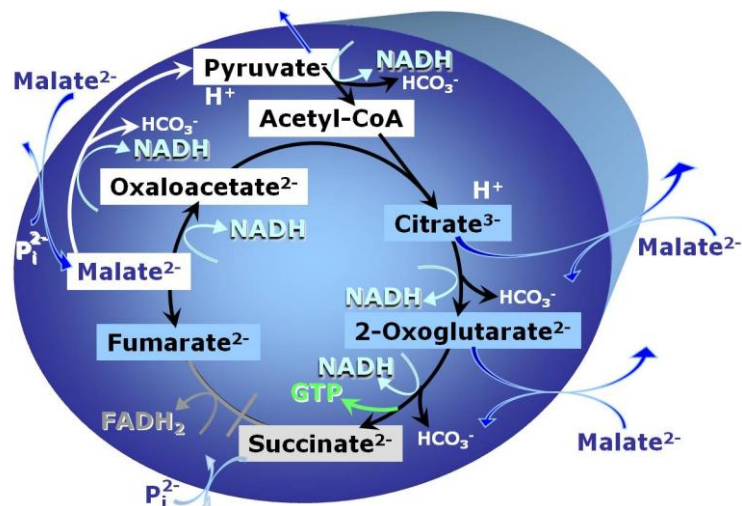
### Carriers for malate (malic acid, $C_4H_6O_5$ )

1. The dicarboxylate carrier catalyses the electroneutral exchange of malate<sup>2-</sup> or succinate<sup>2-</sup> for  $HPO_4^{2-}$ . It is more active in liver than heart mitochondria.
2. The tricarboxylate carrier exchanges malate<sup>2-</sup> for citrate<sup>3-</sup> or isocitrate<sup>3-</sup> (with co-transport of  $H^+$ ). It is highly active in liver, but low in heart mitochondria.
3. The 2-oxoglutarate carrier exchanges malate<sup>2-</sup> for 2-oxoglutarate<sup>2-</sup>.

Many mammalian and non-mammalian mitochondria have a mt-isoform of  $NADP^+$ - or  $NAD(P)^+$ -dependent malic enzyme (ME), the latter being particularly active in proliferating cells. Then malate alone can support high respiratory activities.

### Fig. 3.2. Malate and mt-malic enzyme.

Dismutation of malate by malate dehydrogenase (MDH) and mt-malic enzyme (mtME). Pyruvate accumulates in the medium or re-enters the TCA cycle via acetyl-CoA (PDH) and citrate synthase, thus re-entering oxaloacetate into the TCA cycle.





## 2. Pyruvate & Malate, PM

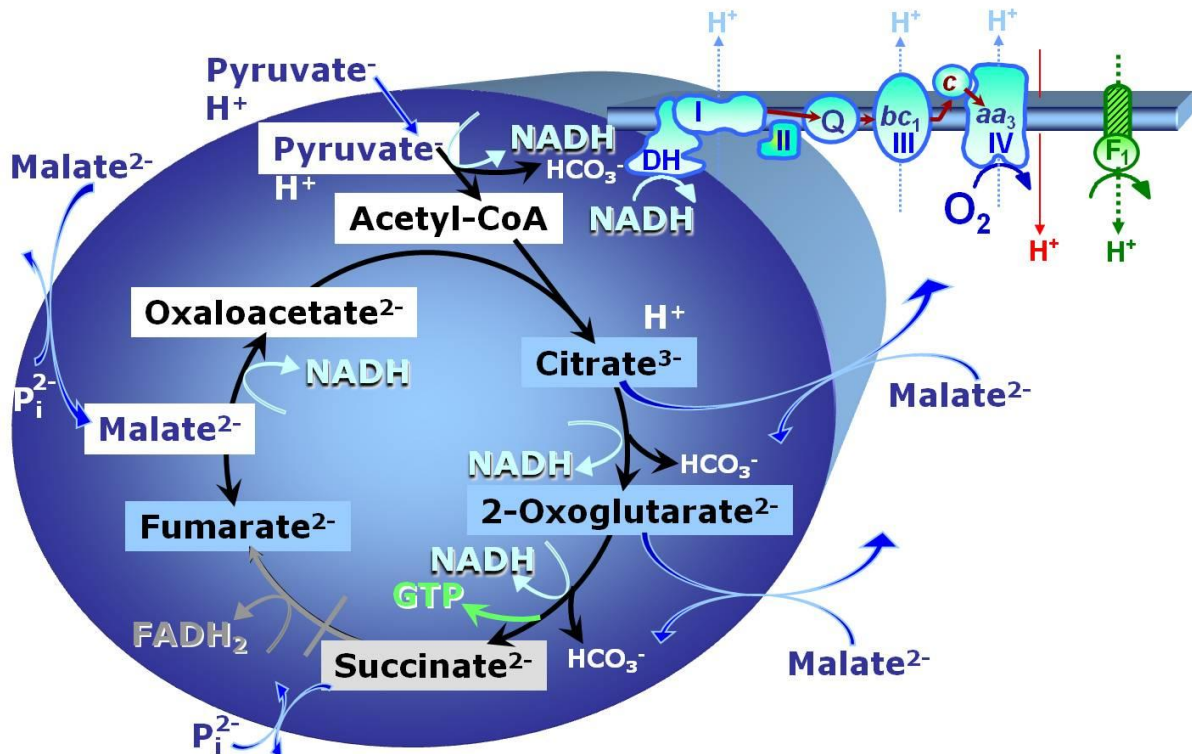


**Fig. 3.3. Pyruvate&malate (PM).** Oxidative decarboxylation of pyruvate is catalyzed by pyruvate dehydrogenase and yields acetyl-CoA. Malate dehydrogenase located in the mitochondrial matrix oxidises malate to oxaloacetate. Condensation of oxaloacetate with acetyl-CoA yields citrate (citrate synthase). 2-oxoglutarate ( $\alpha$ -ketoglutarate) is formed from isocitrate (isocitrate dehydrogenase).

### The pyruvate carrier (pyruvic acid, $C_3H_4O_3$ )

The monocarboxylic acid  $pyruvate^-$  is exchanged electroneutrally for  $OH^-$  by the pyruvate carrier.  $H^+$ /anion symport is equivalent to  $OH^-$ /anion antiport. Above a pyruvate concentration of 5 mM (compare Tab. A2.1), pyruvate transport across the membrane is partially noncarrier-mediated. Above 10 mM pyruvate, hydroxycinnamate cannot inhibit respiration from pyruvate.

Complex II is not or only to a small extent involved in respiration on pyruvate&malate (PM) in isolated mitochondria (Fig. 3.3). The malate-fumarate equilibrium is catalyzed by fumarase with an equilibrium ratio of malate to fumarate of 4.1 in mitochondrial incubation medium. High added malate concentrations, therefore, equilibrate with fumarate, which inhibits flux from succinate to fumarate, in addition to any inhibition of succinate dehydrogenase by oxaloacetate. This prevents formation of  $FADH_2$  in conjunction with the loss of 2-oxoglutarate and succinate into the medium. Due to the high activity of the tricarboxylate carrier in liver mitochondria, citrate is lost from the mitochondria in exchange for malate, before it can be oxidised. Taken together, these were the arguments of using high malate concentrations (2 mM; compare Tab. A2.1), particularly



in studies of  $\sim P/O$  ratios through Complex I. Malonate may be added to inhibit the succinate-fumarate reaction, which exerts only a minor effect on liver mitochondrial respiration. Pyruvate alone yields only 2.1% of OXPHOS capacity with PM in rat skeletal muscle mitochondria.

Uncoupling stimulates coupled OXPHOS respiration,  $PM_p$ , with an apparent excess  $E-P$  capacity relative to  $E$  of 0.15 in human vastus lateralis and rat skeletal muscle, 0.35 to 0.40 in human heart and NIH3T3 fibroblasts, but essentially zero in mouse skeletal muscle (Fig. 5.3).

### 3. Glutamate, G

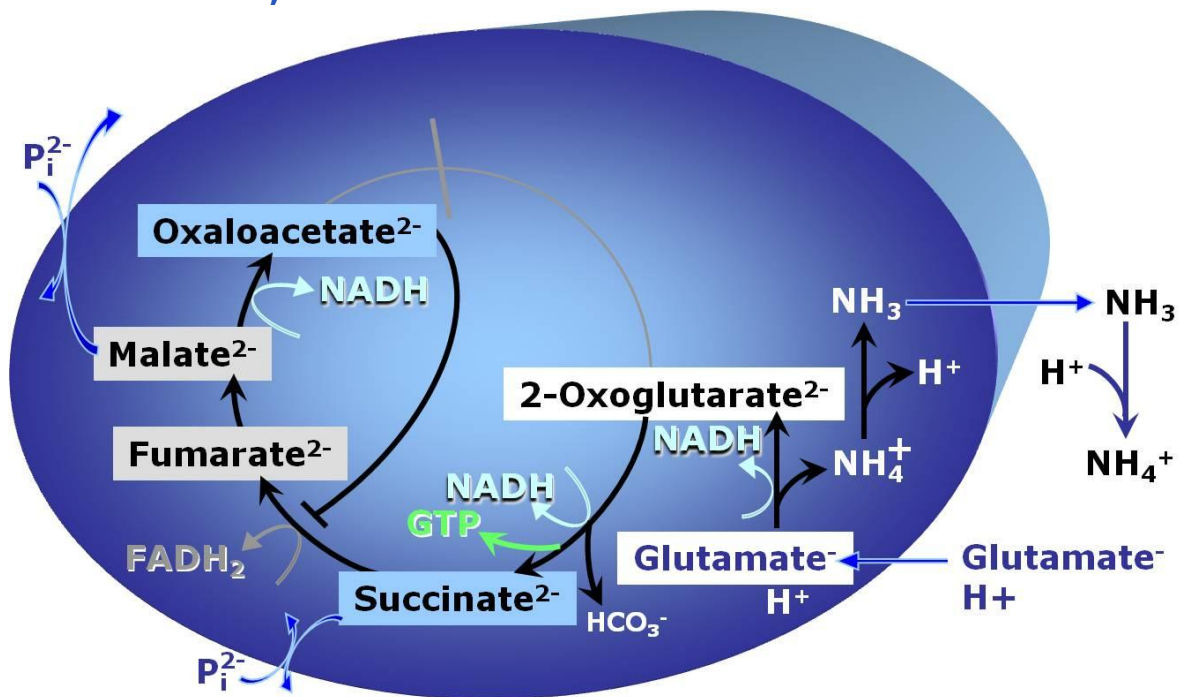


**Fig. 3.4. Glutamate** as the sole fuel substrate is transported by the electroneutral glutamate<sup>-</sup>/OH<sup>-</sup> exchanger, and is oxidised via glutamate dehydrogenase in the mitochondrial matrix. Ammonia can pass freely through the mitochondrial membrane. Compare with Fig. 3.5.

#### Carriers for glutamate (glutamic acid, C<sub>5</sub>H<sub>9</sub>NO<sub>4</sub>)

1. The glutamate-aspartate carrier catalyzes the electrogenic antiport of glutamate<sup>-</sup>+H<sup>+</sup> for aspartate<sup>-</sup>. It is an important component of the malate-aspartate shuttle in many mitochondria. Due to the symport of glutamate<sup>-</sup>+H<sup>+</sup>, the glutamate-aspartate antiport is not electroneutral and may be impaired by uncoupling. Aminooxyacetate is an inhibitor of the glutamate-aspartate carrier.
2. The electroneutral glutamate<sup>-</sup>/OH<sup>-</sup> exchanger is present in liver and kidney mitochondria.

In human skeletal muscle mitochondria, OXPHOS capacity with glutamate alone (Fig. 3.4) is 50% to 85% of respiration with glutamate&malate (Fig. 3.6). Accumulation of fumarate inhibits succinate dehydrogenase and glutamate dehydrogenase.

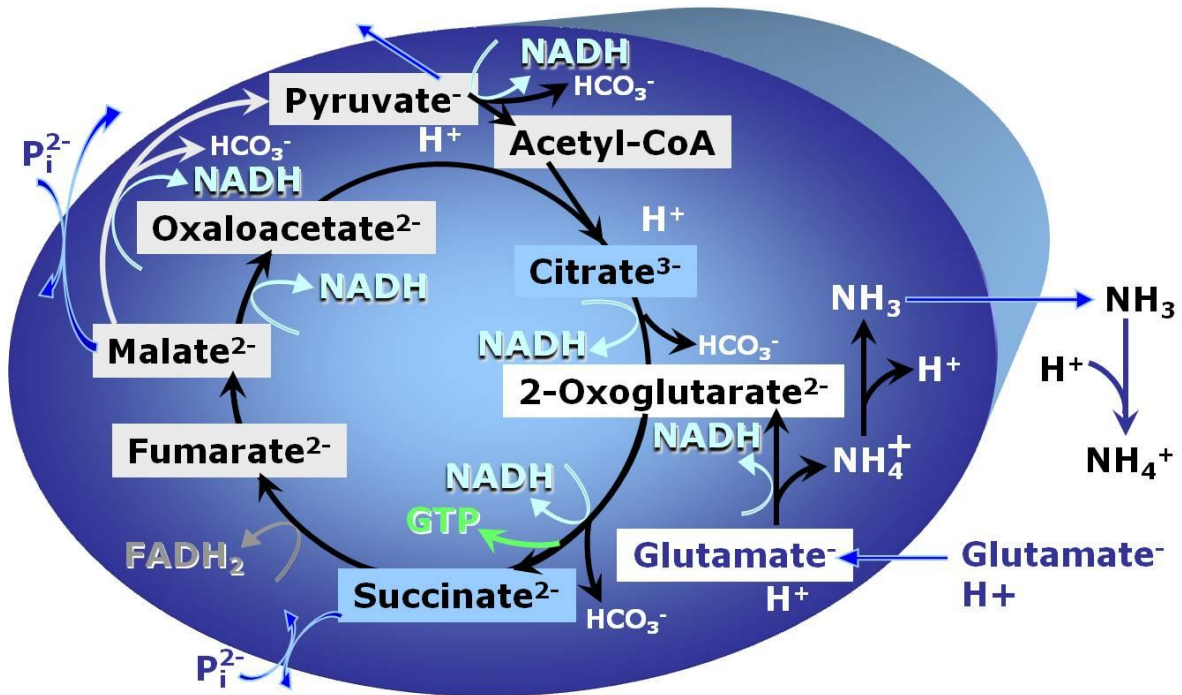


**Fig. 3.5. Glutamate and mt-malic enzyme.** Glutamate derived from hydrolyzation of glutamine is an important aerobic substrate in cultured cells. Mitochondrial glutamate dehydrogenase is particularly active in astrocytes, preventing glutamate induced neurotoxicity. mtNAD-malic enzyme supports an anaplerotic pathway when carbohydrate is limiting.

**4. Glutamate & Malate, GM**

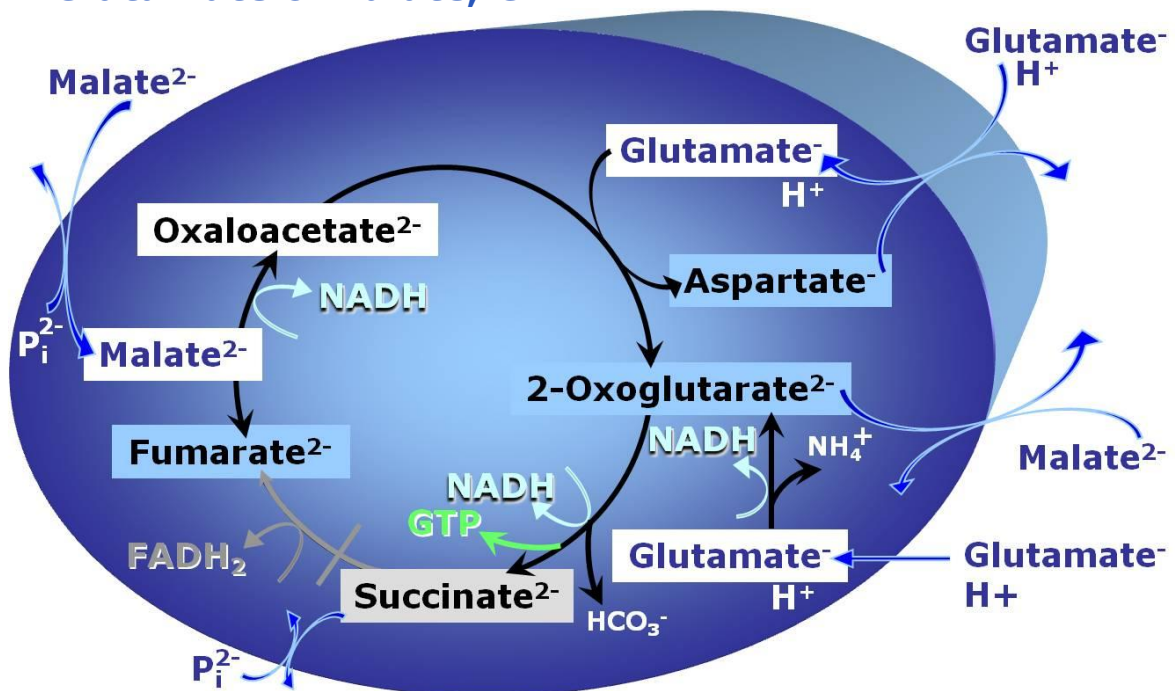


**Fig. 3.6. Glutamate&malate (GM).** When glutamate&malate are added to isolated mitochondria or permeabilized cells, glutamate and transaminase are responsible for the metabolism of oxaloacetate, comparable to the metabolism with acetyl-CoA and citrate synthase (Fig. 3.3).



In human skeletal muscle mitochondria, respiration with glutamate&malate (Fig. 3.6) in the presence of ADP ( $GM_p$ ) is identical or 10% higher than with pyruvate&malate ( $PM_p$ ). These results on isolated mitochondria agree with permeabilized fibres, although there are reports on respiratory capacity for  $PM_p$  being 16% to 25% higher than for  $GM_p$ . In fibroblasts,  $GM_p$  supports a higher respiratory flux than  $PM_p$ .

The  $PM_p/GM_p$  flux ratio shifts from  $<1$  in white muscle to  $>1$  in red skeletal muscle fibres from turkey. In rat heart mitochondria, respiration is 33% higher for  $GM_p$  compared to  $PM_p$ , and OXPHOS with succinate and rotenone is marginally higher than with GM. 2-Oxoglutarate efflux with GM is limited at low malate concentrations, and is half-maximal at 0.36 mM. Glutamate&malate support a higher OXPHOS respiration ( $GM_p$ ) than  $PM_p$  in rat liver mitochondria. The  $PM_p/GM_p$  ratio is strongly temperature dependent in permeabilized mouse heart fibres. Taken together, this suggests that a critical evaluation is required for interpreting CI-linked respiration on a particular substrate in terms of limitation by Complex I.

Uncoupling stimulates respiration above OXPHOS in human skeletal and cardiac muscle mitochondria, whereas respiration is not under the control of the phosphorylation system in mouse skeletal and cardiac muscle and red fibre type pigeon breast muscle mitochondria.  $GM_p$  is severely limited by the phosphorylation system in fibroblasts, since uncoupling exerts a strong stimulation above maximally ADP-stimulated respiration (compare Fig. 5.3).

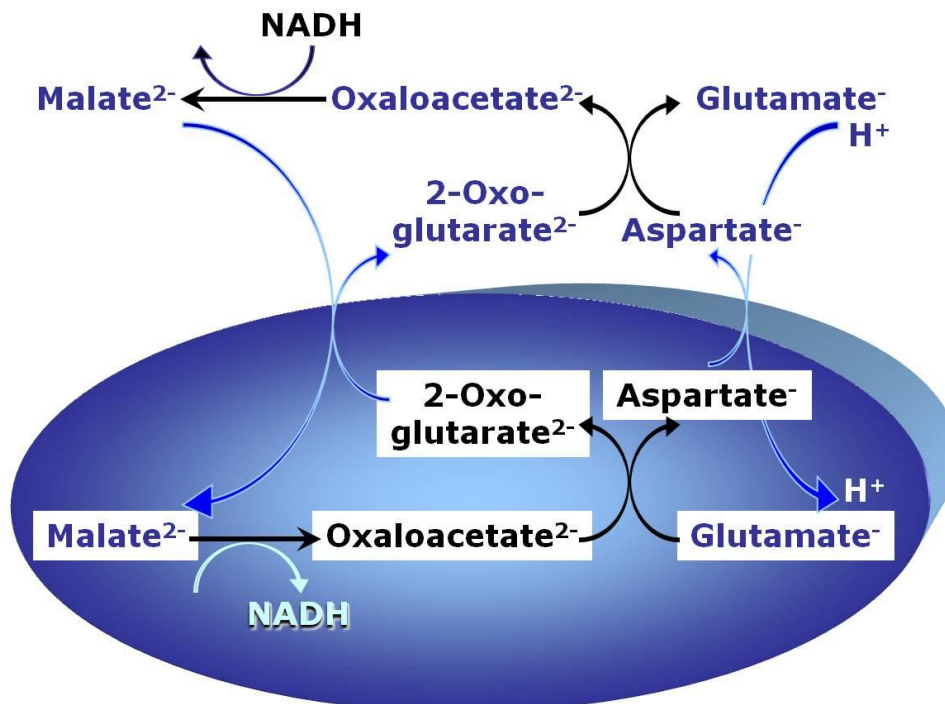


**Fig. 3.7. The malate-aspartate shuttle** involves the glutamate-aspartate carrier and the 2-oxoglutarate carrier exchanging malate<sup>2-</sup> for 2-oxoglutarate<sup>2-</sup>. Cytosolic and mitochondrial malate dehydrogenase and transaminase complete the shuttle for the transport of cytosolic NADH into the mitochondrial matrix. It is most important in heart, liver and kidney.



The overall reaction stoichiometry of the malate-aspartate shuttle is (Fig. 3.7):



After transamination in the cytosol (Fig. 3.8),



The net reaction is,



At high cardiac workload, the 2-oxoglutarate-malate transporter cannot effectively compete for the same substrate of the 2-oxoglutarate dehydrogenase, thus limiting the activity of the malate-aspartate shuttle and transfer of cytosolic NADH into the mitochondria, reducing the cytosolic glutamate pool, and activating cytosolic reoxidation of NADH through lactate production despite sufficient oxygen availability. Regulation of cytosolic NADH levels by the glutamate-aspartate carrier is implicated in glucose-stimulated insulin secretion in beta-cells.

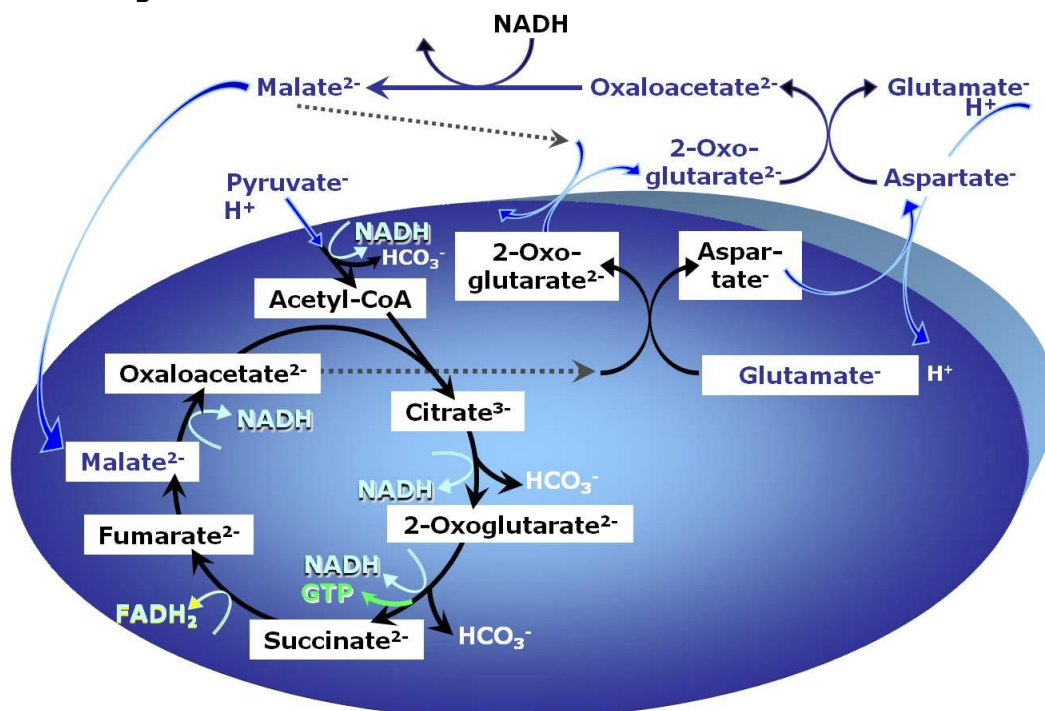
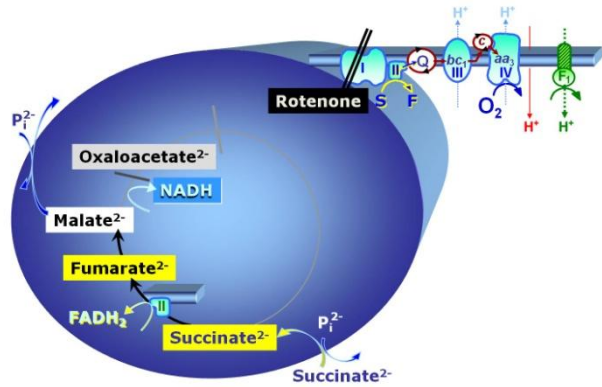


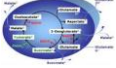
**Fig. 3.8. Malate-aspartate shuttle in the intact cell.** Cytosolic NADH is utilized for respiration at the cost of a proton transported along the electrochemical gradient back into the mitochondrial matrix. This reduces the effective  $\sim P/O$  ratio.





## Chapter 4. Mitochondrial pathways to Complexes II, glycerophosphate dehydrogenase and electron-transferring flavoprotein



Section		Page
	1. Succinate and Rotenone, S(Rot) .....	39
	2. Succinate, S .....	40
	3. Glycerophosphate, Gp .....	42
	4. Electron-transferring flavoprotein, CETF .....	42

Complex II (CII) is the only membrane-bound enzyme in the tricarboxylic acid cycle (TCA) and is part of the electron transfer system. The flavoprotein succinate dehydrogenase (SDH) is the largest polypeptide of CII, located on the matrix face of the inner mt-membrane. Following succinate oxidation, CII transfers electrons to the quinone pool. Whereas reduced NADH is a *substrate* of Complex I linked to dehydrogenases of the TCA cycle and mt-matrix *upstream* of CI, reduced FADH<sub>2</sub> is a *product* of Complex II with *downstream* electron flow from CII to Q. NADH and succinate (not FADH<sub>2</sub>) are the comparable substrates of CI and CII.

### 1. Succinate and Rotenone, S(Rot)

Succinate, S(Rot), supports electron flux through CII via flavin adenine dinucleotide (FADH<sub>2</sub>). After inhibition of CI by rotenone, the NADH-linked dehydrogenases become inhibited by the redox shift from NAD<sup>+</sup> to NADH (Fig. 4.1). Succinate dehydrogenase is activated by succinate and ATP, which explains in part the time-dependent increase of respiration in isolated mitochondria after addition of rotenone (first), succinate and ADP.

#### Carrier for succinate (succinic acid, C<sub>4</sub>H<sub>6</sub>O<sub>4</sub>)

The dicarboxylate carrier catalyses the electroneutral exchange of succinate<sup>2-</sup> for HPO<sub>4</sub><sup>2-</sup>, and accumulation of malate is also prevented by exchange of malate and inorganic phosphate.

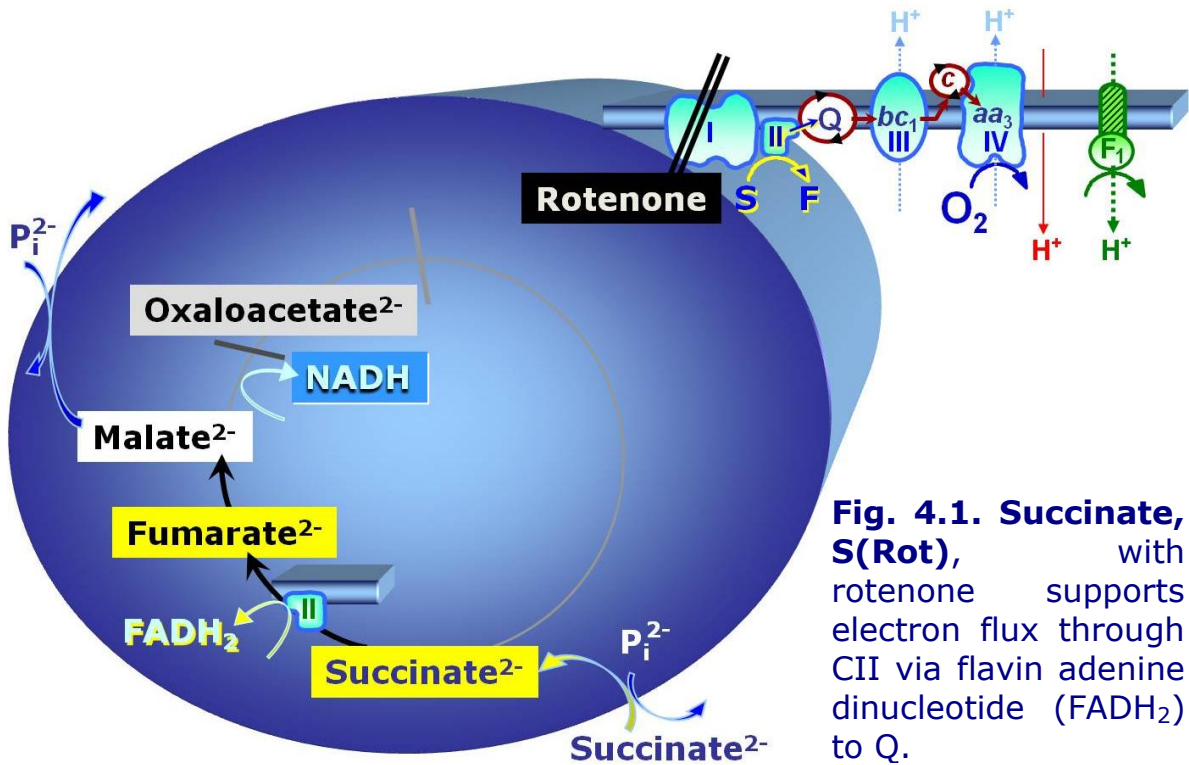


**Fig. 4.1. Succinate, S(Rot),** with rotenone supports electron flux through CII via flavin adenine dinucleotide (FADH<sub>2</sub>) to Q.

**2. Succinate, S**

When succinate is added without rotenone (Fig. 4.2), oxaloacetate is formed from malate by the action of malate dehydrogenase. Oxaloacetate accumulates and is a more potent competitive inhibitor of succinate dehydrogenase than malonate even at small concentration. Reverse electron flow from CII to CI is known to stimulate production of reactive oxygen species under these conditions to extremely high, nonphysiological

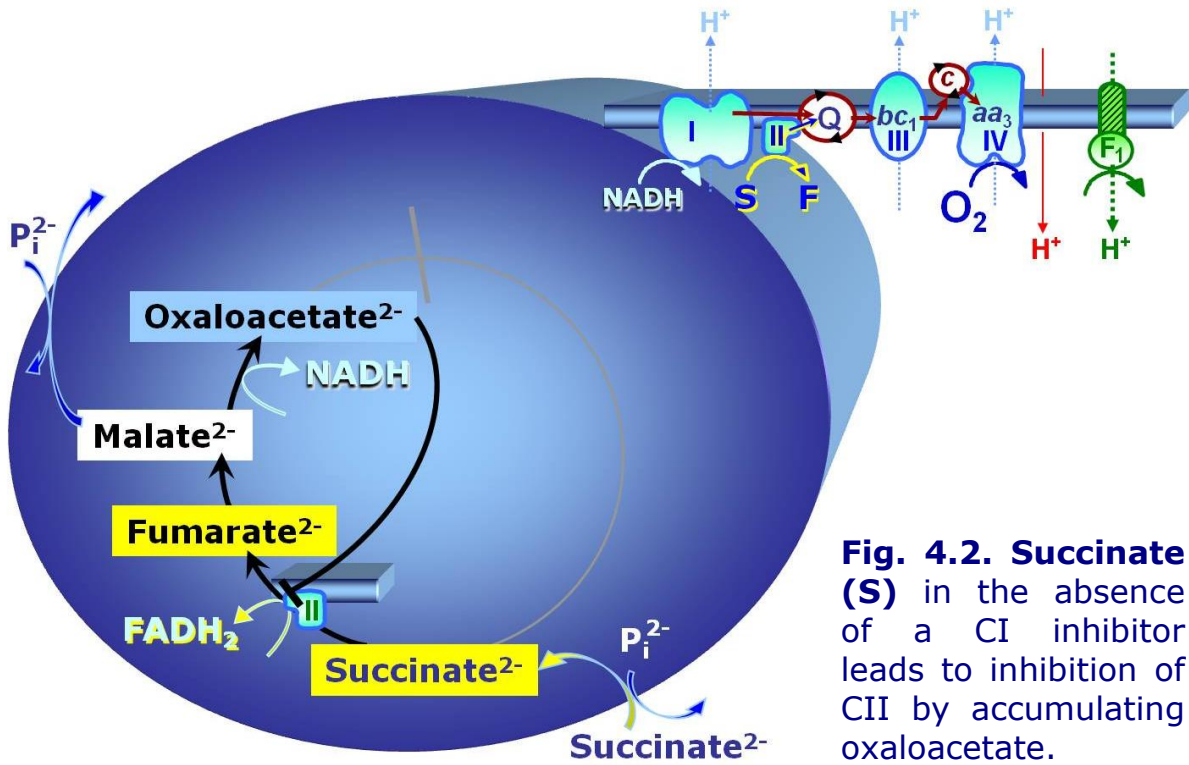


**Fig. 4.2. Succinate (S)** in the absence of a CI inhibitor leads to inhibition of CII by accumulating oxaloacetate.

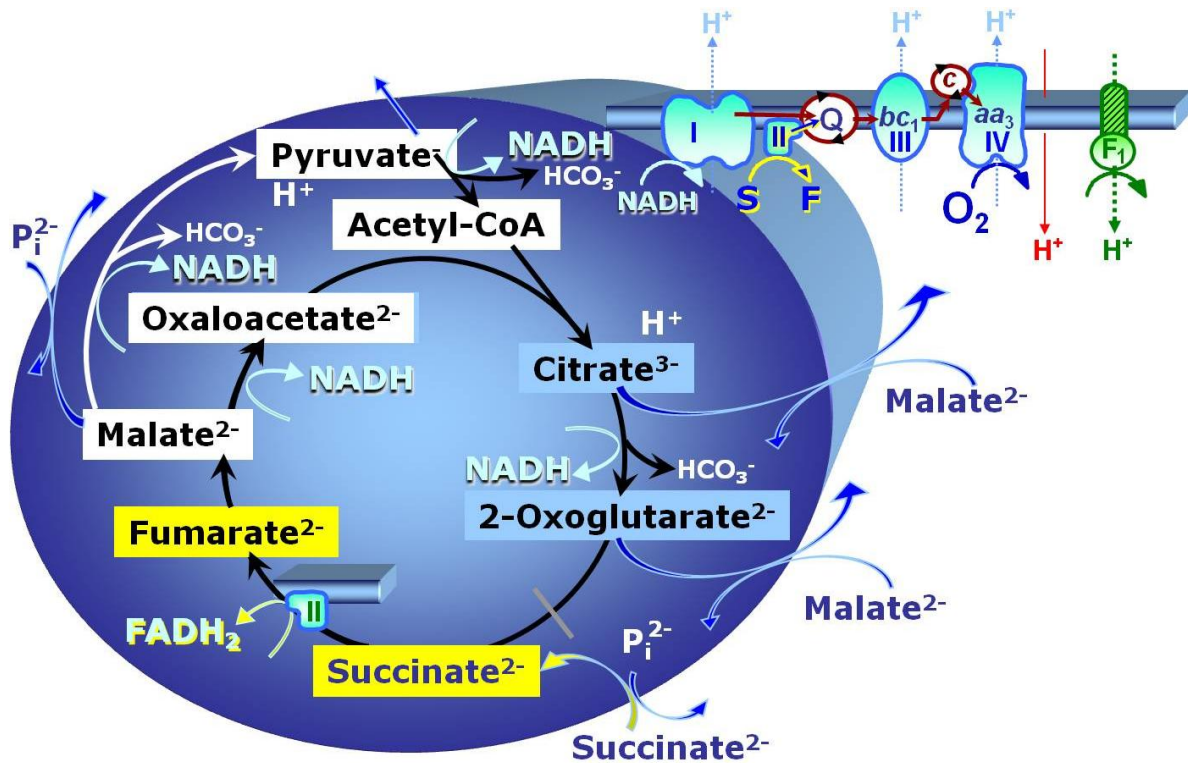


**Fig. 4.3. Succinate and mtME.** mt-Malic enzyme (mtME) catalyzes the formation of pyruvate from malate. Acetyl-CoA from pyruvate (PDH) is then available for removal of oxaloacetate through citrate synthase, thus preventing or reducing inhibition of succinate dehydrogenase by oxaloacetate.

levels. Addition of malate reduces superoxide production with succinate, probably due to a shift in the redox state and oxaloacetate inhibition of CII.

OXPHOS capacity with succinate alone,  $S_D$ , is 30-40% lower than flux with succinate and rotenone,  $S(\text{Rot})_D$ , in human and rat skeletal muscle mitochondria, due to inhibition of succinate dehydrogenase by accumulating oxaloacetate. This is similar in mammalian liver, where <10% of malic enzyme is cytosolic.

Conditions with succinate as the sole substrate are different if mt-malic enzyme plays a significant role, as is the case in proliferating cells. Measurement of the  $\sim P/O_2$  ratio in CII-linked respiration with and without rotenone provides an indication of the extent to which CI is stimulated by NADH, which is generated through the mtME and PDH pathway in parallel with formation and removal of oxaloacetate through the MDH-CS pathway. The exported malate may be too dilute for an active antiport against citrate and 2-oxoglutarate (Fig. 4.3; compare malate with mtME in Fig. 3.2). However, generation of NADH in the presence of mtME activity will counteract reverse CII to CI electron transfer and thus play an important role in the regulation of ROS production under these experimental conditions.



### 3. Glycerophosphate, Gp

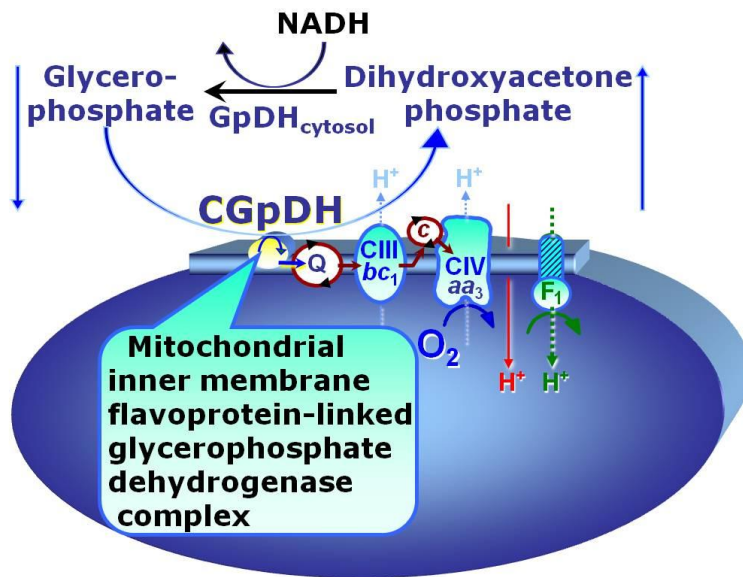


**Fig. 4.4. The glycerophosphate shuttle** represents an important pathway, particularly in liver, of making cytoplasmic NADH available for mitochondrial oxidative phosphorylation. Cytoplasmic NADH reacts with dihydroxyacetone phosphate catalyzed by cytoplasmic glycerophosphate dehydrogenase. On the outer face of the inner mitochondrial membrane,

mitochondrial glycerophosphate dehydrogenase oxidises glycerophosphate back to dihydroxyacetone phosphate, a reaction not generating NADH but reducing a flavin prosthetic group. The reduced flavoprotein donates its reducing equivalents to the electron transfer system at the level of CoQ.

Glycerophosphate oxidation (Fig. 4.4) is 10-fold higher in rabbit gracilis mitochondria (fast-twitch white muscle; 99% type IIb) compared to soleus (slow-twitch red muscle; 98% type I). Activity is comparatively low in human vastus lateralis. Glycerophosphate is an important substrate for respiration in brown adipose tissue mitochondria.

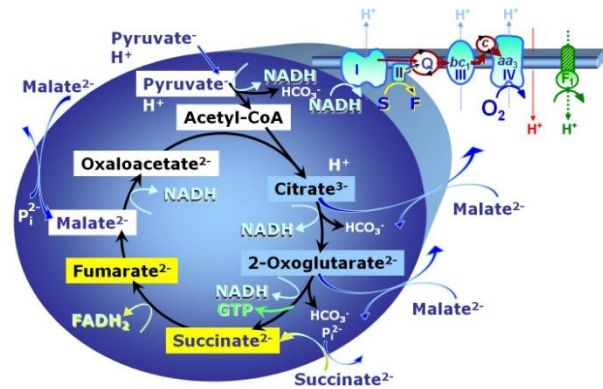
### 4. Electron-transferring flavoprotein complex

Electron-transferring flavoprotein complex (ETF) is located on the matrix face of the inner mt-membrane, and supplies electrons from fatty acid  $\beta$ -oxidation (FAO) to CoQ. FAO cannot proceed without a substrate combination of fatty acids & malate, and inhibition of CI blocks FAO completely. Fatty acids are split stepwise into two carbon fragments forming acetyl-CoA, which enters the TCA cycle by condensation with oxaloacetate (CS reaction). Therefore, FAO implies simultaneous electron transfer into the Q-junction through ETF and CI (Fig. 5.4).

Fatty acids (short chain with 4–8, medium-chain with 6–12, long chain with 14–22 carbon atoms) are activated by fatty acyl-CoA synthases (thiokinases) in the cytosol. The outer mt-membrane enzyme carnitine palmitoyltransferase 1 (CPT-1) generates an acyl-carnitine intermediate for transport into the mt-matrix. Octanoate but not palmitate (eight- and 16-carbon saturated fatty acids) may pass the mt-membranes, but both are frequently supplied to mt-preparations in the activated form of octanoylcarnitine or palmitoylcarnitine.



# Chapter 5. Mitochondrial pathways to Complexes I & II: convergent electron transfer at the Q-junction and additive effect of substrate combinations



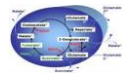
'..the O<sub>2</sub> uptake of intact cells represents the global result of the activity of several respiratory systems.'

Keilin D (1929) Cytochrome and respiratory enzymes. Proc R Soc London Ser B 104: 206-52.

'It is not at all easy to draw a sharp line between cases where what is happening could be called "addition", and where some other word is wanted.'

Douglas R Hofstadter (1979) Gödel, Escher, Bach: An eternal golden braid. A metaphorical fugue on minds and machines in the spirit of Lewis Carroll. Penguin Books.

Section	1. Electron transfer system and ET chain .....43	Page
	2. Historical perspectives .....46	
	3. Pyruvate&Glutamate&Malate, PMG .....53	
	4. Pyruvate&Malate&Succinate, PMS .....53	
	5. Glutamate&Malate&Succinate, GMS .....54	
	6. Pyruvate&Malate&Glutamate&Succinate, PMGS .....56	
	7. Additive effect of Gp and FAO.....56	
	8. Implications .....57	



## 1. Electron transfer system and ET chain

The term 'electron transfer chain' (or electron transport chain, ETC) is a misnomer. Understanding mitochondrial respiratory control has suffered greatly from this inappropriate terminology, although textbooks using the term ETC make it sufficiently clear that electron transfer systems are not arranged as a chain: the 'ETC' is in fact not a simple chain but an arrangement of electron transfer complexes in a non-linear, convergent electron transfer system (ETS; Fig. 5.1).

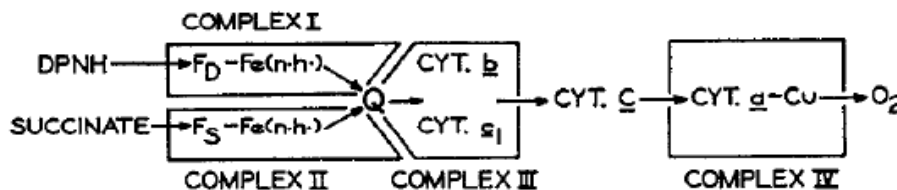


**Fig. 5.1. Electron transfer system:** The four primary Complexes and their arrangement in the electron transfer system (Hatefi et al 1962). DPNH is NADH.

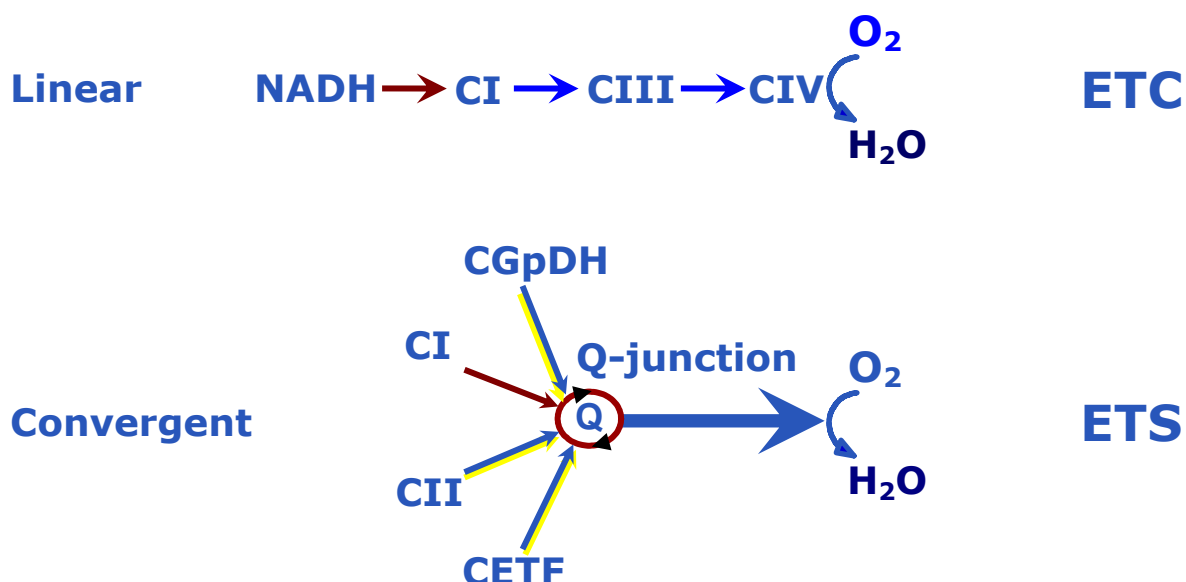


**Fig. 5.2. ETC vs ETS.** Electron transfer chain (ETC, linear) versus electron transfer system (ETS, convergent). CI to CIV, Complex I to IV; CGpDH, glycerophosphate dehydrogenase complex; CETF, electron-transferring flavoprotein complex. Electron gating (ETC) limits flux upstream if convergent electron supply exerts an additive effect on ETS capacity.

The convention of defining the electron transfer chain as being comprised of four respiratory complexes has conceptual weaknesses. (a) In fact, there are at least six Complexes of mitochondrial electron transfer: In addition to Complexes I and II, the Complexes glycerophosphate dehydrogenase (CGpDH) and electron-transferring flavoprotein (CETF) are involved in electron transfer to Q and Complex III (Fig. 5.2). (b) The term 'chain' suggests a linear sequence, whereas the functional structure of the electron transfer system can only be understood by recognizing the convergence of electron flow at the Q-junction, followed by a chain of Complexes III and IV, mediated by cytochrome c (Fig. 5.1 and 5.2).

Electrons flow to oxygen from either Complex I (CI) with a total of three coupling sites, or from Complex II (CII) and other flavoproteins, providing multiple entries into the Q-cycle with two coupling sites downstream. A novel perspective of mitochondrial physiology and respiratory control by simultaneous supply of various fuel substrates emerged from a series of studies based on high-resolution respirometry. Substrate-uncoupler-inhibitor-titration (SUIT) protocols for real-time OXPHOS analysis (Fig. 5.3) are based on a biochemical analysis of convergent pathways comprising the mitochondrial electron transfer system (Fig. 5.4). When the TCA cycle is in full operation in the intact cell with influx of pyruvate, electron flow into the Q-junction converges according to a NADH:succinate ratio of 4:1 (Fig. 5.4). SUIT protocols are designed for reconstitution of TCA cycle function and sequential separation of branches of mitochondrial pathways for OXPHOS analysis.

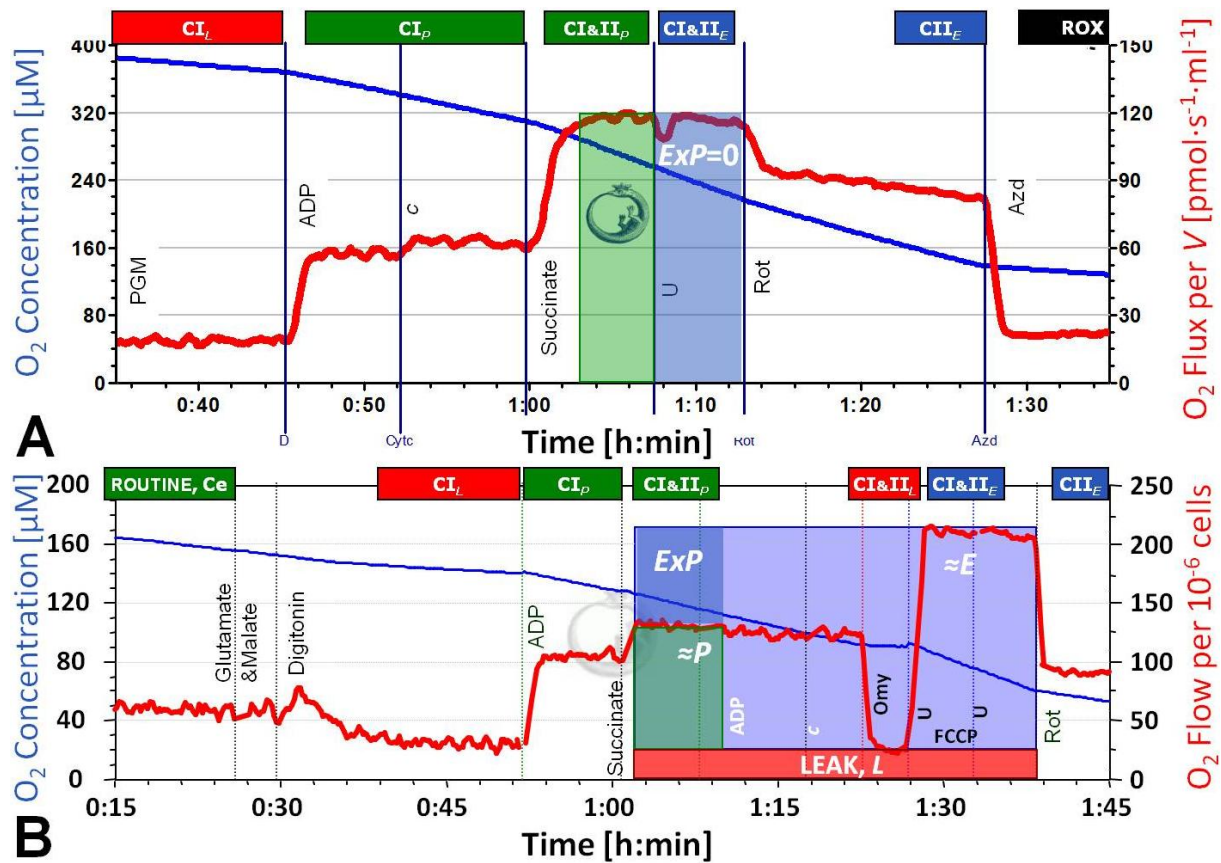


**Fig. 5.3. SUIT protocols for OXPHOS analysis.** Multiple substrate-inhibitor protocols for high-resolution respirometry in permeabilized muscle fibres and permeabilized cells. Measurements at 37 °C in the 2 ml chamber of the OROBOROS Oxygraph-2k in mitochondrial respiration medium (MiRO5). Blue lines: O<sub>2</sub> concentration [μM]; red lines: O<sub>2</sub> flux or flow. **A:** Permeabilized mouse skeletal muscle fibres: PGM<sub>N</sub>+D+c+S+U+Rot+Azd. PGM pyruvate & glutamate & malate, c cytochrome c, S succinate, U FCCP, Rot rotenone, Azd azide. Succinate stimulates flux two-fold (CI/CI&II=0.5), and the phosphorylation system is not limiting (zero excess E-P capacity, ExP=0) (IOC39). **B:** NIH3T3 fibroblasts; 0.24·10<sup>6</sup> cells/ml (I<sub>O2</sub> [pmol O<sub>2</sub>·s<sup>-1</sup>·10<sup>-6</sup> cells]): C<sub>e</sub>+GM+Dig→GM<sub>N</sub>+D+S+c+Omy+U+Rot+Ama. After ROUTINE endogenous respiration, glutamate&malate (GM) were added, and cells were permeabilized by digitonin, inducing state GM<sub>N</sub> (LEAK; L<sub>N</sub>, no adenylates). ADP (1 mM) stimulated respiration inducing state GM<sub>P</sub> (OXPHOS). Succinate (S) increased respiration with convergent CI&II electron input (GMS<sub>P</sub>). 3 mM ADP and 10 μM cytochrome c were without stimulatory effect (GMS<sub>C<sub>P</sub></sub>). After inhibition by oligomycin (L<sub>Omy</sub>; LEAK state GMS<sub>L</sub>), stimulation by FCCP (ETS state GMS<sub>E</sub>) indicated strong limitation of OXPHOS by the phosphorylation system and a correspondingly high excess ETS-OXPHOS capacity, ExP=E-P. Thus the free ETS capacity (≈E=E-L) is nearly twice as high as the free OXPHOS capacity (≈P=P-L), comparable to human cardiac mitochondria (Fig. 5.8) Inhibition by rotenone (Rot) revealed a low capacity of respiration on succinate alone, ETS state S(Rot)<sub>E</sub>: the CII/CI&II substrate control ratio was less than 0.5. These SUIT protocols reveal highly divergent OXPHOS fingerprints in the two types of mitochondria.

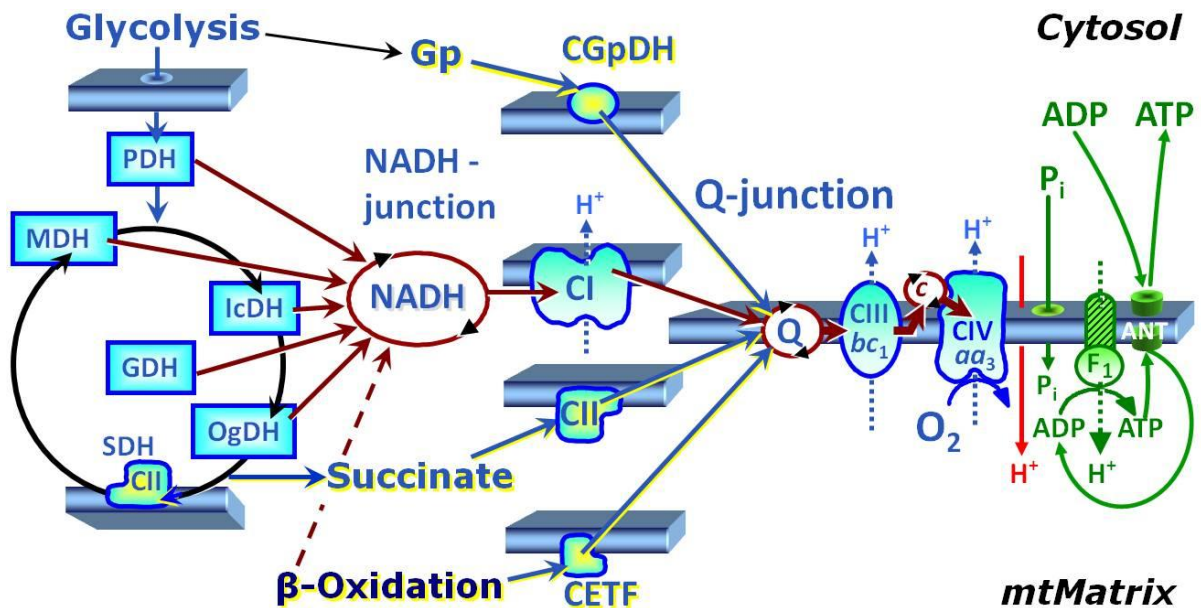


**Fig. 5.4. Convergent electron transfer** at the levels of the Q-junction (CI, CII, CGpDH and CETF) and at the level of the NADH pool. Dehydrogenases are PDH, pyruvate DH; MDH, malate DH; IDH, isocitrate DH; OgDH, 2-oxoglutarate DH, SDH, succinate DH - yielding a NADH:succinate ratio of 4:1 in the full TCA cycle. GDH, mt-glutamate DH.

## 2. Historical perspectives of protocols with substrate combinations: beyond the State 3 or ETC paradigm of bioenergetics

An additive effect of CI&II-linked substrate combinations was described more than 50 years ago by Hatefi et al (1962), introducing the concept of the Q-junction (Gutman et al 1971).

Convergent CI&II electron transfer is a complexity to be avoided for analyzing site-specific H<sup>+</sup>:e and ~P:O ratios. For this aim, segments of the electron transfer system are separated into linear thermodynamic cascades, forming distinct electron transfer *chains*, using either NADH-linked substrates or the classical succinate-rotenone combination. This analytical approach pioneered by Chance and Williams (1955) has then been applied mainly in the functional diagnosis of OXPHOS. The experimental separation of convergent electron transfer by electron gating was common to the extent of establishing an 'ETC paradigm of bioenergetics' in mitochondrial studies.

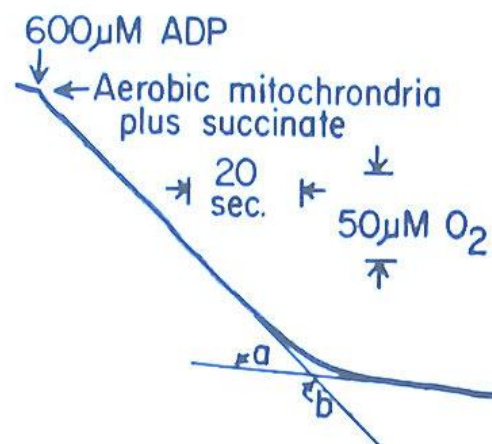


**Fig. 5.5.** Recording of the kinetics of initiation and cessation of rapid respiration in rat liver mitochondria. Chance and Williams (1955 I) Fig. 5A.



## 2.1. Intersubstrate competitions

Restriction of permeability of the inner mitochondrial membrane for various substrates of the TCA cycle raised the question on inter-substrate competition for transport, intramitochondrial concentrations and oxidation.

*Biochem. J.* (1963) **86**, 432

### **Substrate Competition in the Respiration of Animal Tissues**

THE METABOLIC INTERACTIONS OF PYRUVATE AND  $\alpha$ -OXOGLUTARATE  
IN RAT-LIVER HOMOGENATES

BY R. J. HASLAM\* AND H. A. KREBS

*Medical Research Council Unit for Research in Cell Metabolism, Department of Biochemistry,  
University of Oxford*

(Received 23 July 1962)

A readily oxidizable substrate—an intermediate or a starting material—often inhibits the oxidation of other substrates when added to respiring material (Krebs, 1935; Edson, 1936). In terms of enzyme chemistry this means that oxidizable substrates

\* Present address: Sir William Dunn School of Pathology, University of Oxford.

and intermediates derived from them compete with each other for the joint pathway of electron transport to molecular oxygen or for a shared co-factor. The present investigation is concerned with the detailed study of the competitive and other interactions of pyruvate,  $\alpha$ -oxoglutarate and endogenous substrates in respiring rat-liver homogenates.

Succinate accumulation is decreased by malate, and titration of phosphate or malate in the presence of succinate and rotenone progressively inhibit respiration of rat liver mitochondria (Harris and Manger 1968). In general, *'when two substrates are presented together the respiratory rate obtainable with maximal stimulation by uncoupler can exceed, be equal to or be less than the sum of the rates obtained with the respective substrates separately'* (Harris and Manger 1969). Various mechanisms for explaining these different effects have been recognized, in particular that *'the stimulation of the oxidation of either malate or succinate by the addition of glutamate is due to the removal of oxaloacetate by transamination'* (Harris and Manger 1969; Fig. 3.6 and 5.11). When  $\beta$ -hydroxybutyrate is added to NADH-linked substrates (either citrate, malate, glutamate, oxoglutarate or pyruvate), then *'with these pairs the total rate of oxidation obtainable is equal to the sum of the respective rates measured separately'*. Since the *'respiratory rate obtainable from other pairs of substrates can be less than the sum of the separate rates, even though there is no known inhibition of the enzymes by the conjugate substances'*, the available conclusion was that *'in this circumstance mutual competition between the two anions for permeation and accumulation is presumed'* (Harris and Manger 1969).

It is important to note that these investigations were based on noncoupled flux, removing any downstream limitation of flux by the phosphorylation system. Without the concepts of (i) a shift of flux control under different metabolic conditions of substrate supply to different enzyme-catalyzed steps, and (ii) convergent versus linear pathways, however, interpretation of these results on rat liver mitochondria was only



possible in terms of intersubstrate competition of substrate transport. The focus, therefore, was on inhibitory mechanisms. Although stimulation of respiration of rat liver mitochondria was observed when succinate was added to pyruvate (without succinate and rotenone as a control for an additive effect), the interpretation was that '*succinate oxidation did not inhibit pyruvate oxidation*' (König et al 1969). Although these early studies clearly showed that succinate plays an important regulatory role for mitochondrial respiration in the presence of CI-linked substrates, they appear to have had little or no influence on later concepts on mitochondrial respiratory capacity and respiratory control.

## 2.2. Scattered observations with substrate combinations

It is difficult to trace the history of observations on mitochondrial respiration with specific substrate combinations that lead to convergent electron flow through CI&II (Hatefi et al 1962) or CI&GpDH. The reason for this difficulty is related to the apparent lack of an explicit conceptual framework (Torres et al 1988), rendering valuable results scattered as observations without specific interpretation.

(i) The group of Alberto Boveris reports OXPHOS capacities ( $P$ ) with glutamate&succinate ( $GS_p$ ) which is 1.9-fold higher than glutamate&malate ( $GM_p$ ) in rat heart mitochondria (Costa et al 1988). While no values were reported for succinate in heart, liver mitochondria were studied with succinate and rotenone,  $S(Rot)_p$ , and  $GM_p$ . The same group measured OXPHOS capacity of rat muscle and liver mitochondria in states  $GS_p$  and  $GM_p$ : The  $GM_p/GS_p$  flux ratios are 0.7 to 0.8 in liver (Llesuy et al 1994). No conclusion on an additive effect of the CI&II-linked substrates is possible, since succinate(rotenone) alone supports a higher flux than glutamate&malate in liver mitochondria and permeabilized liver tissue. In fact, the  $GM_p/S(Rot)_p$  flux ratio is 0.6 (Costa et al 1988). Similarly, the  $GM_p/GS_p$  flux ratios of 0.5 and 0.8 for rat heart and skeletal muscle mitochondria cannot be interpreted without direct comparison to flux in state  $S(Rot)_p$ .

(ii) Jackman and Willis (1996) report an additive effect of multiple substrates on flux: The sum of OXPHOS activities with glycerophosphate ( $Gp_p$ ) and pyruvate&malate ( $PM_p$ ) adds up to the respiration measured in state  $PMGp_p$ . The physiological importance of this additive effect of convergent electron flow can be evaluated only with information on the additive succinate effect, since subsequent addition of Gp may then exert a lower stimulatory effect on respiration from state  $PMS_p$  to  $PMSGp_p$ .

(iii) Kuznetsov et al (1996) note that respiration of permeabilized cardiac fibres was measured in a medium containing '*10 mM glutamate + 5 mM malate as mitochondrial substrates or additionally 10 mM succinate and 0.08 mM cytochrome c*'. The fundamentally different effects of succinate and cytochrome *c* are neither distinguished nor even presented. Later, Kunz et al (2000) report a  $GM_p/GMS_p$  ratio of 0.7 in permeabilized human muscle fibres. The apparent excess capacity of cytochrome *c*



oxidase is lower with reference to the higher flux in state  $GMS_p$ , compared to the lower  $GM_p$  reference flux. This finding was interpreted by Kunz et al (2000) as a salient feature of permeabilized fibres (or intact cells) in contrast to isolated mitochondria, rather than the consequence of the multiple substrate supply (Fig. 1.6). A less misguided interpretation might have been chosen with reference to the data on mitochondria isolated from rat muscle (Llesuy et al 1994), and to the  $GM_p/GS_p$  ratio of 0.5 and 0.7 for isolated mitochondria from pigeon skeletal muscle and human vastus lateralis (Rasmussen and Rasmussen 1997; 2000).

### 2.3. Maximum flux: functional assays and noncoupled cells

(iv) Hans and Ulla Rasmussen (1997; 2000) developed the concept of '*functional assays of particular enzymes*' by using various substrates and substrate combinations in respiratory studies of mitochondria isolated from skeletal muscle. A functional assay is based on the stimulation of flux to a maximum, which then is limited by a defined system or particular enzyme. Their concept on the application of substrate combinations (glutamate&succinate) has been largely ignored in the literature, perhaps on the basis of the argument that flux control is distributed over several enzymes along a pathway. Limitation by a single enzyme, which then has a flux control coefficient of 1.0, is a rare event, even under conditions of a 'functional assay'. Importantly, however, the 1.4- or even 2.0-fold higher flux in state  $GS_p$ , compared to the conventional State 3 paradigm, using states  $PM_p$ ,  $GM_p$  or  $S(Rot)_p$ , raises the critical issue of the physiologically appropriate reference state for measuring flux control coefficients and excess capacities of a particular enzyme such as cytochrome c oxidase (Fig. 1.6). For general consideration, Rasmussen et al (2001) state: "*The tricarboxylic acid cycle cannot be established in optimal, cyclic operation with isolated mitochondria, but parts of the in vivo reaction scheme may be realized in experiments with substrate combinations*".

(v) Attardi and colleagues dismiss isolated mitochondria as a suitable model for respiratory studies, on the basis of the fact that 'State 3' in permeabilized cells (with Complex I-linked substrates) is low compared to endogenous respiration of intact cells, which then "*raises the critical issue of how accurately the data obtained with isolated mitochondria reflect the in vivo situation*" (Villani, Attardi 1997). This ignores the scattered observations on multiple substrate effects. Low OXPHOS capacity may be directly related to artefacts in the isolation of mitochondria. Thus the 'ETC paradigm of State 3' is converted into a paradigm of maximum flux, obtained by studying 'intact' cells in the noncoupled state. Whereas it is highly informative to uncouple intact cells and thus measure ETS capacity as maximum respiration, cells are not bioenergetically intact after uncoupling. This trivial fact is dismissed under the paradigm of maximization of flux (bold added): '*KCN titration assays, carried out on intact uncoupled cells, have clearly shown that the COX capacity is in low excess (16-40%) with respect to that required to support the endogenous respiration rate*' (Villani et al 1998). Uncoupling eliminates



flux control by the phosphorylation system, hence the reference state of the noncoupled cell is nonphysiological, unless the phosphorylation system exerts no control over coupled respiration. The three-compartment model of OXPHOS has to be replaced by four-compartmental OXPHOS analysis (Chapter 2.2).

## 2.4. Mitochondrial physiology and mitochondrial pathways

A rapidly growing number of studies on various tissues and cells points to the importance of the additive effect of substrate combinations on OXPHOS capacity (Gnaiger 2009). Convergent CI&II electron flow to the Q-junction resolves discrepancies between intact cells and mitochondria. This additive effect indicates a high downstream excess capacity of respiratory complexes including cytochrome *c* oxidase (CIV) over Complexes CI and CII. Convergent electron transfer yields a maximum (additive) effect on OXPHOS when CII, CIV and the phosphorylation system exert a minimum (zero) flux control. Convergent electron transfer corresponds to the operation of the TCA cycle and mitochondrial substrate supply *in vivo*. In isolated mitochondria and permeabilized cells or tissue, conventional measurements of State 3 with pyruvate&malate, glutamate&malate or succinate(rotenone) underestimate maximum OXPHOS capacity, since external succinate is required for reconstitution of the TCA cycle and stimulating convergent CI&II electron flow under these conditions. By establishing the physiological reference state of maximum *coupled* respiration, convergent CI&II electron flow provides the proper basis for (i) quantifying excess capacities and interpreting flux control by various enzymes such as cytochrome *c* oxidase and components such as the phosphorylation system, and (ii) evaluation of specific enzymatic defects in mitochondrial respiratory physiology and pathology (Fig. 1.6). The concept on convergent electron transfer at the Q-junction (ETS) challenges conventional OXPHOS analysis based on the ETC terminology and a way of thinking about the mitochondrial 'electron transfer chain' (Fig. 5.2).

The excess ETS-OXPHOS capacity yields important information on the limitation of OXPHOS capacity by the phosphorylation system. Electron gating (ETC) limits flux artificially upstream of the Q-junction, thereby obscuring the quantitative importance of physiological flux control by the phosphorylation system (Fig. 5.4).

Specifically designed substrate-uncoupler-inhibitor titrations (SUIT) extend experimental protocols for OXPHOS analysis in the diagnosis of mitochondrial respiratory function. An important added value of SUIT protocols is the sequential measurement of mitochondrial function in multiple respiratory states of substrate and coupling control (Fig. 5.3; 5.6 to 5.8). This increases the information obtained from a limited amount of biological sample and allows the calculation of statistically robust internal flux control ratios and corresponding flux control factors, in contrast to the separate assays applied previously (Chapter 6).



**Fig. 5.6. SUIIT protocols for OXPHOS analysis: human vastus lateralis. A:** Mass-specific oxygen flux [ $\text{pmol O}_2 \cdot \text{s}^{-1} \cdot \text{mg}^{-1} W_w$ ] with substrates for fatty acid oxidation (FAO), Complex I (CI), and Complex II (CII). Permeabilized fibres, 37 °C, MiR06, 2 ml chamber (modified from Pesta and Gnaiger 2012).

Protocol:  $\text{OctM}_N + \text{D}_{2.5} + \text{G} + \text{S} + \text{D}_5 + \text{U}_{1.25} + \text{Rot} + \text{Mna} + \text{Myx} + \text{Ama}$ .

1.  $\text{OctM}_N$ :  $\text{FAO}_L$  in the LEAK state  $L$  (no adenylates,  $N$ ).
2.  $\text{OctM}_{\text{D}2.5}$ :  $\text{FAO}_P$ , OXPHOS state  $P$  (2.5 mM ADP).
3.  $\text{GMOct}_{\text{D}2.5}$ :  $\text{CI}\&\text{FAO}_{\text{D}2.5}$ , OXPHOS is ADP-limited at 2.5 mM.
4.  $\text{GMSOct}_{\text{D}2.5}$ :  $\text{CI}\&\text{II}\&\text{FAO}_{\text{D}2.5}$ .
5.  $\text{GMSOct}_{\text{D}5}$ :  $\text{CI}\&\text{II}\&\text{FAO}_P$ , OXPHOS capacity at 5 mM ADP.
6.  $\text{GMSOct}_E$ :  $\text{CI}\&\text{II}\&\text{FAO}_E$ , ETS capacity after uncoupler titration to 1.0  $\mu\text{M}$  FCCP, inhibition at 1.25  $\mu\text{M}$ .
7.  $\text{S}(\text{Rot})_E$ :  $\text{CII}_E$ .
8.  $(\text{Mna}\&\text{Myx}\&\text{Ama})_{\text{ROX}}$ : residual oxygen consumption, ROX.

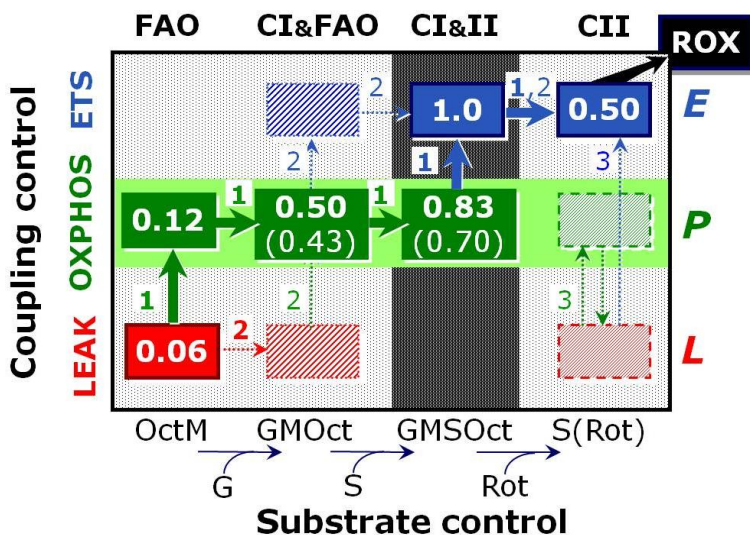


**Fig. 5.7. Coupling/substrate control diagram** with flux control ratios (FCR) normalized relative to ETS capacity with convergent CI&II (&FAO) electron input (arrows 1, corresponding to panel A; FCR in parentheses are pseudo-state  $P$  at 2.5 mM ADP). Additional protocols (arrows 2 and 3) are required to fill in the

dashed coupling/substrate states, including overlapping respiratory state  $\text{S}(\text{Rot})_E$  in all cases; 2:  $\text{OctM}_N + \text{G} + \text{D} + \text{U} + \text{S} + \text{Rot}$ ; 3:  $\text{Rot}\&\text{S} + \text{D} + \text{U}$  or  $\text{Rot}\&\text{S} + \text{D} + \text{Omy} + \text{U}$ . Residual oxygen consumption (ROX) is determined as a common step in the three protocols on integrated pathways (+Mna+Myx+Ama); abbreviations in Appendix (Pesta, Gnaiger 2012).

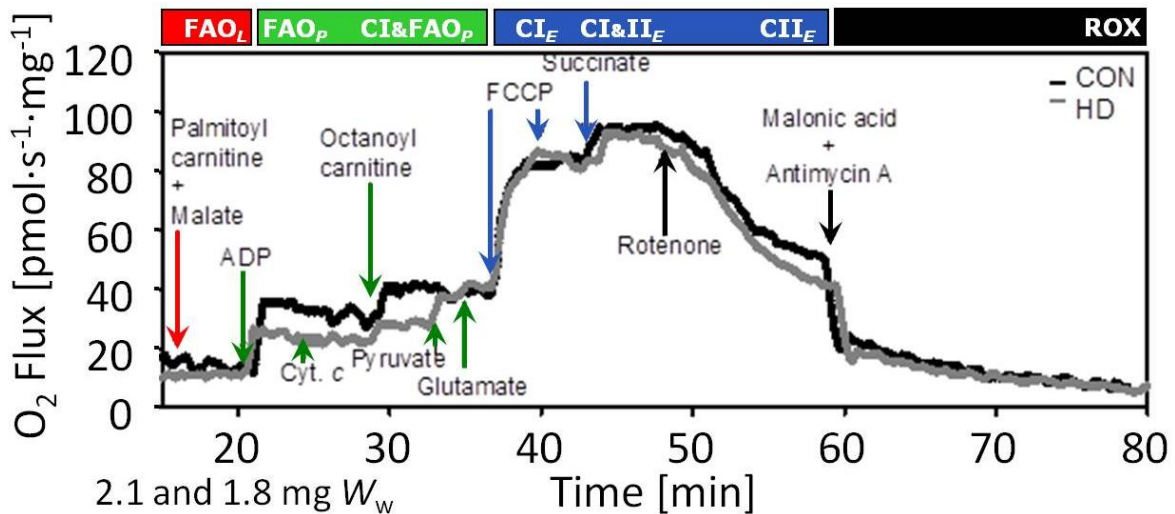


**Fig. 5.8. SUIIT protocols for OXPHOS analysis: human heart.** Permeabilized myocardial fibres from healthy controls. SUIIT protocol for electron flux through fatty acid oxidation (FAO); after addition of pyruvate&glutamate, electron flux is through CI&FAO. Superimposed traces are shown of tissue mass-specific respiratory flux as a function of time for a control and heart disease patient (CON and HD). Arrows indicate titrations, identical for both traces; continued with ascorbate&TMPD (modified from Lemieux et al 2011).

Protocol: **PaIM<sub>N</sub>**+**D**+**c**+**Oct**+**P**+**G**+**U**+**S**+**Rot**+**Mna**+**Ama**.

1. **PaIM<sub>N</sub>**: **FAO<sub>L</sub>** in the LEAK state *L* (no adenylates, *N*).
2. **PaIM<sub>P</sub>**: **FAO<sub>P</sub>**, OXPHOS state *P* (2.5 mM ADP, saturating).
3. **PaIM<sub>C<sub>P</sub></sub>**: **FAO<sub>P</sub>**, state *P* with cytochrome *c*.
4. **PaIOctM<sub>P</sub>**: **FAO<sub>P</sub>**.
5. **PMPaIOct<sub>P</sub>**: **CI&FAO<sub>P</sub>**.
6. **PMGPaIOct<sub>P</sub>**: **CI&FAO<sub>P</sub>**.
7. **PMGPaIOct<sub>E</sub>**: **CI&FAO<sub>E</sub>**, ETS state *E*, capacity after FCCP titration.
8. **PMGSPaIOct<sub>E</sub>**: **CI&II&FAO<sub>E</sub>**.
9. **S(Rot)<sub>E</sub>**: **CII<sub>E</sub>**.
10. **(Mna&Myx&Ama)<sub>ROX</sub>**: residual oxygen consumption, **ROX**.

Human skeletal and cardiac muscle are compared in Fig. 5.6 and 5.8. Note the pronounced additive effect of CI&II-linked respiration in skeletal muscle (as well as in mouse skeletal muscle and human fibroblasts, Fig. 5.3). In contrast, human heart mitochondria show a minor additive effect upon addition of succinate to the CI-substrate state, whereas the *P/E* ratio is significantly higher in skeletal muscle mitochondria (lower excess *E-P* capacity, smaller uncoupling effect, Fig. 5.6) and *P/E* is 1.0 in mouse muscle (zero excess; Fig. 5.3A). The OXPHOS flux control pattern of human fibroblasts (Fig. 5.3B) is more comparable to the human heart and human skeletal muscle, but very different from mouse skeletal muscle (Fig. 5.3A). For a detailed discussion of these SUIIT protocols see Lemieux et al (2011), Pesta et al (2011), Pesta and Gnaiger (2012) and Votion et al (2012).



### 3. Pyruvate & Glutamate & Malate, PGM

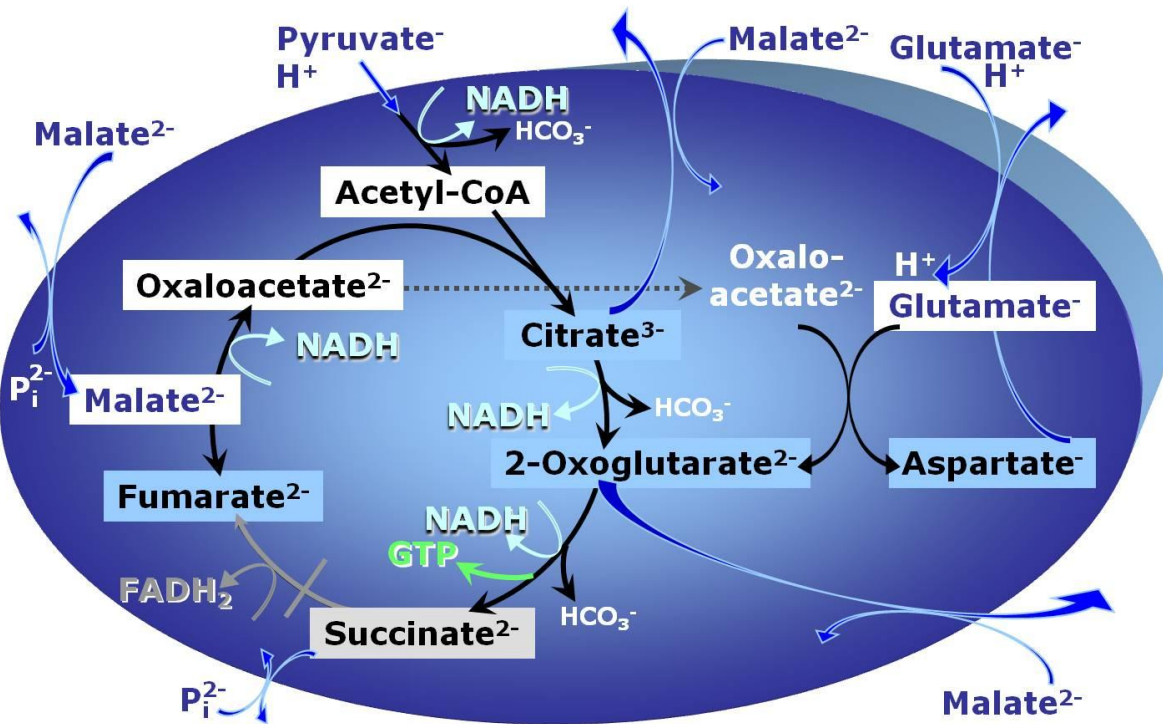


**Fig. 5.9. PGM.** Respiratory capacity through Complex I may be limited by substrate supply. The addition of pyruvate and glutamate with malate (PMG; compare Fig. 5.4) yields respiration in the presence of both pyruvate and the malate-aspartate shuttle.

Mitochondria from red muscle fibres (rabbit soleus) exhibit a 15% higher flux in state  $\text{PGM}_p$  (Fig. 5.9) compared to  $\text{PM}_p$ , whereas white muscle fibre mitochondria (rabbit gracilis) show a slight inhibition by glutamate added to  $\text{PM}_p$  (Jackman and Willis 1996). Paradoxically, a significant inhibition of flux by addition of pyruvate to  $\text{GM}_p$  was observed in horse skeletal muscle fibres (Votion et al 2012). Addition of glutamate to pyruvate&malate increases respiratory capacity in human skeletal muscle (Winkler-Stuck et al 2005; although  $\text{PM}_p$  is 16% higher than  $\text{GM}_p$ ). There is a strong additive effect of the PGM-substrate combination on respiratory capacity of mouse heart fibres (Lemieux et al 2006). High malate concentrations limit the flux through CII by product inhibition of SDH and thus support more specifically the CI-linked activity of respiration.

### 4. Pyruvate & Malate & Succinate, PMS

Reconstitution of TCA cycle function in isolated mitochondria or permeabilized tissues and cells requires addition of succinate to the conventional substrates for Complex I (Fig. 5.10). The TCA cycle does not form a full functional loop when using the substrate combination pyruvate&malate, when citrate and 2-oxoglutarate are exchanged rapidly for malate by the tricarboxylate and 2-oxoglutarate carrier (Fig. 3.3). Then succinate dehydrogenase activity is fully dependent on a high external succinate concentration.

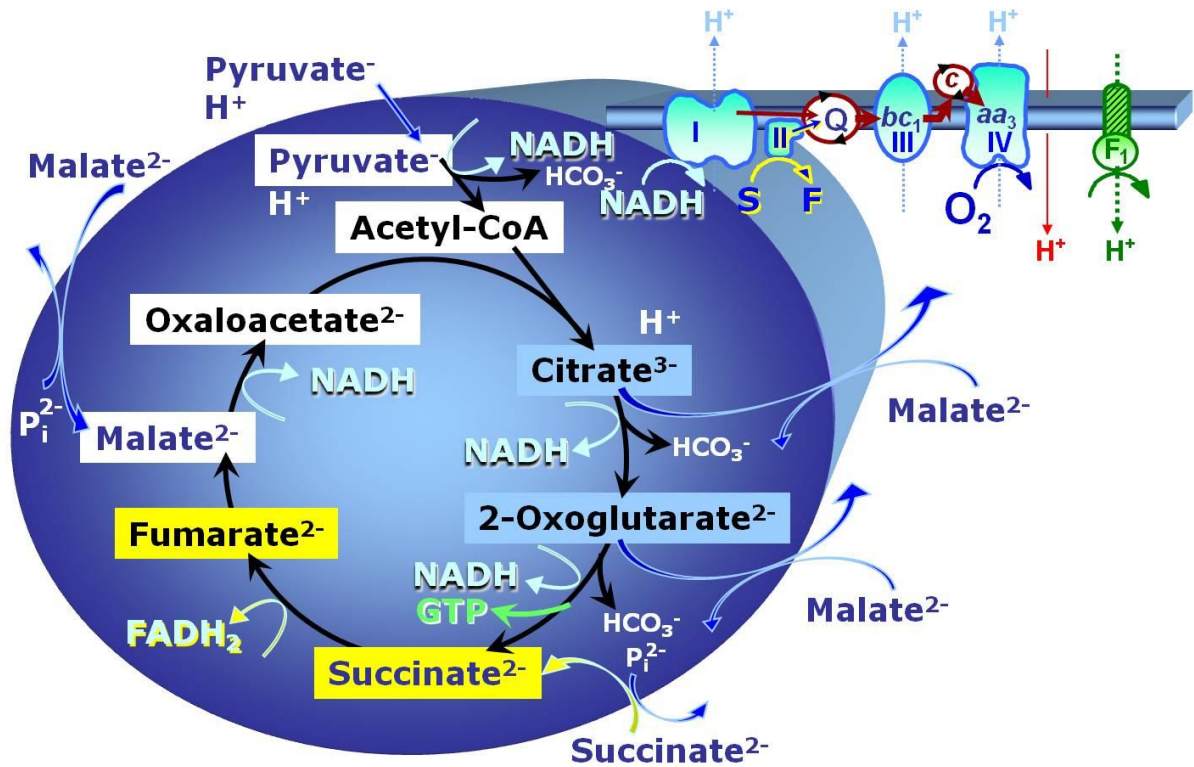


**Fig. 5.10. PMS.** Convergent electron flow to the Q-junction with substrate combination pyruvate&malate&succinate.

### 5. Glutamate & Malate & Succinate, GMS

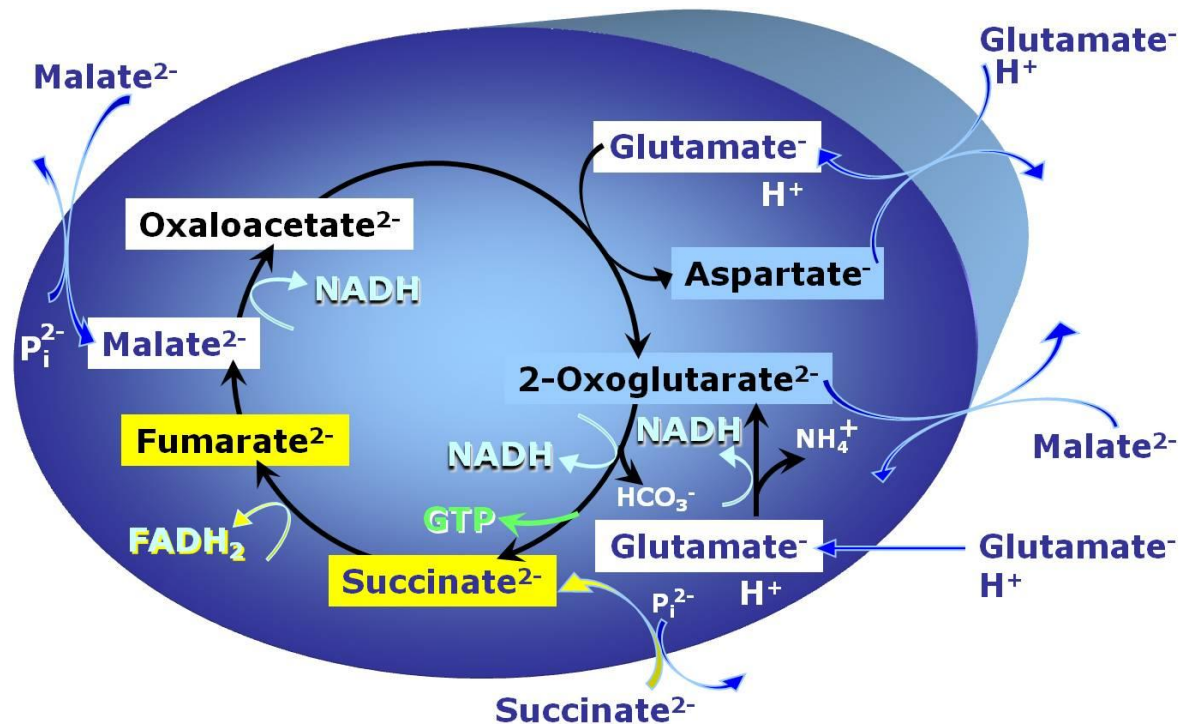


**Fig. 5.11. GMS.** Convergent electron flow to the Q-junction with substrate combination glutamate&malate&succinate (GMS).



Transaminase catalyzes the reaction from oxaloacetate to 2-oxoglutarate, which then establishes a cycle without generation of citrate. OXPHOS is higher with glutamate&succinate (CI&II) compared to glutamate&malate (CI) or succinate and rotenone (CII). This documents an additive effect of convergent CI&II electron flow to the Q-junction, with consistent results obtained with permeabilized muscle fibres and isolated mitochondria (Gnaiger 2009). In human skeletal muscle mitochondria (25 °C), Rasmussen and Rasmussen (2000) obtained CI/CI&II flux ratios of 0.7 (0.6) for OXPHOS (or ETS) with glutamate&malate (8+4 mM) and glutamate&succinate (4+8 mM), and CII/CI&II flux ratios of 0.8 (0.6) for OXPHOS (or ETS). The  $GM_P/GMS_E$  and  $S(Rot)_E/GMS_E$  flux control ratios are 0.50 and 0.55 in human vastus lateralis (Pesta et al 2011).

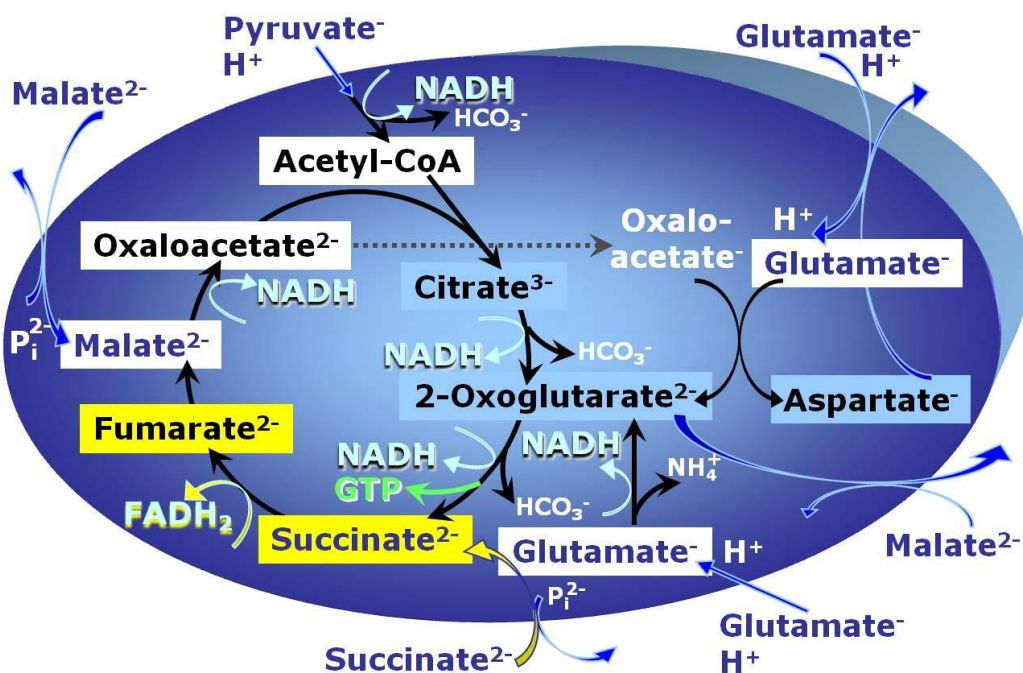


**Fig. 5.12. PGMS:** Convergent electron flow to the Q-junction with substrate combination pyruvate&glutamate&malate &succinate (PGMS).

Due to the lower  $H^+/O_2$  stoichiometry in succinate respiration compared to CI-linked respiration (two versus three coupling sites), the CI/CI&II ratio is lower for LEAK respiration (0.3 to 0.4; Garait et al 2005) compared to OXPHOS capacity.

In human skeletal muscle, the phosphorylation system is more limiting at the highest OXPHOS activity with glutamate&succinate, at a  $P/E$  ratio ( $GS_P/GS_E$ ) of 0.69 versus 0.80 with glutamate&malate (Rasmussen and Rasmussen 2000). Failure of obtaining a further stimulation of coupled OXPHOS in human skeletal muscle mitochondria with GMS by uncoupling (Kunz et al 2000) can be explained by the high FCCP concentration applied (10  $\mu M$ ) which is known to inhibit respiration (Steinlechner-Maran et al 1996). In mouse skeletal muscle, however, the  $P/E$  ratio is actually 1.0 (Aragones et al 2008), which contrasts with the



significant limitation of OXPHOS capacity by the phosphorylation system in humans (Fig. 5.3B, 5.6 and 5.8).

## 6. Pyruvate & Glutamate & Malate & Succinate, PGMS

2-oxoglutarate is produced through the citric acid cycle from citrate by isocitrate dehydrogenase, from oxaloacetate and glutamate by the transaminase, and from glutamate by the glutamate dehydrogenase. If the 2-oxoglutarate carrier does not outcompete these sources of 2-oxoglutarate, then the TCA cycle operates in full circle with external pyruvate&malate&glutamate&succinate (Fig. 5.12).

Recent studies showed that CII- and CI&II-linked OXPHOS capacity is inhibited by 2 mM malate concentrations as applied in most SUIT protocols. This inhibition is less pronounced at 0.5 mM malate (Tab. A2.1).

## 7. Additive effect of glycerophosphate dehydrogenase complex and electron-transferring flavoprotein complex

On the outer face of the inner mt-membrane, glycerophosphate dehydrogenase complex oxidises glycerophosphate to dihydroxyacetone phosphate, reducing a flavin prosthetic group that donates its reducing equivalents to the electron transfer system at the level of CoQ. Electron-transferring flavoprotein complex (CETF) is located on the matrix face of the inner mt-membrane, and supplies electrons from fatty acid  $\beta$ -oxidation to CoQ.

Glycerophosphate oxidation in rabbit skeletal muscle mitochondria (gracilis, fast-twitch white muscle, 99% type IIb; and soleus, slow-twitch red muscle, 98% type I) exhibits an additive activity with pyruvate oxidation (Jackman and Willis 1996).

Oxygen flux in the presence of glycerophosphate is increased by subsequent addition of succinate to brown adipose tissue mitochondria (Rauchova et al 2003). It has yet to be shown if there is an additive effect of applying these two substrates, or if respiratory capacity with succinate(rotenone) is already sufficient for supporting the maximum flux.

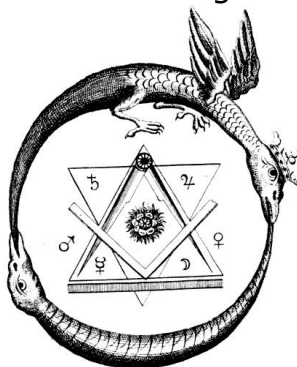
Red and white rabbit muscle mitochondrial respiration is slightly increased when palmitoylcarnitine is added to  $PM_p$  (Jackman and Willis 1996). Similarly, ATP production in mitochondria isolated from human muscle is higher with a substrate combination (pyruvate&malate&2-oxoglutarate&palmitoylcarnitine) that supports convergent CI&FAO electron input into the Q-junction, than with electron input into either CI or CII (Tonkonogi et al 1999; Short et al 2005).



## 8. Implications

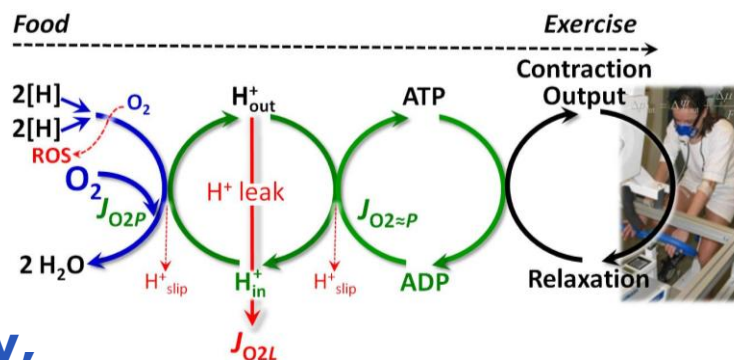
Application of physiological fuel substrate combinations is a hallmark of the extension of mitochondrial bioenergetics to mitochondrial physiology and real-time OXPHOS analysis. Conventional studies with various substrates for NADH-linked dehydrogenases prevent the simultaneous stimulation of CII or other convergent pathways into the Q-junction (Fig. 5.4). Convergent electron input into the Q-cycle characterizes mitochondrial function *in vivo*, with a minimum of 1/5<sup>th</sup> to 1/4<sup>th</sup> of electron flow through Complex II, even for respiration on pure carbohydrate.

- (i) For appreciation of the diversity of mitochondrial function in different animals and tissues, mitochondrial respiratory capacity has to be generally re-assessed with application of substrate combinations appropriate for reconstitution of the TCA cycle.
- (ii) Limitations of SUIT protocols are observed with variations of substrate concentrations, particularly malate and fatty acids. A compromise may have to be made between optimum conditions for FAO-, CI-linked versus CI&II- and CII-linked respiration in a protocol.
- (iii) Interpretation of excess capacities of various components of the electron transfer system and of flux control coefficients is largely dependent on the metabolic reference state. Appreciation of the concept of the Q-junction provides new insights into the functional design of the respiratory system.
- (iv) The conventional view of a drop of mitochondrial membrane potential with an increase of flux from the LEAK to OXPHOS state (high to moderate membrane potential) has to be modified, based on the appreciation of the important control of flux by substrate supply. The relation between membrane potential and flux is reversed when an increase in flux is affected by a change in substrate supply.
- (v) Based on the relationship between ROS production and reversed electron flow from Complex II to Complex I, multiple substrates have been supplied in investigations of oxidative stress related to mitochondrial metabolism. The dependence of ROS production on membrane potential and metabolic state will have to be investigated further, to resolve pertinent controversies on the role of mitochondria in cellular ROS production.
- (vi) Supercomplex formation, metabolic channelling and partially additive effects on flux suggest that convergent electron input into the Q-junction only partially proceeds through a common CoQ pool.





## Chapter 6. Normalization of flux - past the RCR: on efficiency, coupling and substrate control factors



Section	1. Intact cells and mt-preparations .....	58	Page
	2. Cell ergometry: <i>P</i> and <i>E</i> coupling efficiency .....	60	
	3. Flux control ratios, <i>FCR</i> .....	62	
	4. Flux control factors, <i>FCF</i> .....	63	

### 1. Intact cells and mitochondrial preparations

Intact cells, *C*, play an important role in mitochondrial physiology, since bioenergetic function depends on viability as much as cell viability depends on mitochondrial function. While intact cells are characterized by cell viability, mitochondria studied in preparations without intact cell membranes cannot be defined as viable. In contrast to free-living bacteria, mitochondria (and chloroplasts and various parasitic microbes) are bioblasts which cannot *live*, but can *function* when properly isolated from their intracellular environment. Therefore, functional mitochondrial *competence* rather than *viability* can be tested, progressing from the experimental level of quality control of preparation to the biomedical level of physiological competence. Any loss of mitochondrial competence induced artificially by the preparation procedure must be distinguished from various states of pathophysiological mitochondrial competence as a readout of real-time OXPHOS analysis and functional scoring.

Cell viability is scored as the fraction of cells with intact plasma membranes (*C*), staining permeable dead cells (*Pc*) with plasma membrane permeable dyes (e.g. trypan blue). A respirometric test is based on the impermeability of cell membranes for ADP (general) and succinate in most types of intact cells. Cell viability of  $C/(C+Pc)=0.95$  is frequently considered as a threshold for respirometry with intact cells. High  $Ca^{2+}$  concentrations in culture media cause swelling and disruption of mitochondria in *Pc* and inhibit mt-respiration subsequently. When ROX-corrected respiration is expressed on the basis of viable cell count (*C*), the assumption is made that non-viable cells (*Pc*) contribute only to ROX. Complex culture media are used as respiration media, which may be supplemented with substrates for respiration and growth in the cellular ROUTINE state. In media without energy substrates, cells respire on



endogenous substrates (Ce). Different media and external substrate supply modify the potential limitation of ETS capacity by intracellular substrates and influence the level of ROUTINE respiration. Definition of the 'basal metabolic rate' (BMR) of cells is open to a wide scope of speculation and controversial references to ROUTINE or LEAK respiration.

**Table 6.1. Mitochondrial preparations**

Symbol	Name and description
Imt	<b>Isolated mitochondria</b> , integrity of inner and outer mt-membrane
SmtP	<b>Submitochondrial particles</b> , no integrity of outer mt-membrane, cytochrome <i>c</i> depleted, stimulated by addition of NADH
Thom	<b>Tissue homogenate</b> , integrity of inner and outer mt-membrane
Pfi	<b>Permeabilized muscle fibres</b> , selective permeabilization of the plasma membrane mechanically and with saponin, integrity of the mt-cytoskeletal structure
Ptic	<b>Permeabilized tissue or cells</b> , selective permeabilization of the plasma membrane mechanically and with mild detergents, integrity of the mt-cytoskeletal structure
Pc	<b>Permeabilized cells</b> , selective permeabilization of the plasma membrane with digitonin, integrity of the mt-cytoskeletal structure

Defined coupling states (Chapter 2) and substrate states (Chapters 3 to 5) are established in mt-preparations suspended in mt-respiration media (Tab. 6.1). Coupling and substrate states are complementary (Fig. 5.7). To remove the plasma membrane barrier in mt-preparations, the cell membranes and organelles can be (i) separated by mechanical disruption from the mitochondria, which then are isolated and purified by low and high spin centrifugation (Imt and SmtP) or by crude enrichment (low spin, crude Thom). (ii) Alternatively, cell membranes are selectively permeabilized by mechanical fracture (Thom, Ptic) or chemical permeabilization (Pfi, Ptic, Pc) with all intracellular structures remaining in the sample. Then soluble cytosolic components are either washed out (Pfi, Ptic) or highly diluted in mt-respiration medium (Thom, Pc, Pfi). The quality of mt-preparations is evaluated by functional tests on the integrity of the outer mt-membrane (cytochrome *c* test in specific respiratory states; except for SmtP).

With careful preparation, the entire mt-population is recovered in Thom, Pfi and Ptic including Pc. Then oxygen flux can be expressed on the basis of tissue wet weight ( $W_w$ ; strictly mass [mg]; Chapter 1.3).  $W_w$  is determined before (Thom) or after preparation (Pfi) before addition of samples to the Oxygraph chamber. Tissue or cell protein mass can be determined in samples recovered from the Oxygraph chamber (subsamples of Thom and Pc; complete washout of Pfi). The accuracy of measurement of tissue or protein content and mt-markers (e.g. CS activity) is limited by incomplete recovery from the chamber and large background corrections for protein (BSA and catalase in MiR06). mt-normalization or structured analysis of the aerobic performance of tissues and cells separates effects related to mt-density (structural elements per tissue mass) from those related to mt-quality (Chapter 1.3).



**Tab. 6.2.** Electron transfer system capacity,  $E$ , ROUTINE and netROUTINE flux control ratio, and ETS coupling efficiency in the phosphorylation control protocol with intact human (and 32D mouse) cells (37 °C; mean  $\pm$  SD). Details and references in Pesta and Gnaiger (2012).

Cell type	ETS ( $E$ , $I_{O_2E}$ ) pmol·s <sup>-1</sup> ·10 <sup>-6</sup>	ROUTINE $R/E$	netROUTINE $\approx R/E=(R-L)/E$	ETS-LEAK $j_{\approx E}=1-L/E$	Residual ROX/ $E'$
HEK 293	14 $\pm$ 2	0.31 $\pm$ 0.03	0.23 $\pm$ 0.02	0.91 $\pm$ 0.00	0.01 $\pm$ 0.00
32D (mouse)	81 $\pm$ 11	0.39 $\pm$ 0.02	0.29 $\pm$ 0.02	0.90 $\pm$ 0.02	0.03 $\pm$ 0.01
CEM, control	54 $\pm$ 11	0.40 $\pm$ 0.03	n.d.	n.d.	0.02 $\pm$ 0.03
CEM, G1- phase, apopt.	31 $\pm$ 6	0.41 $\pm$ 0.03	n.d.	n.d.	0.03 $\pm$ 0.03
CEM, S- phase, apopt.	85 $\pm$ 13	0.38 $\pm$ 0.03	n.d.	n.d.	0.01 $\pm$ 0.01
HUVEC	114 $\pm$ 18	0.26 $\pm$ 0.02	0.13 $\pm$ 0.00	0.87 $\pm$ 0.02	0.05 $\pm$ 0.04
HPMC, control	181 $\pm$ 58	0.40 $\pm$ 0.09	0.31 $\pm$ 0.08	0.91 $\pm$ 0.01	0.005 $\pm$ 0.01
HPMC, +IL-1 $\beta$	142 $\pm$ 47	0.41 $\pm$ 0.09	0.32 $\pm$ 0.08	0.92 $\pm$ 0.02	0.02 $\pm$ 0.01
Fibroblasts, young	111 $\pm$ 24	0.34 $\pm$ 0.03	0.20 $\pm$ 0.02	0.86 $\pm$ 0.02	0.07 $\pm$ 0.03
Fibroblasts, young-arrest	138 $\pm$ 22	0.23 $\pm$ 0.01	0.18 $\pm$ 0.02	0.95 $\pm$ 0.01	0.05 $\pm$ 0.00
Fibroblasts, senescent	285 $\pm$ 72	0.42 $\pm$ 0.05	0.21 $\pm$ 0.05	0.79 $\pm$ 0.04	0.07 $\pm$ 0.03

Normalization of flux per chamber volume (Fig. 1.2) for cell density yields oxygen flow,  $I_{O_2}$ , per cell number (Tab. 6.2; column 2). Variation of cell size needs to be considered (Fig. 1.3). OXPHOS analyses expressing oxygen flux per mass of tissue or cells (units [mg], not number) take into consideration the fact that intracellular mt-density is a vitally important component of mitochondrial competence. Tissue-mass or cell-mass specific LEAK, OXPHOS and ETS capacities,  $J_{O_2}$  [pmol O<sub>2</sub>·s<sup>-1</sup>·mg<sup>-1</sup>], are of physiological relevance, integrating mt-specific function and mt-density. This unstructured analysis becomes more powerful by determination of mitochondrial markers (mt-markers) to obtain mt-specific fluxes,  $J_{mt,O_2}$ .

## 2. Cell ergometry: OXPHOS and ETS coupling efficiency

Analogous to ergometric measurement of  $V_{O_2max}$  or  $V_{O_2peak}$  on a cycle or treadmill, cell ergometry is based on OXPHOS analysis to determine OXPHOS capacity,  $P=J_{O_2P}$  [pmol O<sub>2</sub>·s<sup>-1</sup>·mg<sup>-1</sup>], at the cellular and mitochondrial level.  $V_{O_2peak}$  and  $J_{O_2P}$  provide reference values for a subject's or a cell's aerobic or mitochondrial competence.  $V_{O_2peak}$  of human endurance athletes is 60 up to 80 ml O<sub>2</sub>·min<sup>-1</sup>·kg<sup>-1</sup> body mass (45 to 60 nmol·s<sup>-1</sup>·g<sup>-1</sup>). When aerobic competence declines in sedentary obese humans to 25 ml O<sub>2</sub>·min<sup>-1</sup>·kg<sup>-1</sup> (20 nmol·s<sup>-1</sup>·g<sup>-1</sup>), mitochondrial competence is diminished in skeletal muscle (vastus lateralis) from a high health score of 140 nmol O<sub>2</sub>·s<sup>-1</sup>·g<sup>-1</sup> to 50 nmol·s<sup>-1</sup>·g<sup>-1</sup> in deep mitochondrial fever (expressing CI&II-linked OXPHOS capacity per tissue wet weight; Fig. 5.6).



To convert oxygen consumption into energy units of **power** (=exergy per time), aerobic catabolic flux ( $J_{O_{2peak}}$  for cycle ergometry,  $J_{O_{2P}}$  for cell OXPHOS capacity [ $\text{nmol}\cdot\text{s}^{-1}\cdot\text{g}^{-1}$ ]) is multiplied by the catabolic Gibbs force ( $F_{O_{2,k}}=\Delta_k G_{O_2}$ ; typically  $-0.47$  mJ/nmol  $O_2$ ; Eq. 1.7). This yields the mass-specific aerobic input power [ $\text{mW}\cdot\text{g}^{-1}$ ]. In cycle *ergometry*, the corresponding mechanical output power results in *ergodynamic* efficiencies,  $\varepsilon$ =output power/-input power, of about 0.25. In OXPHOS analysis, the output power is the product of mitochondrial ATP production,  $\sim P=J_{\sim P}$  [ $\text{nmol}\ \sim P\cdot\text{s}^{-1}\cdot\text{g}^{-1}$ ] and Gibbs force of phosphorylation ( $F_{\sim P}=\Delta_p G_{\sim P}$ ).  $F_{\sim P}$  is typically 48 to 62 kJ/mol  $\sim P$ . The cell ergodynamic output/input power efficiency is partitioned into a flux ratio, the famous  $\sim P/O_2$  ratio ( $J_{\sim P}/J_{O_2}$ ; ATP yield per oxygen consumed), and force ratio.  $\varepsilon_P$  is the efficiency of oxidative phosphorylation at saturating ADP (state  $P$ ):

$$\text{Ergodynamic efficiency: } \varepsilon_P = \frac{J_{\sim PP}}{J_{O_{2P}}} \cdot \frac{F_{\sim P}}{-F_{O_{2,k}}} = \frac{\sim P/P}{\nu_{\sim P/O_2}} \cdot \left( \frac{-F_{O_{2,k}}}{F_{\sim P} \cdot \nu_{\sim P/O_2}} \right)^{-1} = \frac{j_{\sim P}}{f_{\sim P}} \quad (6.1)$$

Ergodynamic efficiency not only depends on coupling of flux but also on the force ratio or force efficiency,  $f_{\sim P}$ . At ergodynamic equilibrium,  $\varepsilon=1.0$ , fluxes vanish to zero when  $j_{\sim P} = f_{\sim P} = 1$ . In Eq. 6.1,  $j_{\sim P}$  results from normalization of the *measured*  $\sim P/O_2$  ratio ( $\sim P/P$ ) by the *mechanistic*  $\sim P:O_2$  ratio (stoichiometric number of a fully coupled reaction,  $\nu_{\sim P/O_2}$ ). With a theoretical range from 0.0 to 1.0,  $j_{\sim P}$  is the proper expression of the OXPHOS coupling efficiency,

$$\text{OXPHOS coupling efficiency: } j_{\sim P} = \frac{\sim P/\nu_{\sim P/O_2}}{P} = \frac{P-L}{P} = 1 - \frac{L}{P} = 1 - \frac{1}{\text{RCR}} \quad (6.2)$$

ATP production,  $\sim P$ , is converted to a stoichiometrically equivalent partial oxygen consumption,  $\approx P$ , which is the free OXPHOS capacity tightly coupled to phosphorylation (Fig. 2.4; Tab. 2.2),

$$\text{Free OXPHOS capacity: } \approx P = \sim P/\nu_{\sim P/O_2} = P-L \quad (6.3)$$

To avoid overestimating the dissipative LEAK component,  $L$  can be measured in a LEAK state with the protonmotive force,  $\Delta p_{mt}$ , adjusted to the slightly lower value maintained in the OXPHOS state  $P$ . Any turnover-dependent components of proton leak and slip, however, are underestimated under these conditions. Insertion of Eq. 6.3 into the first term in Eq. 6.2 yields  $j_{\sim P} = \approx P/P$ . This defines OXPHOS coupling efficiency as a flux control factor, which is linked to the  $L/P$  coupling control ratio and is exclusively based on respirometric OXPHOS analysis (Tab. A1.3). Eq. 6.2 shows the hyperbolic relation between  $j_{\sim P}$  and the RCR (Fig. 6.1).

The OXPHOS state can be established experimentally in mt-preparations, adding ADP and  $P_i$  at kinetic saturation and fuel substrate combinations which reconstitute physiological TCA cycle function (Chapter 5). The free OXPHOS capacity may be kinetically limited by the phosphorylation system to utilize  $\Delta p_{mt}$ . Then ETS capacity is in excess of

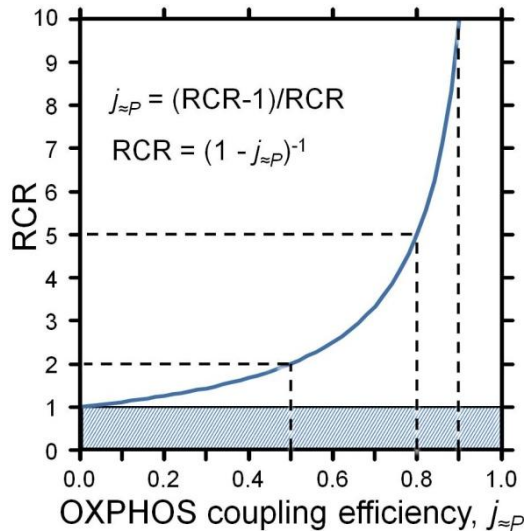


**Fig. 6.1. Respiratory acceptor control ratio, RCR, as a function of OXPHOS coupling efficiency,  $j_{\approx P}$ .** RCR is the State 3/State 4 flux ratio, equal to  $P/L$  if State 3 refers to saturating  $[ADP]$  and  $[P_i]$ . RCR ranges from 1.0 to infinity and is highly non-linear in the typical experimental range of RCR from 3 to 10: when  $j_{\approx P}$  increases from 0.8 to 0.9, RCR doubles from 5 to 10. RCR increases to infinity at the limit of  $j_{\approx P}=1.0$ . Statistical analyses of  $RCR \pm SD$  require linearization by transformation to  $j_{\approx P}$ .

OXPHOS capacity by the factor  $j_{EXP}=(E-P)/E$  (Tab. A1.3). Such kinetic limitation restricts the effective  $j_{\approx P}$  in addition to the mechanism of coupling. The free OXPHOS capacity potentially available for ATP production is, therefore, not only confined by incomplete coupling, which determines the dissipative limitation of efficiency by LEAK, but also by kinetic OXPHOS restriction expressed by the excess  $E-P$  capacity (Fig. 2.4). The corresponding respiratory reserve for OXPHOS cannot be studied with intact cells. The phosphorylation-kinetic component is separated from the coupling component when expressing the biochemical coupling efficiency as ETS coupling efficiency, defined as  $j_{\approx E}=(E-L)/E$  (compare Eq. 6.2).  $j_{\approx E}$  and  $j_{\approx P}$  are related by taking into account the apparent ETS excess capacity (Fig. 2.4, 5.3, 5.6-5.8),

$$\text{ETS coupling efficiency: } j_{\approx E} = j_{\approx P} \cdot (1 - j_{EXP}) + j_{EXP} \quad (6.4)$$

$j_{\approx P}$  can be determined in intact cells and mt-preparations (Fig. 1.2, 5.3, Tab. 6.2), whereas extended cell ergometry for determination of OXPHOS coupling efficiency requires OXPHOS analysis based on mt-preparations.

The derivation of flux efficiencies from principles of thermodynamics provides a theoretical framework for the generalized definition of flux control factors and and flux control ratios.

### 3. Flux control ratios, $FCR$

Flux control ratios are oxygen fluxes,  $Y_i$ , in various respiratory states  $i$ , expressed relative to a *common* respiratory reference state  $Z$ ,

$$\text{Flux control ratio: } FCR_i = \frac{Y_i}{Z} \quad (6.5)$$

$Z$  can be considered as an *internal* functional mt-marker for normalization of flux. For conceptual and statistical reasons, the reference state is chosen such that  $Z$  is a high or the maximum flux in a SUIT protocol. Therefore, CI&II-linked ETS capacity is frequently selected as  $Z$  (Fig. 2.3,



5.3, 5.6-5.8). Internal normalization (Eq. 6.1) is a general concept for structured OXPHOS analysis, to distinguish unequivocally changes of mt-quality versus mt-density. For a given protocol or set of respiratory protocols (Fig. 5.7), flux control ratios provide a fingerprint of coupling and substrate control independent of (i) mt-content of cells or tissues, (ii) purification in preparations of isolated mitochondria, and (iii) assay conditions for determination of tissue mass or mt-markers external to a respiratory protocol (CS, protein, stereology, etc.). For these methodological reasons, flux control ratios yield higher statistical resolution of changes in mt-quality compared to OXPHOS analysis based on *external* mt-markers.

Coupling control ratios are *FCR* at a constant substrate state, whereas substrate control ratios are *FCR* at a constant coupling state (Fig. 5.7).

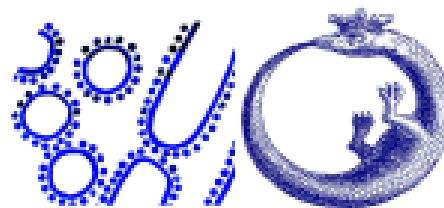
#### 4. Flux control factors, *FCF*

Complementary to the concept of flux control ratios as expressions of various respiratory *states*, *i* (Eq. 6.5), flux control factors (*FCF*) express the control of respiration in a *step* caused by a specific metabolic control variable, *X*. The  $FCF_X$  is the dimensionless fractional change of flux normalized by the reference state,  $Z_X$ , with high (stimulated or uninhibited) flux.  $Y_X$  is the background state at low flux, upon which *X* acts. *X* is either added (stimulation, activation) or removed (reversal of inhibition) to yield a flux  $Z_X$  with background  $Y_X$ . Note that *X*,  $Y_X$  and  $Z_X$  denote both, the metabolic control variable (*X*) or respiratory state ( $Y_X$ ,  $Z_X$ ) and the corresponding step change of respiratory flux or flow,  $X=Z_X-Y_X$ . Experimentally, inhibitors are added rather than removed; then  $Z_X$  is the initial state and  $Y_X$  the final state in the presence of the inhibitor. The flux control factor of *X* upon background  $Y_X$  is expressed as the change of flux from  $Y_X$  to  $Z_X$ , normalized for the reference state  $Z_X$ :

$$\text{Flux control factor: } FCF_X = \frac{Z_X - Y_X}{Z_X} = 1 - \frac{Y_X}{Z_X} \quad (6.6)$$

Substrate control factors express the relative change of oxygen flux in response to a transition of substrate availability in a defined coupling state. Coupling and phosphorylation control are determined in an ETS-competent substrate state.

A general concept of normalization of mt-respiration is derived here. This provides a consistent expression of biochemical coupling efficiencies, distinguishing OXPHOS and ETS coupling efficiency, which are normalizations of free OXPHOS and ETS capacities (Tab. 2.2). Efficiencies range from 0.0 at zero coupling to 1.0 at the limit of a completely coupled system. The terminology is to be considered as an effort to express the relations derived from the four-compartmental OXPHOS model in a consistent framework summarized in Appendix A.1.



## Chapter 7. Conversions of metabolic fluxes

### 1. Temperature adjustment of flux

Manometric techniques ('Warburg apparatus') require good temperature control and were used extensively at 37 °C for respirometry with mammalian cells up to the middle of the last century, and later occasionally with isolated mitochondria. Spectrophotometers and Clark-type Oxygraphs had comparatively poor or no temperature control and thus measurements were performed at room temperature (Chance and Williams 1955). This conceptually trivial (technically less simple) reason is largely forgotten, but a convention is continued, and frequently mammalian mitochondrial respiration is still measured at 25 °C or 30 °C in 'modern' bioenergetics. Mitochondrial physiology requires functional measurements at physiological temperature. A  $Q_{10}$  of 2 (multiplication factor for an increase by 10 °C) is frequently assumed for adjustment to physiological temperature, but can be considered as an approximation only.

Metabolic reactions are not a linear function of temperature.  $Q_{10} = 2$  (Eq. 7.1a) is an approximation for the temperature dependence of chemical reactions in general (Arrhenius equation) and metabolic fluxes in particular. To adjust flux,  $J_1$ , measured at temperature  $T_1$  (for instance,  $T_1=25$  °C; Tab. 7.1) to the physiological temperature,  $T_2=37$  °C, the exponential relation (Eq. 7.1) is used to calculate  $J_2$  (37 °C),

$$J_2 = 10^{\log J_1 - \log Q_{10} / (\frac{10}{T_1 - T_2})} \quad (7.1)$$

The derivation is obtained from the definition of the  $Q_{10}$ ,

$$Q_{10} = \left(\frac{J_1}{J_2}\right)^{\frac{10}{T_1 - T_2}} \quad (7.1a)$$

In log transformation, Eq. 7.1a is,

$$\log Q_{10} = (\log J_1 - \log J_2) \cdot \left(\frac{10}{T_1 - T_2}\right) \quad (7.1b)$$

Division by the term  $10/(T_1 - T_2)$  yields,

$$\log Q_{10} / \left(\frac{10}{T_1 - T_2}\right) = \log J_1 - \log J_2 \quad (7.1c)$$



and solving for  $\log J_2$ ,

$$\log J_2 = \log J_1 - \log Q_{10} / \left( \frac{10}{T_1 - T_2} \right) \quad (7.1d)$$

Eq. 7.1 is then obtained by inserting Eq. 7.1d into Eq. 7.1e,

$$J_2 = 10^{\log J_2} \quad (7.1e)$$

For any given  $Q_{10}$  and temperature difference  $\Delta T = T_1 - T_2$ , a multiplication factor  $F_{\Delta T}$  can be calculated from Eq. 7.1 to obtain  $J_2$  (Tab. 7.1),

$$J_2 = J_1 \cdot F_{\Delta T} \quad (7.2a)$$

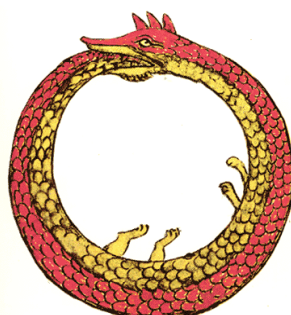
$$F_{\Delta T} = 10^{-\log Q_{10} / \left( \frac{10}{T_1 - T_2} \right)} \quad (7.2b)$$

The  $Q_{10}$  is the  $F_{\Delta T}$  (Eq. 7.2b) for a temperature difference of 10 °C. Obviously, if  $T_2$  is 37 °C and  $T_1$  is 27 °C ( $T_1 - T_2 = -10$ ), then the exponent in Eq. 7.2b is  $\log Q_{10}$ , and  $F_{\Delta T} = Q_{10}$ . For  $T_1$  of 25 °C or 30 °C and  $Q_{10} = 2$ , the  $\Delta T$ -factor  $F_{\Delta T}$  is 2.30 and 1.62, respectively. Clearly, if respiratory flux at physiological temperature is of interest, respiration should be measured at this temperature rather than adjusted on the basis of potentially inaccurate assumptions about the  $Q_{10}$ .

In HRR, experimental temperature is controlled in the range of 4 °C to 47 °C at a stability better than  $\pm 0.002$  °C.

**Tab. 7.1.** Conversion of metabolic flux from experimental temperature  $T_1$  to adjusted temperature  $T_2$ , based on  $Q_{10}$  values of 2.0, 1.8 and 2.2.

$Q_{10}$	2.00			1.80			2.20		
$T_1$ °C	25	30	37	25	30	37	25	30	37
$T_2$ °C	$F_{\Delta T}$								
25	1.00	0.71	0.44	1.00	0.75	0.49	1.00	0.67	0.39
30	1.41	1.00	0.62	1.34	1.00	0.66	1.48	1.00	0.58
35	2.00	1.41	0.87	1.80	1.34	0.89	2.20	1.48	0.85
37	2.30	1.62	1.00	2.02	1.51	1.00	2.58	1.74	1.00
38	2.46	1.74	1.07	2.15	1.60	1.06	2.79	1.88	1.08
39	2.64	1.87	1.15	2.28	1.70	1.12	3.02	2.03	1.17
40	2.83	2.00	1.23	2.41	1.80	1.19	3.26	2.20	1.27





## 2. Conversion factors for units of oxygen flux

Comparability of quantitative results on respiratory fluxes is aided by using common units. Considering the variety of units used in various disciplines of respiratory physiology (e.g.  $V_{O2max}$ ), a common basis may only be found with reference to proper *SI* units (Gnaiger 1983, 1993).

$$1 \text{ ml O}_2 \cdot \text{min}^{-1} \cdot \text{kg}^{-1} = 0.744 \text{ } \mu\text{mol} \cdot \text{s}^{-1} \cdot \text{kg}^{-1} \text{ at STPD}$$

When respiratory activity is expressed per volume of the Oxygraph chamber or volume-specific oxygen flux, the base *SI* unit is  $[\text{mol} \cdot \text{s}^{-1} \cdot \text{m}^{-3}]$ . Since oxygen concentration in pure water at equilibrium with air at standard barometric pressure of 100 kPa is 254.8 to 207.3  $\mu\text{mol} \cdot \text{dm}^{-3}$  (25 to 37 °C), it is most practical to express oxygen concentration in  $\mu\text{M}$  units,

$$1 \text{ } \mu\text{mol O}_2/\text{litre} = 1 \text{ } \mu\text{mol}/\text{dm}^3 = 1 \text{ } \mu\text{M} = 1 \text{ nmol}/\text{ml} = 1 \text{ nmol}/\text{cm}^3$$

**Table 7.2. Conversion of various units into *SI* units** when expressing respiration as mass-specific oxygen flux.

$J$	[Unit <sub><i>i</i></sub> ]	x	Factor	=	$J_{O_2}$ [ <i>SI</i> -Unit]
					nmol O <sub>2</sub> ·s <sup>-1</sup> ·g <sup>-1</sup>
					pmol O <sub>2</sub> ·s <sup>-1</sup> ·mg <sup>-1</sup>
12	ng.atom O·min <sup>-1</sup> ·mg <sup>-1</sup>	x	8.33	=	100
12	$\mu\text{mol O} \cdot \text{min}^{-1} \cdot \text{g}^{-1}$	x	8.33	=	100
12,000	natom O·min <sup>-1</sup> ·g <sup>-1</sup>	x	0.00833	=	100
6	nmol O <sub>2</sub> ·min <sup>-1</sup> ·mg <sup>-1</sup>	x	16.67	=	100
6	$\mu\text{mol O}_2 \cdot \text{min}^{-1} \cdot \text{g}^{-1}$	x	16.67	=	100
6	mmol O <sub>2</sub> ·min <sup>-1</sup> ·kg <sup>-1</sup>	x	16.67	=	100

The proper *SI* unit,  $\mu\text{mol O}_2 \cdot \text{s}^{-1} \cdot \text{dm}^{-3}$ , is used for the corresponding respiratory flux in the classical bioenergetic literature (Chance and Williams 1956). In the bioenergetic context of  $\text{H}^+ / 2 \text{ e}$  or  $\text{H}^+ / \text{O}$  ratios (Mitchell and Moyle 1967) or P:O ratios, corresponding fluxes were then frequently expressed as  $J_p / J_{O_2}$ , where  $J_{O_2} = 2 \cdot J_{O_1}$ , the latter in 'bioenergetic' units [ $\text{natoms O} \cdot \text{s}^{-1} \cdot \text{ml}^{-1}$ ] (Slater et al 1973). In bioenergetics a variety of expressions is used for units of amount of oxygen (natoms oxygen; natoms O; ng.atom O; nmol O), with the identical meaning: 0.5 nmol O<sub>2</sub>.

## 3. Fundamental constants and conversion factors

Boltzmann constant	$k$	$1.3807 \cdot 10^{-23} \text{ J} \cdot \text{K}^{-1}$
Gas constant	$R$	$8.314510 \text{ J} \cdot \text{mol}^{-1} \cdot \text{K}^{-1}$
Avogadro constant	$N_A$	$6.02214 \cdot 10^{23} \text{ mol}^{-1}$
Elementary charge	$e$	$1.602177 \cdot 10^{-19} \text{ C}$
Farady constant	$F = eN_A$	$96,485.3 \text{ C} \cdot \text{mol}^{-1}$ (96.4853 kJ·mol <sup>-1</sup> /V)
Absolute temperature	$T$	273.15; 298.15; 310.15 K at 0; 25; 37 °C
$RT$		2.271; 2.479; 2.579 kJ·mol <sup>-1</sup> at 0; 25; 37 °C
$\ln(10)$		2.3026
$RT \cdot \ln(10)$		5.229; 5.708; 5.938 kJ·mol <sup>-1</sup> at 0; 25; 37 °C
$(RT/F) \cdot \ln(10)$		54.20; 59.16; 61.54 mV at 0; 25; 37 °C
$1/4F$		2.591 $\mu\text{mol}/(4 \text{ C})$



**P R E L - ROX**

**Appendix: Abbreviations**

Section A1. Respiratory coupling states and rates ..... 67 Page  
 A2. Substrates, uncouplers, inhibitors - SUIT ..... 69

**A1. Respiratory coupling states and rates**

**Table A1.1. Respiratory coupling states, corrected for ROX.**

Symbol	Definition	mt-Preparations, ETS competent substrate states	Intact cells, exogenous or endogenous substrates
State <i>i</i>	$J_{O2i}$ or $I_{O2i}$		
<i>P</i>	<b>OXPHOS capacity</b> , oxidative phosphorylation capacity, coupled, $\Delta p_{mt}$ supports $J_{-P}$	Saturating ADP and $P_i$ , or $J_{max}$ from ADP kinetics	Difficulties to achieve saturating ADP and $P_i$
<i>R</i>	<b>ROUTINE activity</b> , physiological control of energy turnover in the theoretical range from <i>L</i> to <i>P</i> , variable $\Delta p_{mt}$	Limiting steady-state ADP levels simulating states of routine activity above <i>L</i> and below <i>P</i>	Physiological control of cellular substrate uptake, intermediary metabolism and energy turnover
<i>E</i>	<b>ETS capacity</b> , electron transfer system capacity, noncoupled, low but not zero $\Delta p_{mt}$	Optimal uncoupler concentration for maximum respiration	Optimal uncoupler concentration for maximum respiration
<i>L</i>	<b>LEAK respiration</b> , nonphosphorylating, maximum $\Delta p_{mt}$	$L_N$ and $L_{Omy}$ : general; $L_T$ : excluding ATPase activity	$L_{Omy}$
ROX	<b>Residual oxygen consumption</b>	Substrate depletion, or inhibition of CI to CIV	Inhibition of CI to CIV

Conditions vary for measurement and expression of respiration (flux,  $J_{O2}$ ; flow,  $I_{O2}$ ). If these conditions are defined and remain consistent within a given context, then the symbols for respiratory states (*P*, *R*, *E*, *L*) can be used to substitute the explicit expressions for flows (or fluxes):

$$P, R, E, L = I_{O2P}, I_{O2R}, I_{O2E}, I_{O2L} \text{ or } J_{O2P}, J_{O2R}, J_{O2E}, J_{O2L}$$

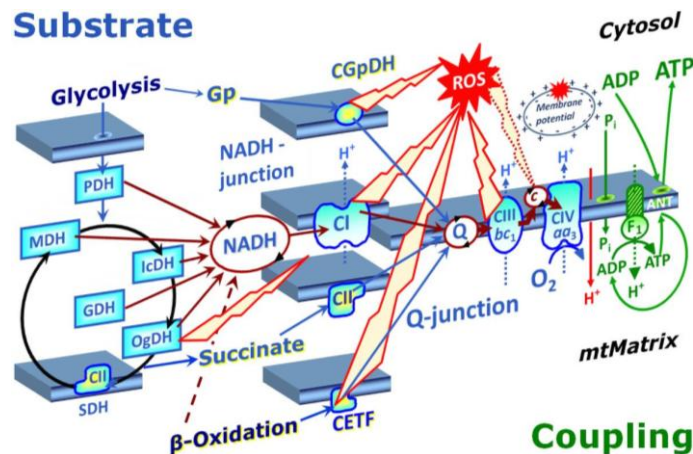




**Table A1.2. Coupling control ratios related to free and excess capacities.**

Free and excess capacities are defined in Tab. 2.2.

FCR	Coupling control ratio, CCR	$X_i$	$Y_i$	Z
L/P	<b>L/P coupling control ratio</b> , 1/RCR, combines the effects of coupling and OXPHOS capacity. Free OXPHOS capacity: $\approx P = P - L$	D*	L	P
L/R	<b>L/R coupling control ratio</b> , combines the effects of cell physiological state, mitochondrial coupling and OXPHOS capacity. Free ROUTINE activity: $\approx R = R - L$	Omy	L	R
L/E	<b>LEAK control ratio</b> , L/E coupling control ratio, combines the effects of coupling and ETS capacity. Free ETS capacity: $\approx E = E - L$	U	L	E
P/E	<b>OXPHOS control ratio</b> , phosphorylation system control ratio, P/E coupling control ratio, combines the effects of coupling and limitation by the phosphorylation system, phosphorylation system control ratio. Excess E-P capacity: $ExP = E - P$	U	P	E
R/E	<b>ROUTINE control ratio</b> , R/E coupling control ratio, combines the effects of cell physiological state, coupling, OXPHOS capacity and excess capacity, ExP. Excess E-R capacity: $ExP = E - R$	U	R	E
$\approx P/E$	<b>netOXPHOS control ratio</b> , $\approx P/E$ control ratio = $(P - L)/E$ .	U	$\approx P$	E
$\approx R/E$	<b>netROUTINE control ratio</b> , $\approx R/E$ control ratio = $(R - L)/E$ .	U	$\approx R$	E

**Table A1.3. Coupling control factors for free and excess capacities.**

FCF	Coupling control factor, CCF	j	Net ratio	1-CCR	X	$Y_x$	$Z_x$
$\approx P/P$	<b>OXPHOS coupling efficiency</b> , P-L control factor, 1-RCR <sup>-1</sup>	$j_{\approx P} = (P - L)/P$	$= (P - L)/P$	$= 1 - L/P$	D*	L	P
$\approx R/R$	<b>ROUTINE coupling efficiency</b> , R-L control factor	$j_{\approx R} = (R - L)/R$	$= (R - L)/R$	$= 1 - L/R$	Omy	L	R
$\approx E/E$	<b>ETS coupling efficiency</b> , E-L control factor	$j_{\approx E} = (E - L)/E$	$= (E - L)/E$	$= 1 - L/E$	U	L	E
ExP/E	<b>Excess E-P capacity factor</b> , E-P control factor	$j_{ExP} = (E - P)/E$	$= (E - P)/E$	$= 1 - P/E$	U	P	E
ExR/E	<b>Excess E-R capacity factor</b> , E-R control factor	$j_{ExR} = (E - R)/E$	$= (E - R)/E$	$= 1 - R/E$	U	R	E



[http://www.bioblast.at/index.php/Bioblast Glossary: Respiratory states](http://www.bioblast.at/index.php/Bioblast_Glossary:_Respiratory_states)

[http://www.bioblast.at/index.php/Bioblast Glossary: Respiratory control ratios](http://www.bioblast.at/index.php/Bioblast_Glossary:_Respiratory_control_ratios)

$$j_{\approx P} = \frac{P - L}{P} = 1 - \frac{L}{P} = 1 - \frac{1}{RCR}$$

$$FCR_i = \frac{Y_i}{Z}$$

$$FCF_x = \frac{Z_x - Y_x}{Z_x}$$

$$\approx P = \frac{\approx P}{V_{-P/O_2}} = P - L = 1 - \frac{Y_x}{Z_x}$$



## A2. Substrates, uncouplers, inhibitors - SUIT



### A2.1. Oxygraph-2k manual titrations: mitochondria, homogenate, permeabilized cells and tissues

**Tab. A2.1.** Manual titrations for O2k-Chamber volume of 2.0 ml

Substrates	Event	Concentration in syringe (solvent)	Storage [°C]	Final conc. in 2 ml	Titration [μl]	Syringe [μl]
Pyruvate	P	2 M (H <sub>2</sub> O)	fresh	5 mM	5	25
Malate	M	0.4 M (H <sub>2</sub> O)	-20	0.5 mM	2.5	25
Glutamate	G	2 M (H <sub>2</sub> O)	-20	10 mM	10	25
Succinate	S	1 M (H <sub>2</sub> O)	-20	10 mM	20	50
Octanoylcarnitine	Oct	0.1 M (H <sub>2</sub> O)	-20	0.2 mM	4	10
Ascorbate	As	0.8 M (H <sub>2</sub> O)	-20	2 mM	5	25
TMPD	Tm	0.2 M (H <sub>2</sub> O)	-20	0.5 mM	5	25
Cyt. c	c	4 mM (H <sub>2</sub> O)	-20	10 μM	5	25
ADP+ Mg <sup>2+</sup>	D	0.5 M (H <sub>2</sub> O)	-80	1 - 5 mM	4 - 20	25
ATP+ Mg <sup>2+</sup>	T	0.5 M (H <sub>2</sub> O)	-80	1 - 5 mM	4 - 20	25
<b>Uncoupler</b>						
CCCP*	U	0.1 mM (EtOH)	-20	0.05 μM steps	1 μl steps	10
CCCP*	U	1.0 mM (EtOH)	-20	0.5 μM steps	1 μl steps	10
<b>Inhibitors</b>						
Rotenone	Rot	1 mM (EtOH)	-20	0.5 μM	1	10
Malonic acid	Mna	2 M (H <sub>2</sub> O)	fresh	5 mM	5	25
Antimycin A	Ama	5 mM (EtOH)	-20	2.5 μM	1	10
Myxothiazol	Myx	1 mM (EtOH)	-20	0.5 μM	1	10
Sodium azide	Azd	4 M (H <sub>2</sub> O)	-20	≥100 mM	≥50	50
KCN	Kcn	1 M (H <sub>2</sub> O)	fresh	1.0 mM	2	10
Oligomycin	Omy	5 mM (EtOH)	-20	2.5 μM	1	10
Carboxyatractyloside	Cat	5 mM (H <sub>2</sub> O)	-20	0.75 mM	2	10
<b>Cell perm.</b>						
Digitonin	Dig	10 mg/ml (DMSO)	-20	10 μg·10 <sup>-6</sup> cells	1 μl 10 <sup>-6</sup>	10
<b>Other</b>						
Catalase in MiR06	Ctl	112,000 U/ml	-20	280 U/ml	5	25

\*0.1 mM stock for mt-preparations with high uncoupler sensitivity; 1 mM stock for mt-preparations with low uncoupler sensitivity, intact cells in various culture media (e.g. RPMI, DMEM, EGC) and for TIP2k.



[http://www.bioblast.at/index.php/MiPNet09.12\\_O2k-Titrations](http://www.bioblast.at/index.php/MiPNet09.12_O2k-Titrations)

SUIT symbols have evolved for daily laboratory practice with the requirement to keep abbreviations short. They are not intended for use outside the SUIT framework.



## A2.2. Substrates of the TCA cycle and major entries

Single capital letters for the most commonly used fuel substrates

CI	CI-linked substrate state, at defined coupling state
CII	CII-linked substrate state, at defined coupling state
CI&II	Substrate state with CI- and CII-linked substrates added in combination, at a defined coupling state
CI+CII	Flux or flow calculated as the arithmetic sum of CI-linked plus CII-linked respiration measured separately
CI/CI&II	Substrate control ratio at a defined coupling state
CI&FAO	Substrate state with FA and a CI-competent substrate combination (e.g. GMOct)
P	Pyruvate; if added after GM: $FCF_P = 1 - GM/PGM$
G	Glutamate; if added after PM: $FCF_G = 1 - PM/PGM$
M	Malate; inhibition by $\Delta$ concentration Z to Y: $FCF_{\Delta c} = 1 - M_Y/M_Z$
S	Succinate; if added after CI: $FCF_{CII} = 1 - CI/CI&II$
FA	Fatty acid
FAO	FA oxidation, involving Complexes CETF & CI (e.g. OctM)
Fu	Fumarate
Og	Oxoglutarate
Ce	Cellular substrates <i>in vivo</i> , endogenous
Cex	Cellular substrates <i>in vivo</i> , with exogenous substrate supply

## A2.3. Other substrates and respiratory redox components

Oca	Octanoate
Paa	Palmitate
Oct	Octanoylcarnitine
Pal	Palmitoylcarnitine
As	Ascorbate
Tm	TMPD
c	Cytochrome c; c control factor: $FCF_c = 1 - J_{CHO}/J_{CHOc}$
Gp	Glycerophosphate



[http://www.bioblast.at/index.php/Bioblast Glossary: Substrates and metabolites](http://www.bioblast.at/index.php/Bioblast%20Glossary%3A%20Substrates%20and%20metabolites)

## A2.4. Inhibitors of respiratory complexes, dehydrogenases or transporters

Atr	Atractyloside (state $L_{Atr}$ ); ANT
Ama	Antimycin A; CIII
Azd	Sodium azide; CIV
Hci	Hydroxycinnamate; pyruvate carrier
Kcn	KCN; CIV
Mna	Malonate; CII
Myx	Myxothiazol; CIII
Omy	Oligomycin (state $L_{Omy}$ ); CV
Rot	Rotenone; CI; if added after CI&II: $FCF_{CI} = 1 - CII/CI&II$



[http://www.bioblast.at/index.php/Bioblast Glossary: Inhibitors](http://www.bioblast.at/index.php/Bioblast%20Glossary%3A%20Inhibitors)



## A2.5. Phosphorylation system

Adenylates,  $P_i$ , uncouplers, downstream inhibitors of ATP synthase, ANT, or phosphate are denoted by subscripts. If  $P_i$  is always present at saturating concentration, it does not have to be indicated in the titration protocols.

$P_i$	Inorganic phosphate
$\sim P$	phosphorylation of ADP+ $P_i$ to ATP
$\sim P$	Flux of phosphorylation, $\sim P = J_{\sim P}$
$\approx P$	Free OXPHOS capacity, partial or net oxygen flux fully coupled to $\sim P$ ; $\approx P = J_{O_2P} - J_{O_2L}$
N	no adenylates added (see state L)
D*	ADP at saturating concentration (state P: saturating [ADP])
D0.2	ADP at specified concentration (saturating versus non-saturating ADP is frequently not specified in State 3); stimulation by $\Delta$ concentration Y to Z: $FCF_{\Delta c} = 1 - D_Y/D_Z$
T	ATP (see state $L_T$ )
TD	ATP&ADP (state P, in the presence of physiological high (mM) ATP concentrations)
T[ADP]	High ATP and varying ADP concentrations, in the range between states T and TD.
U	Uncoupler, titration for optimum concentration at maximum noncoupled flux (state E); excess E-P capacity factor = $1 - P/E$



[http://www.bioblast.at/index.php/Bioblast Glossary: Uncouplers](http://www.bioblast.at/index.php/Bioblast_Glossary:Uncouplers)

## A2.6. Protocols

Letters in normal font are used for the substrates X.

Subscripts are used for effectors of the phosphorylation system and for indicating coupling control states.

Example: In the protocol  $^*:PM_N + D + c + G + S + U + (Rot) + (Myx+..)$ , the respiratory state after addition of rotenone is:  $PMGSc(Rot)_E$ . With reference to this protocol, it may be convenient to use an abbreviation, such as  $S(Rot)_E$ .

\*Suspended cells may be permeabilized in the Oxygraph chamber with digitonin (Dig), after measurement of endogenous respiration in mitochondrial respiration medium. The initial protocol is indicated above as \*, referring to the initial steps of endogenous respiration and permeabilization:  $Ce_R + PM + Dig$ .





## References

Open Access to the full list of references and notes:



[http://www.bioblast.at/index.php/Gnaiger\\_2014\\_MitoPathways](http://www.bioblast.at/index.php/Gnaiger_2014_MitoPathways)

Selected references (mainly sources of figures, tables, and basic concepts):

- Boushel R, Gnaiger E, Schjerling P, Skovbro M, Kraunsoe R, Flemming D (2007) Patients with Type 2 Diabetes have normal mitochondrial function in skeletal muscle. *Diabetologia* 50: 790-796.
- Chance B, Williams GR (1955) Respiratory enzymes in oxidative phosphorylation. I. Kinetics of oxygen utilization. *J Biol Chem* 217: 383-393.
- Chance B, Williams GR (1955) Respiratory enzymes in oxidative phosphorylation. III. The steady state. *J Biol Chem* 217: 409-427.
- Gnaiger E (1993) Nonequilibrium thermodynamics of energy transformations. *Pure Appl Chem* 65: 1983-2002.
- Gnaiger E (1993) Efficiency and power strategies under hypoxia. Is low efficiency at high glycolytic ATP production a paradox? In: *Surviving Hypoxia: Mechanisms of Control and Adaptation*. Hochachka PW, Lutz PL, Sick T, Rosenthal M, Van den Thillart G (eds) CRC Press, Boca Raton, Ann Arbor, London, Tokyo: 77-109.
- Gnaiger E, Méndez G, Hand SC (2000) High phosphorylation efficiency and depression of uncoupled respiration in mitochondria under hypoxia. *Proc Natl Acad Sci U S A* 97: 11080-11085.
- Gnaiger E (2008) Polarographic oxygen sensors, the Oxygraph and high-resolution respirometry to assess mitochondrial function. In: *Mitochondrial Dysfunction in Drug-Induced Toxicity* (Dyken JA, Will Y, eds) John Wiley: 327-352.
- Gnaiger E (2009) Capacity of oxidative phosphorylation in human skeletal muscle. *New perspectives of mitochondrial physiology*. *Int J Biochem Cell Biol* 41: 1837-1845.
- Gutman M, Coles CJ, Singer TP, Casida JE (1971) On the functional organization of the respiratory chain at the dehydrogenase-coenzyme Q junction. *Biochemistry* 10: 2036-2043.
- Harris EJ, Manger JR (1969) Intersubstrate competitions and evidence for compartmentation in mitochondria. *Biochem J* 113: 617-628.
- Hatefi Y, Haavik AG, Fowler LR, Griffiths DE (1962) Studies on the electron transfer system. XLII. Reconstitution of the electron transfer system. *J Biol Chem* 237: 2661-2669.
- Krumschnabel G, Eigentler A, Fasching M, Gnaiger E (2014) Use of safranin for the assessment of mitochondrial membrane potential by high-resolution respirometry and fluorometry. *Methods Enzymol* 542: 163-81.
- LaNoue KF, Schoolwerth AC (1979) Metabolite transport in mitochondria. *Annu Rev Biochem* 48: 871-922
- LaNoue KF, Walajtys EI, Williamson JR (1973) Regulation of glutamate metabolism and interactions with the citric acid cycle in rat heart mitochondria. *J Biol Chem* 248: 7171-7183.





- Lemieux H, Semsroth S, Antretter H, Hoefler D, Gnaiger E (2011) Mitochondrial respiratory control and early defects of oxidative phosphorylation in the failing human heart. *Int J Biochem Cell Biol* 43: 1729-1738.
- Mitchell P (1961) Coupling of phosphorylation to electron and hydrogen transfer by a chemi-osmotic type of mechanism. *Nature* 191: 144-148.
- Mitchell P, Moyle J (1967) Respiration-driven proton translocation in rat liver mitochondria. *Biochem J* 105: 1147-1162.
- Pesta D, Gnaiger E (2012) High-resolution respirometry. OXPHOS protocols for human cells and permeabilized fibres from small biopsies of human muscle. *Methods Mol Biol* 810: 25-58.
- Pesta D, Hoppel F, Macek C, Messner H, Faulhaber M, Kobel C, Parson W, Burtscher M, Schocke M, Gnaiger E (2011) Similar qualitative and quantitative changes of mitochondrial respiration following strength and endurance training in normoxia and hypoxia in sedentary humans. *Am J Physiol Regul Integr Comp Physiol* 301: R1078-R1087.
- Puchowicz MA, Varnes ME, Cohen BH, Friedman NR, Kerr DS, Hoppel CL (2004) Oxidative phosphorylation analysis: assessing the integrated functional activity of human skeletal muscle mitochondria - case studies. *Mitochondrion* 4: 377-385.
- Rasmussen HN, Rasmussen UF (1997) Small scale preparation of skeletal muscle mitochondria, criteria for integrity, and assays with reference to tissue function. *Mol Cell Biochem* 174: 55-60.
- Rasmussen UF, Rasmussen HN (2000) Human quadriceps muscle mitochondria: A functional characterization. *Mol Cell Biochem* 208: 37-44.
- Renner K, Amberger A, Konwalinka G, Gnaiger E (2003) Changes of mitochondrial respiration, mitochondrial content and cell size after induction of apoptosis in leukemia cells. *Biochim Biophys Acta* 1642: 115-123.
- Sjoevall F, Morota S, Hansson MJ, Friberg H, Gnaiger E, Elmer E (2010) Temporal increase of platelet mitochondrial respiration is negatively associated with clinical outcome in patients with sepsis. *Critical Care* 14: R214 doi:10.1186/cc9337
- Torres NV, Mateo F, Sicilia J, Meléndez-Hevia E (1988) Distribution of the flux control in convergent metabolic pathways: theory and application to experimental and simulated systems. *Int J Biochem* 20: 161-165.
- Votion DM, Gnaiger E, Lemieux H, Mouithys-Mickalad A, Sereteyn D (2012) Physical fitness and mitochondrial respiratory capacity in horse skeletal muscle. *PLoS One* 7: e34890.



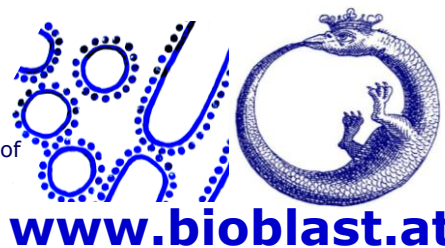
Winfried Platzgummer - Oroboros in thermodynamics (2010)



# Bioblast Wiki

OROBOROS-Team<sup>1</sup>

Integrating the spirit of  
Gentle Science and  
Scientific Social  
Responsibility



**Bioblast** was launched as a glossary and index for high-resolution respirometry (OROBOROS INSTRUMENTS) and mitochondrial physiology ('MitoPedia'), to find topics quickly, as a dynamic tool for summarizing definitions of terms, symbols and abbreviations - an innovative, collaborative wiki database, supporting the growth and function of a [Mitochondrial Global Network](#) [2,3].

**What is the aim?** Bioblast provides a platform for **Gentle Science** [4] in the spirit of Scientific Social Responsibility. Catalytically working as an *Information synthase* (see logo [3]), **Bioblast glossaries** are aimed to develop a consistent nomenclature in the growing field of mitochondrial physiology. **O2k-Protocols** provide up-to-date information on experimental details. Users are encouraged to contribute and share their expertise. The corresponding category **Publications** provides a portal for sharing, disseminating and commenting relevant literature in mitochondrial physiology, with context-related 'filters' for references in the **MiPMap**. Bioblast allows the *evolution* of a scientific publication - providing space for open discussions and extensions of an otherwise static *paper*. This applies specifically to the sections of *Methods and Materials*, *Discussion*, and *References*, which may be limited by space in original publications. Detailed information added and edited should be helpful in practice.

**How to register?** Write to us, and we will register you with your real name, as in a scientific publication. Anonymous or pseudonymous contributions to Bioblast do not follow the scientific attitude of publication. Mail to [instruments@oroboros.at](mailto:instruments@oroboros.at) for registration or contact our team for adding your contributions under your name.

**How does it work?** We invite scientists, students, and technicians in mitochondrial physiology and pathology to join as 'active users' in the spirit of Gentle Science, to ensure that the Bioblast Wiki will develop into a database of top-quality scientific information. This can be achieved only by an expert-moderated wiki - with input and feedback of a large benevolent user community of experts in mitochondrial physiology.

All of you can shape the Bioblast Wiki by bringing together scientists working in divergent disciplines, to discuss, to resolve differences, to spread new knowledge and techniques; thus meeting the demand to integrate current developments in the methodologically and conceptually complex field of mitochondrial physiology.

1. Ondrej Capek, Verena Erhart, Mario Fasching, Sandra Fleischmann, Mona Fontana-Ayoub, Karina Fritz, Erich Gnaiger, David K Harrison, Florian Hoppel, Georg Kandolf, Gerhard Krumschnabel, Verena Laner, Bernd Schöpf - [www.oroboros.at/?O2k-Team](http://www.oroboros.at/?O2k-Team)
2. A *wiki* (Hawaiian, meaning 'fast') is a dynamic and collaborative website. Cunningham Ward: [What is a Wiki](#); WikiWikiWeb: <http://www.wiki.org/wiki.cgi?WhatIsWiki> 2010-09-09
3. The **Bioblast logo** combines mitochondrial art, from 'ATP synthase congregation' by Odra Noel, with the Oroboros, "the tail-eater" - a dragon forming a circle, where 'creation and the created become one in an inseparable process' <http://www.mipart.at/index.php?oroboros-archetypical-symbol>
4. Gentle Science Shapes the World - [http://www.bioblast.at/index.php/Gentle\\_Science](http://www.bioblast.at/index.php/Gentle_Science)

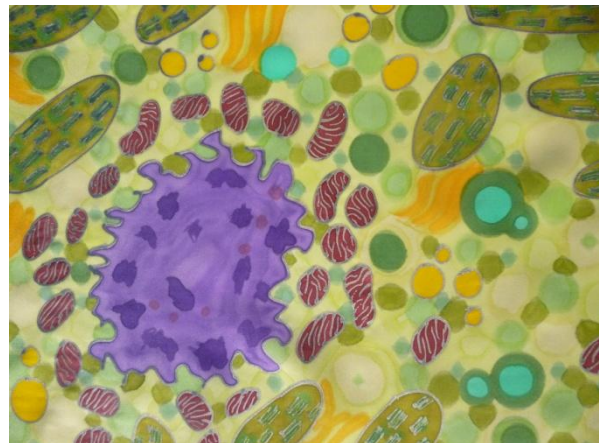
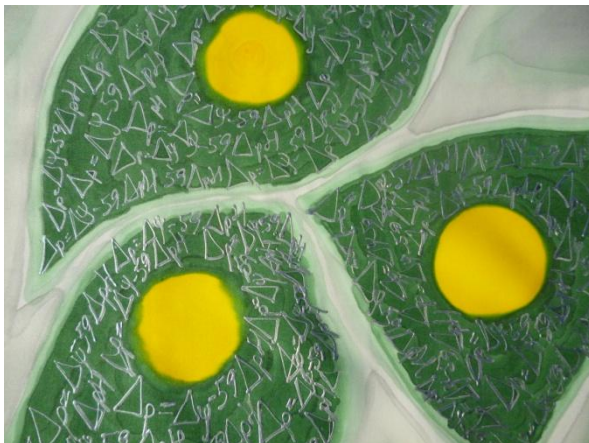


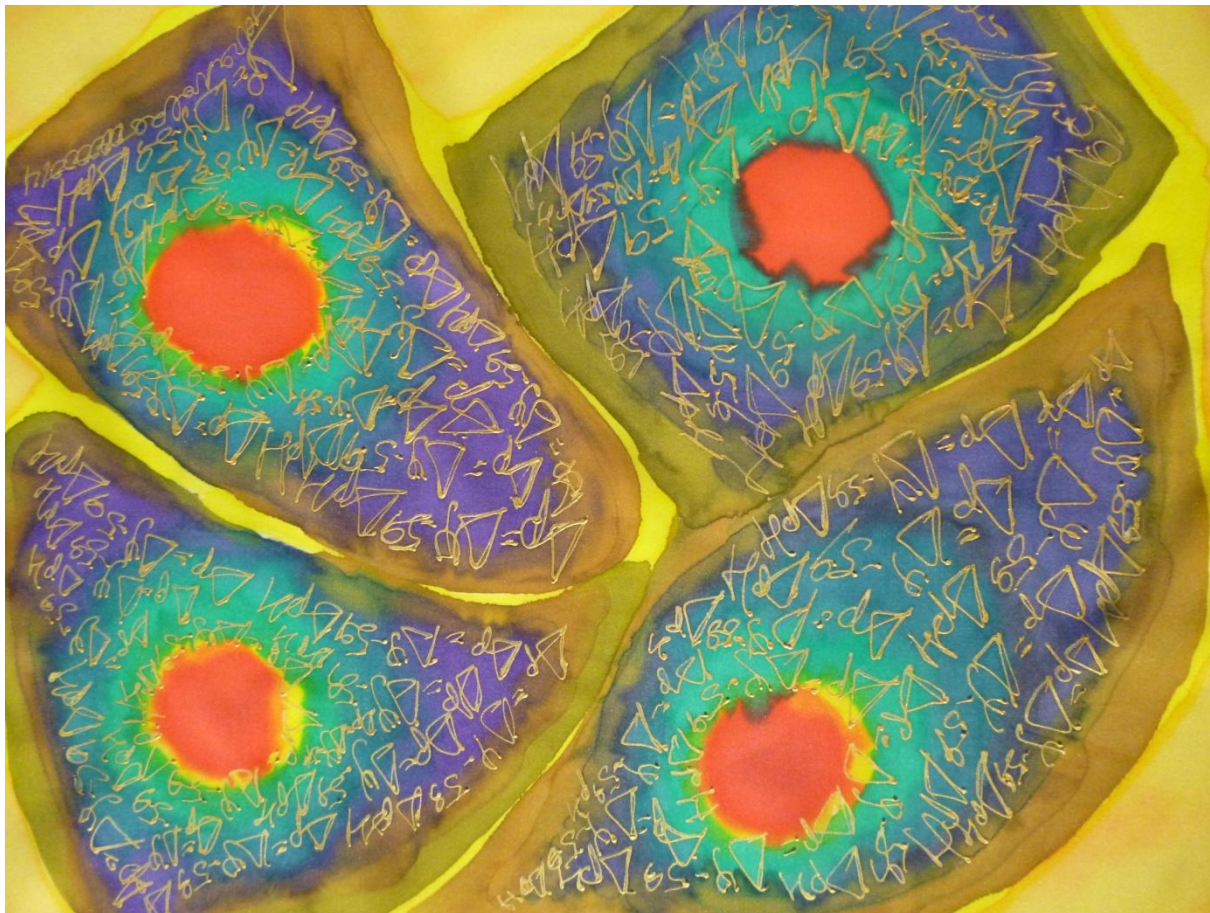
## *MiPart - Mitchell's dream*

by Odra Noel

<http://odranoel.eu/category/mitochondrial-art>

*Science is beautiful: it has truth, it has drama, it is full of wonder. The Mitchell's dream series is a vision of some aspects of science through art. I hope it explains, inspires or makes you curious to find out more.*





## *MiP Art - Mitchell's equation*

by Erich Gnaiger

### *Do you ever dream about an equation?*

The *Mitchell's dream series* by Odra Noel is a dream on equations and shows a dream on the equation that penetrates all of biology since Peter D Mitchell started publishing on the protonmotive force equation [1]. Can we imagine how many dreaming was required until the chemiosmotic hypothesis emerged on energy coupling by the protonmotive force of oxidative phosphorylation in the bioblasts, which comprise the mitochondria, chloroplasts, bacteria and archaea? Seeing Odra Noel's pictures on *Mitchell's dream* provides insights into the equations of biophysics and biochemistry: these equations do not just belong to our books. They do belong to our cells, our bioblasts, to the living world. It is the mitochondria that help us to understand these equations, since the equations are in the mitochondria, they are the visible parts of the mitochondria and open *insights* into function beyond the visible form – this is mitochondrial physiology.

### *Do you feel part of the equation?*

An equation (or it's opposite) connects two sides by the equal (or unequal) sign,

$$= \quad (1)$$

The left side may show simply a symbol,

$$\Delta p_{mt} =$$



This symbol is defined as being equal to a combination of various parts on the right side,

$$\Delta p_{mt} = \text{electric part} + \text{chemical part} \quad (2)$$

and these parts may again be shown simply as symbols,

$$\Delta p_{mt} = \Delta \Psi_{mt} + \Delta \mu_{H^+}/F \quad (3)$$

The *electric* part is the potential difference across the inner mitochondrial (mt) membrane,  $\Delta \Psi_{mt}$ . This suggests that the protonmotive force in the form of Equation 3 should be expressed in the electric unit of volt [V]. *Electric* force of the mitochondrial membrane potential is the electric energy change per 'motive' electron or per electron moved across the transmembrane potential difference, with the number of 'motive' electrons expressed in the unit coulomb [C].

Therefore, the *chemical* part,  $\Delta \mu_{H^+}/F$ , which stems from the difference of pH across the mt-membrane, contains a factor that bridges the gap between the *electric* force [J/C] and the *chemical* force [J/mol]. This factor is the Faraday constant,  $F$ , for conversion between *electric* force expressed in joules per coulomb or Volt [V=J/C] and *chemical* force with the unit joules per mole or Jol [Jol=J/mol],

$$F = 96.4853 \text{ kJol/V} = 96,485.3 \text{ C/mol}$$

Generally, a force is the change of potentially available or 'free' energy (exergy) per 'motive' unit [2]. The *chemical* force or chemical potential of the 'motive' proton is the exergy change [J] per 'motive' amount of substance [mol]. Protonmotive means that the proton is moved across the mt-membrane at  $\Delta pH$  maintained across the mt-membrane,

$$\Delta \mu_{H^+} = -2.3 \cdot RT \cdot \Delta pH \quad (4)$$

This chemical force is the *difference* ( $\Delta$ ) of chemical potential across the inner mitochondrial membrane. Mitchell's equation and Odra Noel's pictures don't show proton *gradients* or membrane potential *gradients* – this dream belongs to another group.

The right side of Equations (2) and (3) helps us to separate the different parts, which require different methods of measurement, are expressed in different units, confuse us with different sign conventions and scientific nomenclature with terminological incompatibilities. On which side of the equation are you at home? Which part is more your part? Do you feel part of the equation?



On the other hand, the left side of the equation brings the different parts together in a unifying concept. With full focus on the equation, do we still see the mitochondria? Odra Noel places the sides and parts of the equation where they belong: They are parts of the bioblasts, they are the essence of the mitochondria themselves. Unification is brought to the limit of reduction in the form of Equation 1:



We have to write  $\Delta \Psi_{mt}$  to point out that the mitochondrial membrane potential difference is in our mind. However,  $\Delta \Psi$  in Odra Noel's pictures *is* the mitochondrion, the mt does not have to be written *into* the pictures, mt is essentially shown *by* the pictures. The *Mitchell's dream series* illustrates the importance of putting a symbol in the right form at the right place for understanding an equation and easily identifying the meaning of the symbol.

*Mitchell's dream* is a symbol of form and function – form and function is the mitochondrial physiologist's dream.

Reprinted from Laner V, Gnaiger E, eds (2014) Mitochondrial physiology – methods, concepts and biomedical perspectives. MiP2014. Mitochondr Physiol Network 19.13: 88 pp.

1. Mitchell P (1961) Coupling of phosphorylation to electron and hydrogen transfer by a chemi-osmotic type of mechanism. Nature 191: 144-148. – Photo: [www.nobelprize.org/nobel\\_prizes/chemistry/laureates/1978/](http://www.nobelprize.org/nobel_prizes/chemistry/laureates/1978/)
2. Gnaiger E (1993) Nonequilibrium thermodynamics of energy transformations. Pure Appl Chem 65: 1983-2002.



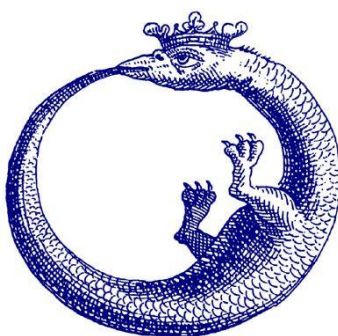
The Oroboros – the open door to OROBOROS INSTRUMENTS and the *MiP*Art Gallery. Steel sculpture by Harald Kirchebner (2008). Foto by Philipp Gradl. – [www.mipart.at](http://www.mipart.at)



## THE OROBOROS

### FEEDING ON NEGATIVE ENTROPY?

The dragon forming a cycle, feeding on its own tail - in alchemy, the Oroboros is an emblem of the eternal, cyclic nature of the universe, combining idea and action, efficiency and power. The Oroboros is grasping the whole by the conception of the opposite, the divine process of creation and the evil backlash of destruction. In thermodynamics, the alchemist's search for the eternal Unity has been continued in the many efforts to construct a machine operating at 100% efficiency, the



Perpetuum Mobile. 100% efficiency is the prerequisite for a truly cyclic nature of energy flux through the biosphere. The notion of the arrow of time, introduced by the Second Law of thermodynamics, replaces the quest for 100% efficiency by the pursuit of a balanced management of the resources of energy and time. Such optimization of efficient material recycling and balanced resource utilization is a vital responsibility of modern society for the protection of local and global ecological systems.

The Oroboros is one of the rare universal examples where feeding on external negative entropy,  $d_e S/dt$ , is not true, as shown by the feedback loop and the system boundaries. In terms of ergodynamics, at any rate, Oroboros is the fine state of *non-thermodynamic equilibrium*.

Graphic from: Abraham Eleazar (1760)  
Uraltes chymisches Werk. 2nd ed, Leipzig

From: *What is Controlling Life? 50 years after Erwin Schrödinger's 'What is Life?'*  
(Gnaiger E, Gellerich FN, Wyss M, eds), Modern Trends in BioThermoKinetics 3  
Innsbruck Univ Press (1994): 316.



# A taste of Gentle Science **Bioblast**



[www.bioblast.at](http://www.bioblast.at)

[www.orooboros.at](http://www.orooboros.at)